Characterization of the Function of the *AtST4* Subfamily Members in Cytokinin-Dependent Growth Control in *Arabidopsis thaliana*

Effat Khodashenas

A Thesis

in

The Department

of

Biology

Presented in Partial Fulfillment of the Requirements
for the Degree of Master of Science (Biology) at
Concordia University
Montreal, Quebec, Canada

March 2010

Your file Votre référence
ISBN: 978-0-494-67280-8
Our file Notre référence
ISBN: 978-0-494-67280-8

ABSTRACT

Characterization of the Function of the *AtST4* Subfamily Members in Cytokinin-Dependent Growth Control in *Arabidopsis thaliana*

Effat Khodashenas

The main objective of our laboratory is to characterize the function of the 18 sulfotransferase-coding genes of *Arabidopsis thaliana*. In this study, we describe the biochemical and biological characterization of the three members of the *AtST4* subfamily (*AtST4a*, *b* and *c*). The analysis of published microarray data as well as transcript expression studies show that the three members of the *AtST4* subfamily are expressed in roots and regulated by cytokinins. *AtST4b* is among the group of genes exhibiting the highest level of induction following treatment with the cytokinin *trans*-zeatin. In contrast, *AtST4c* is repressed under the same experimental conditions.

To elucidate their biological function, we isolated *AtST4a, AtST4b,* and *AtST4c* loss of function mutants. Using metabolite profiling of the knockout mutant and mass spectrometry, we demonstrate that *AtST4b* encodes a cadabicine (cyclic dihydroxycinnamoyl spermidine) sulfotransferase. Even though cadabicine has previously been reported to occur naturally in plants, this is the first report of its occurrence in *A. thaliana* and the first report of the accumulation of its sulfonated conjugate. Phenotypic analysis of the *AtST4b*-knockout mutant showed alternations in root, shoot and reproductive development as compared to wild type plants and a partial loss of sensitivity to cytokinins. Our results seem to indicate that *AtST4b* plays an important role in the cytokinin-mediated effects on growth.

Unfortunately, we could not find the endogenous substrate of AtST4a and AtST4c, and the results of our biochemical and metabolic profiling experiments suggest that they might sulfonate the same substrate or substrates with very similar properties. However, the *AtST4a* and *AtST4c* loss of function mutants show differences in their growth behavior suggesting that they have different functionalities in *A. thaliana*.

تقدیم به مادرم

که سخت کوشی را از او آموختم

TABLE OF CONTENTS

LIST OF FIGURES

LIST OF ABBREVIATIONS

AHKs	Arabidopsis histidine kinase receptors
AHPs	Arabidopsis histidine phosphotransmitter proteins
ARR	Arabidopsis response regulator
BAHD acyl transferase	First letters of the first characterized members of the family: BEAT, AHCT, HCBT and DAT
BRs	Brassinosteroids
CID	Collision induced dissociation
CKs	Cytokinins
CKXs	Cytokinin oxidases
Col-0	Columbia 0
C-terminus	Carboxyl-terminus
DAG	Days after germination
DMSO	Dimethylsulfoxide
DPM	Disintegrations per minute
E.coli	*Escherichia coli*
eFP	Electronic fluorescent pictograph
FT-IMS	Fourier transform-ion mobility spectrometry
GARP motif	First letters of the members in maize GOLDEN2, Arabidopsis response regulators and *Chlamidomonas* PSR1
HCAAs	Hydroxycinnamic acid amides
His-tag	Histidine-tag
HPLC	Reverse phase high performance liquid chromatography

IPT	Isopentenyl dephosphate transferase
Kbp	Kilobase pair
Kda	Kilodalton
KO	Knockout
LB	T-DNA left border
LC-MS/MS	Reverse phase liquid chromatography-tandem mass spectrometry
LFY	*LEAFY* gene
MS media	Murashige and Skoog media
Ni-NTA	Nickel-nitrilotriacetic acid
N-terminus	Amino-terminus
PAPS	3'-phosphoadenosine 5'-phosphosulfate
PAs	Polyamines
PCR	Polymerase chain reaction
Q-TOF mass spectrometer	Tandem quadrupole time-of-flight mass spectrometer
RT-PCR	Reverse transcription-polymerase chain reaction
SCT	Spermidine dicoumaroyl transferase
SD	Standard deviation
SDS-PAGE	Sodium dodecyl sulfate-poly acrylamide gel electrophoresis
SSAT	Spermidine/spermine N1-acetyltransferase
SULTs	Sulfotransferases
TCS	Two-component signaling system
T-DNA	Transfer DNA

TLC	Thin layer chromatography
t-zeatin	*trans*-zeatin

Chapter 1- Review of Literature

1.1) Introduction

This chapter reviews the main topics related to the characterization of the three members of the *AtST4* sulfotransferase (SULT) subfamily from *Arabidopsis thaliana*. At first, we present a brief introduction to SULTs, their structure and functions, with emphasis on plant soluble SULTs. Next, we introduce cytokinins, a class of phytohormones that regulate many physiological processes including the expression of the *AtST4* gene subfamily in *A. thaliana*.

Since the substrate of *AtST4b* is a polyamine conjugate, we conclude this chapter by reviewing the biological significance of the accumulation of polyamines in plants.

1.2) Sulfotransferases

1.2.1) Introduction

SULTs catalyze the transfer of a sulfuryl group (SO_3) from the ubiquitous donor 3'-phosphoadenosine 5'-phosphosulfate (PAPS), which is the active form of inorganic sulfate, to an appropriate hydroxyl group of different substrates in a process called the sulfonation reaction (Fig. 1). These enzymes have highly conserved domains and are found across all kingdoms, from bacteria to plantae and animalia (Varin *et al.* 1997). The sulfonation reaction seems to be very important for life, because a defect in sulfate metabolism or sulfate transport lead to severe skeletal disorders and/or death in human and mouse (ul Haque *et al.* 1998; Rossi and Superti-Furga 2001).

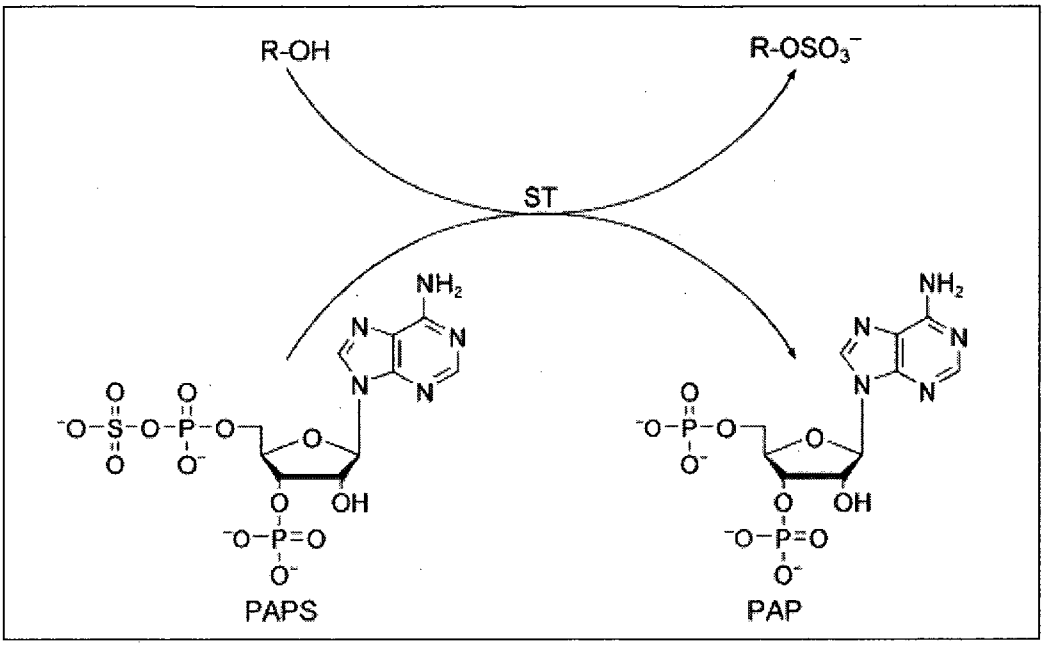

Figure 1. General sulfonation reaction catalyzed by SULTs (Chapman *et al.* 2004).

There are two classes of SULT proteins based on their cellular localization and function: membrane-associated SULTs and cytosolic SULTs. The membrane-associated SULTs are localized in the Golgi apparatus and catalyze the sulfonation of macromolecules such as proteins, peptides and complex carbohydrates. A large number of these enzymes catalyze the sulfonation of biological signaling molecules which are essential for life. Members of this class of enzymes have been characterized only from *Mimosa pudica* and *Oryza sativa* in plants, and are not the interest of this study. The so-called cytosolic SULTs or soluble SULTs sulfonate small organic molecules such as flavonoids, steroids, glucosinolates and hydroxyjasmonates (Honke and Taniguchi 2002; Hernàndez-Sebastiá *et al.* 2008).

The sulfonation reaction has different effects on a metabolite. The sulfated conjugate is more polar and water soluble than the original molecule, therefore the presence of a sulfate group might influence their transport and excretion. For example, mammalian

cytosolic SULTs play an important role in phase II of the biotransformation and excretion of xenobiotics in the liver (Weinshilboum and Otterness 1994; Yasuda *et al.* 2005). Sulfonation also modulates the biological activity of some metabolites such as steroids. For example, the sulfonation and desulfonation reactions are controlling the level of active estrogen in the blood of mammals. The sulfated estrogens are stored and eventually can be converted to the active hormone by sulfatases (Strott 1996). In contrast, the sulfonation can increase the biological activity of some metabolites. For example, the sulfonation of tyrosine residues on the chemokine receptor CCR5 (a principal HIV-1 co-receptor) is a modification that is required for its biological activity and indirectly facilitates entry of HIV-1 (Farzan *et al.* 1999).

In plants, SULTs are involved in the regulation of plant growth, defense and stress responses by the modulation of the biological activity of signal molecules and hormones. For example, it has been shown that the sulfonation of desulfoglucosinolates is required for the activation of their antimicrobial properties (Piotrowski *et al.* 2004; Klein *et al.* 2006). Moreover, the choline sulfate that accumulates under saline conditions is involved in salt or drought stress-tolerance in *Limonium* species and other plants of the Plumbaginaceae family (Klein and Papenbrock 2004). So far, the characterized plant cytosolic sulfotransferases are as follows:

The flavonol SULTs from *Flaveria* species (Varin *et al.* 1992; Varin *et al.* 1997), the choline SULT from *Limonium sativum* (Rivoal and Hanson 1994) and the brassinosteroid SULTs from *Brassica napus* (Rouleau *et al.* 1999; Marsolais *et al.* 2004). The cytosolic SULTs from *A. thaliana* are discussed in detail later in the text.

1.2.2) Sulfotransferase structure

The X-ray crystal structures of four mammalian cytosolic SULTs and one membrane-associated SULT show a globular structure composed of a single α/ß domain with five-stranded parallel ß sheet surrounded by α-helices (Negishi *et al.* 2001). The amino acid sequence alignment of plant and animal cytosolic SULTs revealed four conserved regions named region I to region IV. Using various approaches, the most important structural and functional features of SULTs have been identified:

- **The PAPS-binding region:** All SULTs contain conserved domains involved in PAPS binding (region I and region IV). The consensus amino acid sequence of the PAPS-binding regions of plant SULTs are PKxGTTWLKAL for region I and FRKGxVGDWK for region IV. The glycine-rich domain followed by the conserved lysine of region IV is a motif (GXXGXXK) that is found to be essential in some nucleotide binding proteins (Weinshilboum *et al.* 1997; Klein and Papenbrock 2004; Hernàndez-Sebastiá *et al.* 2008). The lysine residue from region I is required for the formation of the 5'-phosphosulfate loop (PSB loop). Also, the three amino acids RKG from region IV are involved in the formation of the 3'-phosphate binding loop (PB loop).
- **The catalytic binding region:** The crystal structure and site-directed mutagenesis studies have revealed the importance of conserved histidine, serine and arginine residues from region II and of a lysine residue from region I in the formation of an unstable ternary enzyme-PAPS-substrate complex and for the transfer of the sulfonate group to the substrate (Hernàndez-Sebastiá *et al.* 2008).

- **The substrate binding region:** The study of human and Flaveria flavonol SULTs have indicated two domains, in close proximity to region II, with high amino acid divergence. These domains are responsible for the substrate specificity of SULTs (Hernàndez-Sebastiá *et al.* 2008).

1.2.3) *Arabidopsis thaliana* Sulfotransferases

A. thaliana is a small flowering plant that is widely used as a model organism in plant biology. The genome of *A. thaliana* was completely sequenced in 2001 and provided useful information for biochemical and genetics studies of its over 26, 500 genes.

There are 18 SULT coding genes in *A. thaliana* based on sequence similarity to previously characterized SULTs. Of these, one (At3g51210) is a pseudogene that codes for a truncated protein, and seven have been fully characterized: Flavonoid SULT (At3g45070) (Gidda and Varin 2006), desulfoglucosinolate SULTs (At1g74100, At1g74090, At1g18590) (Piotrowski *et al.* 2004), hydroxyjasmonate SULTs (At5g07010) (Gidda *et al.* 2003) and brassinosteroid SULTs (At2g03760 and At2g14920) (Marsolais *et al.* 2004). The phylogenic tree of *A. thaliana* SULTs is shown in Figure 2.

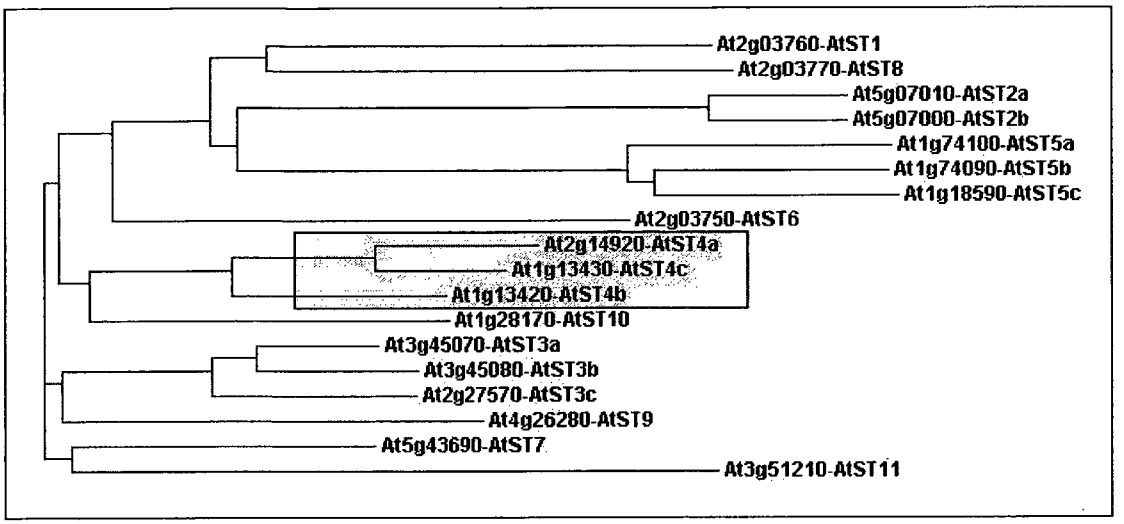

Figure 2. Phylogenic tree of *A. thaliana* SULTs. The respective amino acids sequences of 18 SULTs were grouped using the Clustal W program (http://www.ebi.ac.uk/Tools/clustalw2). The colored box indicates the *AtST4* subfamily and its members.

1.2.4) The *AtST4* subfamily

The *AtST4* subfamily is part of a family of plant SULTs designated as SULT203 (formerly SULT5), based on the recently proposed guidelines for sulfotransferase nomenclature (Blanchard *et al.* 2004). The *AtST4* subfamily contains three members: *AtST4a* (At2g14920), *AtST4b* (At1g13420) and *AtST4c* (At1g13430).

Molecular studies of the *AtST4* subfamily have shown that the three genes are expressed mainly in roots and are regulated by cytokinins (Marsolais *et al.* 2007). The *AtST4a* gene or SUL203A1 is located on chromosome 2 and is more related to *AtST4c* (80% amino acid sequence identity) than *AtST4b* (71% amino acid sequence identity). *AtST4a* has been characterized recently and was shown to code for a brassinosteroid SULT in *in vitro* studies (Marsolais *et al.* 2007). However, the presence of brassinosteroid sulfate has never been demonstrated *in vivo*. *AtST4b* and *AtST4c* are in tandem on chromosome 1.

Despite their high amino acid sequence identity with *AtST4a,* neither *AtST4b* nor *AtST4c* exhibited any activity with brassinosteroids (Marsolais *et al.* 2007).

1.3) Cytokinins

1.3.1) Introduction

Cytokinins (CKs) are a class of phytohormones that play critical roles at different stages of growth and development. The name cytokinin refers to the ability of these molecules to promote cell division and cytokinesis. Miller *et al.* identified the first CK, kinetin, from the autoclaved product of herring sperm DNA as a metabolite that had the ability to promote cell division (Miller *et al.* 1995).

CKs are adenine derivatives and classified based on the substitution on their N^6-side-chain as aromatic or isoprenoid CKs. Both aromatic and isoprenoid CKs are naturally occurring, but the latter is by far the most abundant in plants. The common isoprenoid CKs are; trans-hydroxylated N^6-side chain or *trans*-zeatin (*t*-zeatin), N^6-(Δ^2-isopentenyl) adenine (iP), dihydrozeatin (DZ) and *cis*-zeatin (*c*-zeatin) (Fig. 3A).

The relative abundance of different CKs depends on the plant species, tissue and developmental stages. For example *t*-zeatin is the most abundant CK in *A. thaliana,* whereas *c*-zeatin and its derivatives are the predominant CKs in chickpea seeds and male flower buds of *Mercurialis* (Mok and Mok 2001; Sakakibara 2006).

The aromatic CKs that occur naturally in plants are benzyladenine (BA), *ortho*-topolin and *meta*-topolin. They are not widely distributed and are found in a limited number of plant species (Fig. 3B). All natural CKs may also be present in the corresponding nucleoside, nucleotide and glycoside counterparts in the plant metabolome. There are

also some synthetic metabolites that possess cytokinin activity such as diphenylurea (DPU) but have not been found naturally in plants.

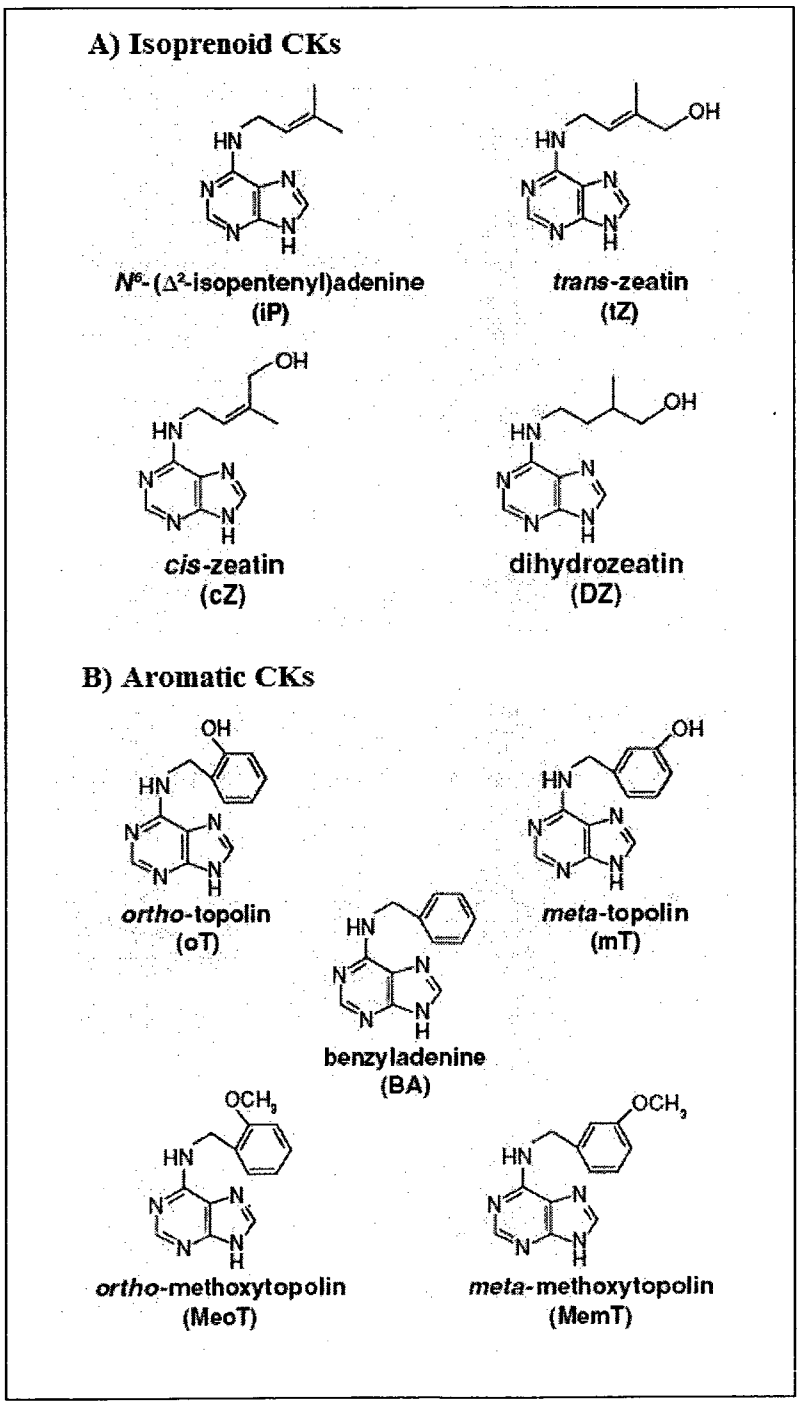

Figure 3. Structure of naturally occurring cytokinins. (A) Isoprenoid CKs, **(B)** Aromatic CKs (Sakakibara 2006).

1.3.2) Cytokinin perception and signal transduction

Since their discovery 50 years ago, scientists have tried to understand the mechanism by which CKs are sensed and perceived in the cell. Early after their discovery, scientists found that the sites of biosynthesis and action of CKs are spatially separated. Isolation of cytokinin-binding-proteins (CBPs) as CK receptors was not successful since none were shown to be a true receptor. With the advent of molecular biology, the mechanism of CK signaling became well understood. The discovery of histidine kinase receptors and downstream components indicated that plants use the two-component signaling system (TCS), initially discovered in bacteria, in the CK signal transduction pathway.

In the next section, the mode of action of TCS in prokaryotes and higher eukaryotes like plants is discussed, and then the components of this system in CK signaling in *A. thaliana* are explained.

1.3.3) Two-component system

Plants like bacteria utilize the two-component system (TCS) to sense and respond to their environment. Basically, TCS consists of two main components: the sensor kinase and the cognate response regulator (RR). The sensor histidine kinase is usually a membrane-bound protein that senses environmental stimuli. It consists of two domains: the "input domain" and the "transmitter domain". The input domain dimerizes upon binding of ligands and autophosphorylates the transmitter domain at a histidine residue (H) (Fig. 4A). This phosphate group is then transferred to the RR. Thus, the sensor histidine kinase directly modulates the activity of RRs in response to stimuli by phosphorylation (Chang and Stewart 1998).

The RR, which propagates the signal through the cytoplasm, consists of two domains: the "receiver domain" that receives the phosphate group on its conserved aspartate (D) residue, and the "output" domain that is not present in all response regulators and has DNA binding activity. Phosphorylation of the receiver domain results in a conformational change in the output domain that will eventually lead to transcription of special sets of genes (Fig. 4A).

The TCS is very well studied in prokaryotes. There are more than 40 different TCSs that have been identified in *Escherichia coli*. Compared to bacteria, plants use a relatively complicated system. They use a hybrid sensor kinase and a multistep phosphorelay cascade in which the phosphoryl group alternates between sequential histidine and aspartate residues of different substrates (Fig. 4B). This allows for longer-lasting signaling in cells in which different pathways can be involved in response to extracellular signals. The output of such complex responses probably leads to a better adaptation to environmental changes.

The components of such a pathway in the model plant *A. thaliana* comprise the Histidine Kinase receptors (AHKs), the Histidine Phosphotransmitter proteins (AHPs) and the Response Regulators (ARRs).

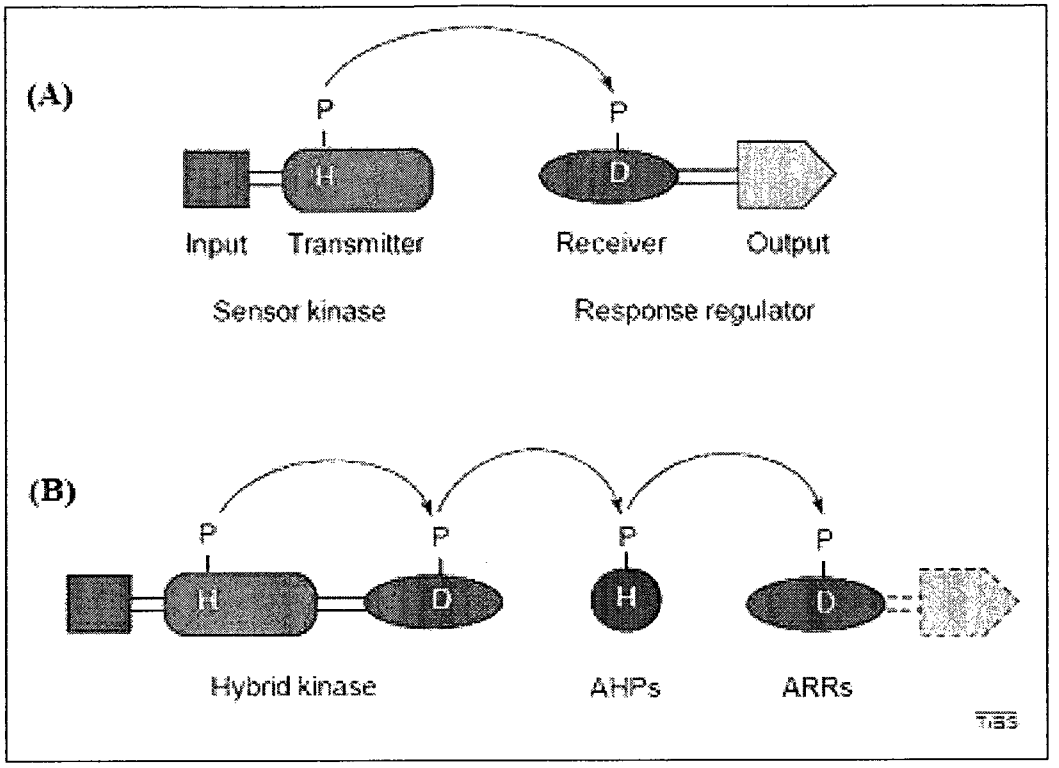

Figure 4. Schematics of two-component system in bacteria and plants (D'Agostino and Kieber 1999). **(A)** Basic prokaryotic two-component system. The input domain (red) is responsible for perceiving external stimuli and modulates the histidine kinase activity of the attached transmitter domain (green). Active sensor kinases act as dimmers. For the sake of simplicity, only a monomer of the sensor kinase is depicted. The phosphate is then transferred to a conserved aspartate residue (D) in the receiver domain (blue) of a cognate response regulator, which activates or inactivates the output domain (yellow). **(B)** The phosphorelay system in plants. The input domain of a hybrid kinase, regulates the activity of the transmitter domain by phosphorylation of its histidine residue. The phosphate is then transferred to an aspartate residue on the fused receiver domain and then to a histidine on an AHP protein (purple) and, finally, to an aspartate residue on an ARR protein. Abbreviations: AHP, Arabidopsis histidine phosphotransfer (HPt) proteins; ARR, Arabidopsis response regulator.

Arabidopsis Histidine Kinase Receptors (AHKs)

Kakimoto identified an Arabidopsis gene, *CKI1* that produces a cytokinin-independent phenotype in calli when overexpressed by transfer DNA (T-DNA) activation tagging. The CKI1 protein contains a sensor histidine kinase domain, a receiver domain, and two potential transmembrane domains in its structure. These characteristics together with the

phenotype of the mutant suggested that CKI1 is a cytokinin receptor (Kakimoto 1996). However, the binding of this protein to CKs has not been demonstrated yet.

The *CRE1/ WOL1/ AHK4* gene was later identified independently in different research studies as a cytokinin receptor coding gene from mutants that exhibited reduced sensitivity to cytokinins. Using forward genetics, Inoue *et al.* found that mutations in the *CRE1* (Cytokinin Response 1) gene produce a cytokinin-insensitive phenotype in Arabidopsis. The cre1 mutants were complemented by introduction of a functional *CRE1* gene. Moreover, expression of *CRE1* conferred a cytokinin-dependent phenotype when introduced in a yeast strain deficient in the endogenous *SLN1* histidine kinase gene (Inoue *et al.* 2001). Molecular and genetic evidences revealed that *CRE1* is allelic to *WOL1* (*WOODEN LEG 1*) and to *AHK4* genes. The *WOL1* gene was initially found to be required for proper formation of root vascular tissue (Mahonen *et al.* 2000).

Almost at the same time, Ueguchi *et al.* found the homologs of *CRE1* as a novel family of sensor histidine kinase genes based on amino acid sequence similarity to the transmitter domain of several sensor histidine kinases in *A. thaliana*. The members of the so-called AHK family (*AHK2*, *AHK3* and *AHK4*) were over 60% identical in the amino acid sequence of their transmitter and receiver domains, and they all encoded plasma membrane associated proteins. Among them, AHK3 and AHK4 were shown to bind directly to cytokinins using a yeast suppression assay (Ueguchi *et al.* 2001; Ueguchi *et al.* 2001). Binding of AHK4 to different types of cytokinins was further demonstrated using heterologous yeast and *E. coli* phosphohorelay systems (Suzuki *et al.* 2001; Yamada *et al.* 2001). Using protoplast transient expression analysis in the presence of cytokinins, all

three putative receptors were able to induce the expression of the *ARR6* promoter which is a cytokinin primary response gene (Hwang and Sheen 2001).

Furthermore, study of *AHK*s expression patterns and *AHK*s single, double and triple mutants revealed distinct, yet overlapping functions of the three receptors in regulating root and shoot growth (Higuchi *et al.* 2004; Nishimura *et al.* 2004; Riefler *et al.* 2006).

AHK1 and *AHK5* (*CKI2*) are also coding for transmembrane histidine kinases in Arabidopsis. However, their potential role in cytokinin signaling has not been demonstrated yet (Kakimoto 1996; Urao *et al.* 1999).

Arabidopsis Histidine Phosphotransmitter Proteins (AHPs)

Identification of sensor histidine kinases as cytokinin receptors suggested the presence of other components of the His-to-Asp phosphorelay system in *A. thaliana* including Histidine Phosphotransmitter proteins (AHPs) and Response Regulators (ARRs). There are at least five putative histidine phosphotransmitter coding genes in the *A. thaliana* genome (Miyata *et al.* 1998; Suzuki *et al.* 2000). AHPs act as cytoplasmic-nuclear shuttles and transfer the signals from AHK, which are mainly localized in the plasma membrane, to ARRs, which are mostly localized in the nucleus (Fig. 5). It was shown that some AHPs (AHP1 and AHP2) transiently translocate from cytoplasm to nucleus upon induction by cytokinins (Hwang and Sheen 2001). Additionally, the binding of AHPs to AHKs and type-B ARRs have been demonstrated using the *E. coli* phosphorelay system and the yeast two-hybrid system, respectively (Suzuki *et al.* 2001; Suzuki *et al.* 2001). Analysis of AHPs loss-of-function mutations indicates the positive and redundant function of these elements in cytokinin signaling (Hutchison *et al.* 2006).

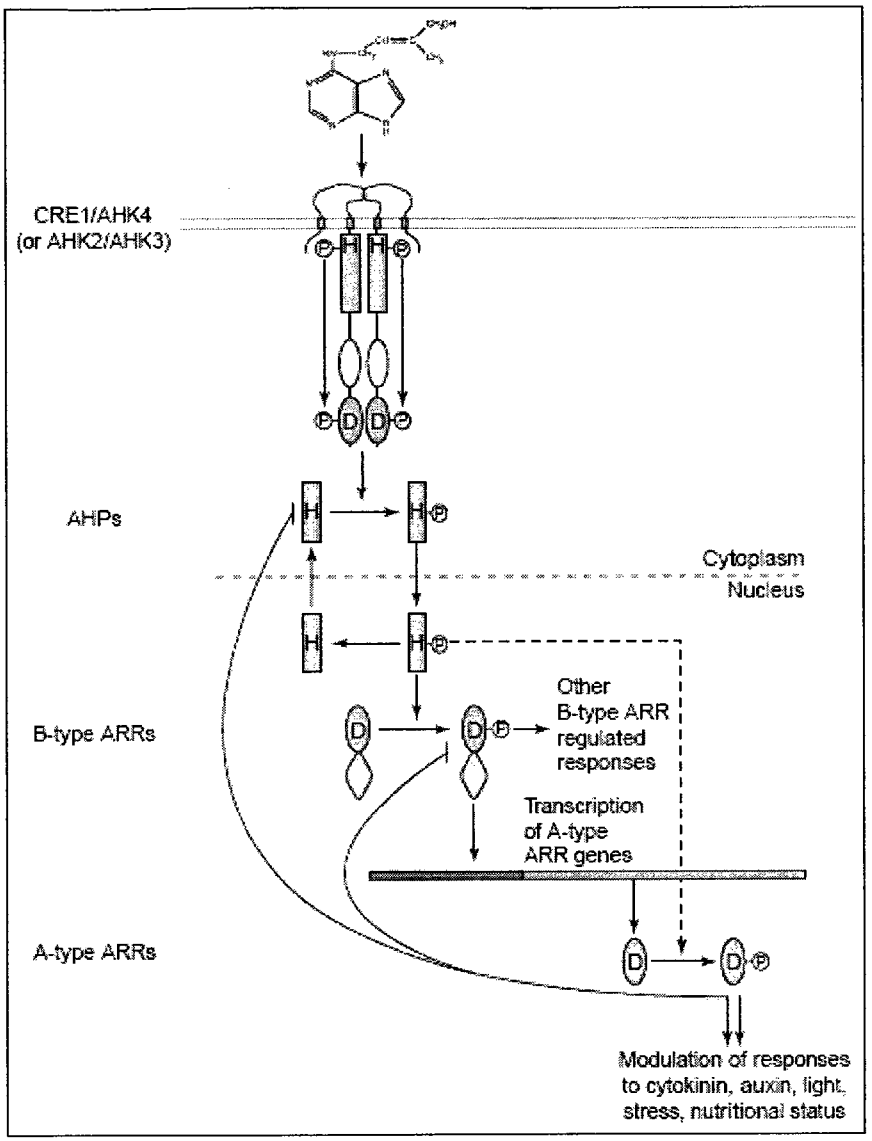

Figure 5. A model for cytokinin signal transduction through His-to-Asp phosphorelay (Heyl and Schmulling 2003). Ligand binding induces receptor dimerization and autophosphorylation. Transfer of the phosphoryl group by activated receptors activates AHPs which transport the signal from the cytoplasm to type-B ARRs in the nucleus. Type-B response regulators transcribe target genes, among them type-A ARR genes. Type-A response regulators may down-regulate the primary cytokinin signal response via a negative feedback loop. Abbreviations: D, aspartate residue, H, histidine residue, P, phosphoryl group.

Arabidopsis Response Regulators (ARRs)

The Response Regulators (ARRs) are the final components of the phosphorelay circuitry in plants. There are at least 22 ARR-coding genes in the Arabidopsis genome that contain

invariant DDK residues in their receiver domain, a hallmark that is also present in response regulators of prokaryotes and yeasts. Based on amino acid sequence similarity and protein structure, ARRs fall into two distinct classes: type-A and type-B. Most of type-A ARRs lack the output domain at their C-terminal ends and show rapid induction upon treatment with cytokinins. In contrast, type-B ARRs contain an extended C-terminal domain having the characteristics of transcriptional activators and their expression is not influenced by cytokinins.

Type-A ARRs: (*ARR3-ARR9, ARR15-ARR17* and *ARR22*): The 11 members of type-A ARRs are mainly composed of a receiver domain with a short extension at their C-terminus (less than 100 amino acids). Their receiver domains are more closely related to each other (60-93% identical in amino acid sequence) than the receiver domain of type-A and type-B ARRs (which are less than 30% identical in amino acid sequence). Type-A ARRs are known as "primary response genes" since their transcript level is rapidly and transiently induced by cytokinins (within 10 minutes). This induction is insensitive to protein synthesis inhibitors (such as cycloheximide) and is specific for cytokinins (D'Agostino *et al.* 2000). Type-A ARRs are located either in the cytoplasm or the nucleus and their transcripts are present in all parts of the plant (Heyl and Schmulling 2003). Most of the type-A ARRs are negative regulators of the cytokinin signaling pathway (Hwang and Sheen 2001; To *et al.* 2004; Lee *et al.* 2007).

Type-B ARRs: (*ARR1, ARR2, ARR10-ARR14*, and *ARR18-ARR21*): Type-B ARRs have a receiver domain and a large carborxy-terminal output domain (250-260 amino acids). The presence of a nuclear localization signal domain (NLS), a GARP DNA-binding domain (or B-motif) and a proline/glutamine-rich domain in the C-terminal

region of all type-B ARRs indicates that they act as transcriptional activators (D'Agostino and Kieber 1999). Recently, a core DNA sequence motif (G/A)GAT(T/C) was identified to be bound by type-B ARRs and be present in the upstream region of most of type-A ARR promoters and putative cytokinin-induced genes (Sakai *et al.* 2000; Rashotte *et al.* 2003).

Studies of several type-B ARR mutant lines suggest distinct but also redundant functions among type-B ARRs (Imamura *et al.* 2003; Tajima *et al.* 2004). The exogenous application of cytokinins does not alter the transcription of type-B ARRs (Imamura *et al.* 1999; Kiba *et al.* 1999).

The expression pattern of different components of the TCS in *A. thaliana* is illustrated in Fig. 6.

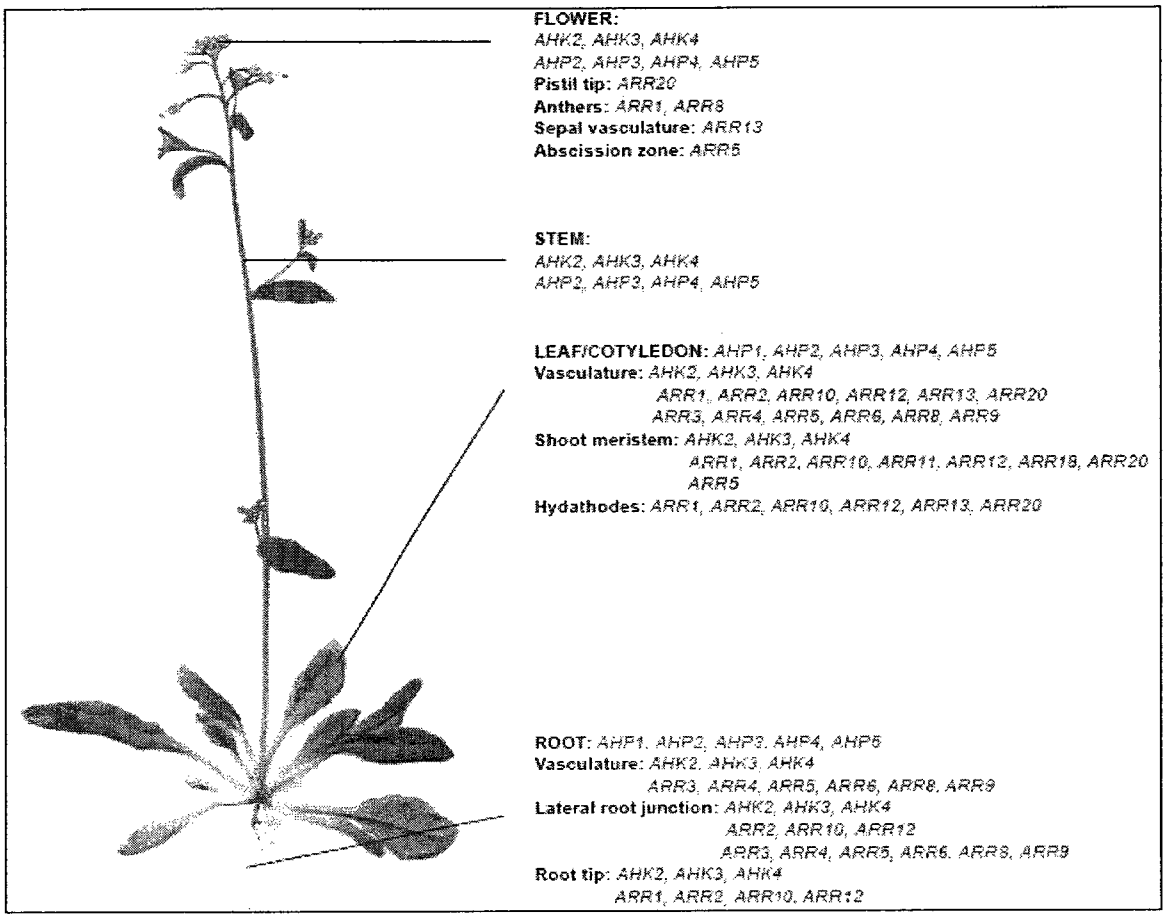

Figure 6. General expression pattern of Arabidopsis cytokinin two-component signaling components (Ferreira and Kieber 2005).

1.3.4) Physiological responses to cytokinins

Cytokinins are involved in many plant growth and developmental processes. In the following section, we first discuss the main downstream target genes which are regulated through the cytokinin signaling pathway. Then, we review the available microarray data showing the cytokinin regulation of the members of *AtST4* subfamily in *A. thaliana.*

Cytokinins and cell division

The cytokinin role in cell division and proliferation was first documented in the 1950s (Miller *et al.* 1995). In 1999, *CycD3* (a member of a D-type cyclin gene family involved

in the G1 to S transition of the cell cycle) was found to be up-regulated in Arabidopsis mutants with high levels of endogenous cytokinins and to be rapidly induced by the exogenous application of cytokinins (Riou-Khamlichi *et al.* 1999). This induction was cycloheximide independent. Moreover, transgenic cells overexpressing the *CycD3* gene were cytokinin independent when grown *in vitro*. Altogether, these results suggest that cytokinins regulate cell cycle progression at the G1-S transition through the positive regulation of *CycD3* expression.

Cytokinins and shoot development

The exogenous application of cytokinins induces shoot formation from calli grown *in vitro*. The analysis of Arabidopsis loss-of-function and gain-of-function mutants with altered cytokinin levels has confirmed the positive role of cytokinins on shoot development. Reduced cytokinin content in the cytokinin-receptor triple mutant (*ahk2,3,4*) and cytokinin-oxidase overexpressor lines (35s::CKXs) resulted in reduced size of shoot apical meristem (SAM), retarded leaf formation and reduced cell production in leaves (Werner *et al.* 2001; Werner *et al.* 2003; Higuchi *et al.* 2004; Nishimura *et al.* 2004). Furthermore, increased levels of cytokinins in transgenic plants overexpressing the bacterial cytokinin biosynthesis gene, isopentyl transferase (*IPT*), led to ectopic shoot formation, reduced apical dominance and increased mesophyll cell layers in leaves. The gene expression studies showed induction of *KNOTTED1* and *STM* homeobox genes in these plants, as well. The *KNOTTED1*-like homeobox genes are expressed exclusively in the SAM and are involved in its development and maintenance (Rupp *et al.* 1999). Moreover, the defect of a recently identified cytokinin biosynthesis enzyme in rice resulted in pre-mature termination of shoot meristem (Kurakawa *et al.* 2007).

Cytokinins and senescence

Leaf senescence is defined as an aging process that is accompanied with the degradation of chlorophyll and photosynthesis proteins. It is a complex mechanism that occurs at final stages of leaf growth and is controlled by many factors. It was shown that cytokinins delay leaf etiolation and senescence (Wingler *et al.* 1998). Overexpression of the cytokinin biosynthesis gene, *IPT,* under the control of a senescence-specific gene promoter delayed senescence in transgenic tobacco (Gan and Amasino 1995). How cytokinins regulate senescence at the molecular level is not known yet, but mutational studies of cytokinin signaling components indicate a primary role for *AHK3* and *ARR2* (a type-B ARR) in this process (To and Kieber 2008).

Cytokinins and root development

In contrast to their promotional role in shoot development, cytokinins reduce root meristem size and inhibit primary root elongation and lateral root formation. Mutants with reduced cytokinin sensitivity (*ahk3* and *arr1,12*) develop an enlarged root meristem and a longer primary root (Dello Ioio *et al.* 2007). Furthermore, cytokinin-deficient mutants that overexpress cytokinin oxidase exhibited an overall enhanced root system (Werner *et al.* 2001; Werner *et al.* 2003). However, reduced cytokinin perception in the receptor triple mutant (*ahk2,3,4*) and in the phosphotransmitter quintuple mutant (*ahp 1,2,3,4,5*) resulted in reduced root development. This implies that although cytokinins have a negative regulatory effect in root development, a certain level of cytokinins is needed for proper root formation. Support for this hypothesis comes from molecular and genetic analysis of the *WOODEN LEG* (*WOL*, an allele of *AHK4/CRE1)* mutant. It was shown that the *wol* mutant develops short roots with fewer embryonic vascular tissues

that give rise only to protoxylem tissue. Interestingly, the defect in root vasculature was complemented by exogenous cytokinin application, indicating a cytokinin requirement for root vascular tissue formation and development (Mahonen *et al.* 2000; Mahonen *et al.* 2006).

Cytokinins and the *AtST4* subfamily

As we have seen, cytokinins play an important role in many physiological and developmental processes in plants. Regulation of these processes requires changes in the expression of cytokinin responsive genes. Many genome-wide microarray analyses have been performed in order to discover the genes downstream of the cytokinin signaling pathway. A review of these studies reveals that members of *AtST4* subfamily are regulated by cytokinins in *A. thaliana.*

Study of genome-wide gene expression of transgenic *A. thaliana* seedlings that carry the bacterial cytokinin-biosynthesis gene (*IPT*) under the control of a chemically inducible promoter showed up-regulation of *AtST4b* (At1g13420) transcript 6 hours and 24 hours after *IPT* induction (Hoth *et al.* 2003).

In the combinational microarray analysis performed by Kiba *et al.*, the *AtST4b* transcript was increased up to 7.3-fold in 21-day old wild type Columbia (Col) seedlings treated for 3 hours with the cytokinin *t*-zeatin. In this study, the *AtST4b* transcript was also up-regulated 11.3-fold in the absence of cytokinin treatment in a transgenic line overexpressing *ARR21* (a type-B ARR) as compared to wild type plants. These results are interesting because based on the kinetics and level of induction, the authors have categorized *AtST4b* as one of the genes that is up-regulated rapidly and specifically by

cytokinins in a manner similar to that of the type-A ARR genes, which are hallmarks of the two-component phosphorelay system (Kiba *et al.* 2005).

Microarray analysis performed on roots of two-week old seedlings of Columbia 0 (Col-0) and *arr10/arr12* double mutant (type-B ARRs) shows that even though *AtST4b* is induced in both cytokinin-treated wild type and mutant line, the level of *AtST4b* induction is attenuated in the mutant line as compared to the wild type plants. These results suggest that ARR10 and ARR11 act as positive regulators of the downstream *AtST4b* gene (Yokoyama *et al.* 2007).

Using genome-wide expression profiling, Brenner *et al.* classified immediate-early (15 min) and delayed (120 min) cytokinin response genes in *A. thaliana.* They also analyzed gene expression in cytokinin deficient transgenic line (35S:AtCKX1). Surprisingly, *AtST4b* is not among the genes whose transcripts have been changed by the exogenous application of cytokinins in wild type and the 35S:AtCKX transgenic line. However, the available data indicates the repression of *AtST4b* transcript in cytokinin oxidase overexpression line compared to wild type plants (Brenner *et al.* 2005).

As mentioned earlier, type-A ARRs are generally negative regulators in the cytokinin signaling circuitry. In order to investigate the downstream components of type-A ARRs, Lee *et al.* produced a transgenic line overexpressing *ARR7* (type-A ARR). Analysis of microarray data showed that *ARR7* overexpression has a distinctively repressive impact on various groups of cytokinin-regulated genes. In particular, the expression of all type-A ARRs (except for *ARR22*), *AHK1* and *AHK4*, most of the cell expansion genes and the cytokinin oxidase genes were repressed in the *ARR7* overexpression line. Surprisingly, regulation of *AtST4b* gene was positively affected by *ARR7.* These results showed that

expression of *AtST4b* is not only up-regulated by cytokinins after 30 min and 2 hours treatment in wild type plants, it is also induced in *ARR7* overexpression line by cytokinin treatments. The high levels of induction in the overexpressor line indicate the great impact of *ARR7* on *AtST4b* regulation.

In the Affymetrix full genome array, the same probe set represents both the *AtST4a* and *AtST4c* genes making it impossible to differentiate these two genes. Based on the GeneChip analysis performed by Lee *et al.* (as opposed to *AtST4b*), the expression of *AtST4c* (and/or *AtST4a*) was repressed by the exogenous application of cytokinins in both wild type and ARR7 overexpressor line (Lee *et al.* 2007).

1.4) Polyamines

Polyamines (PAs) are low molecular weight, nitrogen-containing cationic compounds that are found in almost all organisms. Due to their positive charge, PAs can bind directly to RNA, DNA, nucleotide triophosphates and proteins, and in some cases can modulate their function. PAs play important roles in the regulation of gene expression, modulation of certain ion channels, cell proliferation, programmed cell death or apoptosis, ribosome biogenesis, protein synthesis, membrane rigidity and embryonic development (Igarashi and Kashiwagi 2000; Thomas and Thomas 2001; Kusano *et al.* 2008). The major polyamines in plants are putrescine, spermidine and spermine. The biosynthesis of polyamines in plants is initiated by decarboxylation of the amino acid arginine to form the diamine putrescine. Putrescine is then converted to the triamine spermidine and the tetraamine spermine through the sequential addition of aminopropyl residues (Kusano *et al.* 2007) (Fig. 7). Intracellular PA content is modulated through a complex circuitry of biosynthesis, degradation, cellular uptake and efflux. These mechanisms are controlled

by different enzymes and are tightly regulated to maintain PA homeostasis. The study of loss-of-function and gain-of-function mutation of these genes has confirmed the importance of PAs in plant growth and development. Studies by Imai *et al.* showed that even though spermine is not essential for the survival of Arabidopsis, suppression of the genes coding for the enzymes involved in spermidine biosynthesis (*SPDS1* and *SPDS2*) either by T-DNA insertion or RNA interference is lethal in Arabidopsis and results in embryonic arrest in double mutant seeds (Imai *et al.* 2004; Imai *et al.* 2004). A double mutation of the two putrescine biosynthesis genes (*ADC1* and *ADC2*) leads to a similar developmental defect in the embryo of Arabidopsis (Urano *et al.* 2005). Moreover, overexpression of oat ADC in tobacco resulted in increasing endogenous putrescine levels and toxic phenotypes such as necrosis and dwarfism (Panicot *et al.* 2002). Altogether, these data indicate that putrescine and spermidine are essential for plant growth and embryogenesis, while spermine is not essential for normal growth in Arabidopsis. Furthermore, based on the spermidine biosynthesis pathway and requirement of putrescine for spermidine biosynthesis, it is probably the lack of spermidine that leads to embryonic defects in putrescine biosynthesis mutants.

PAs can be conjugated with a variety of compounds by formation of an amide linkage. In animals, acetylation by spermidine/spermine aceylteransferase (*SSAT*) reduces the positive charges of PAs and their biological activity (Pegg 2008). In plants, however, the acylated conjugates of PAs play an important role in growth and development. A group of these polyamine-based alkaloids are referred as hydroxycinnamic acid amides (HCAAs) and formed by the addition of an acyl moiety (hydroxycinnamic acid in this case) to the acceptor molecules (polyamines) in presence of BAHD acyl transferase

(named after the first letters of the first characterized members of the family; BEAT, AHCT, HCBT and DAT) (D'Auria 2006). The hydroxycinnamoyl component can be replaced with coumaroyl, caffeoyl, hydroxyferuloyl or sinapoyl acyl groups. HCAAs are widely distributed in plants and implicated in several growth and developmental processes such as germination, cell division, flower formation, cell wall formation, as well as stress and defense responses (Facchini *et al.* 2002). For example, Luo *et al.* have characterized two sinapoyl spermidine derivatives that accumulate largely in seeds of Arabidopsis and seem to act as polyamine reserve during germination (Luo *et al.* 2009). Such a storage role for polyamine conjugates have previously been reported in rice seeds, as well (Bonneau *et al.* 1994). Luo *et al.* have also identified a gene coding for spermidine dicoumaroyl transferase (*SCT*) that is specifically expressed in the root tip and induced by cytokinins (Luo *et al.* 2009). Based on its site of expression and induction by cytokinins, the authors have assigned a role in cell division for the *SCT* in roots. Furthermore, spermidine conjugates in the pollen coat of Arabidopsis are responsible for its shape and autofluorescence (Grienenberger *et al.* 2009). Interestingly, a DNA-UV protective function have been suggested for cinnamoyl-derivatized spermidines that accumulate in the pollen (Bienz *et al.* 2005).

In addition to their roles in plants, HCAAs are representing an important class of antioxidant and chemotherapeutic agents that have the potential to be used in the treatment of human diseases and as insecticides (Klose *et al.* 2002; Park and Schoene 2006; Russo *et al.* 2007).

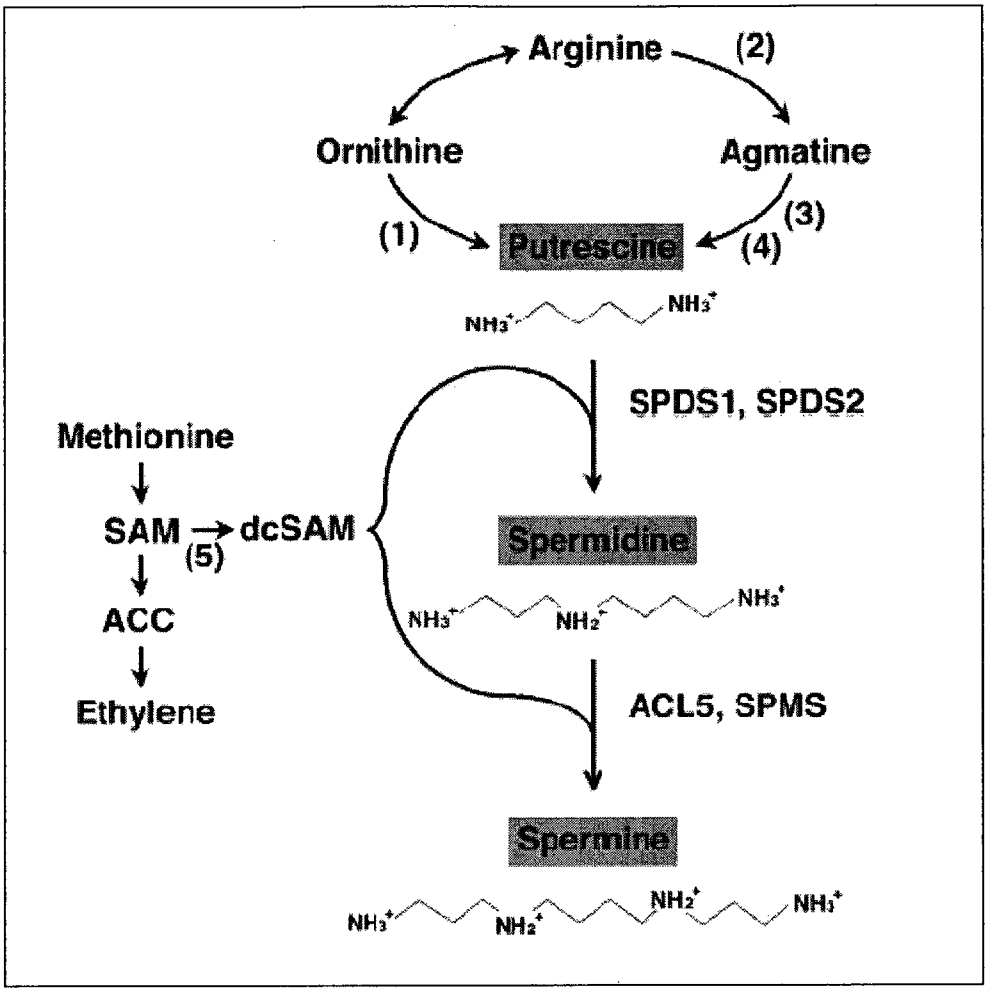

Figure 7. Polyamine biosynthesis pathway in plants (Imai et al. 2004). Enzymes shown in numbers are (1) ODC (ornithine decarboxylase) (2) ADC (arginine decarboxylase) (3) agmatine iminohydrolase (4) N-carbamoylputrescine amidohydrolase and (5) SAMDC (S-adenosylmethionine decarboxylase).

1.5) Purpose of the present study

Based on previous genetic studies and microarray analyses, three SULT-coding genes (*AtST4a*, *AtST4b* and *AtST4c*) were found to be expressed exclusively in roots and regulated by cytokinins in *A. thaliana*. *AtST4a* has been previously partially characterized and was shown to encode a brassinosteroid SULT in *in vitro* studies. The purpose of the present study was to characterize the biochemical and biological function of the other members of the *AtST4* subfamily. To further investigate the role of cytokinins on the

regulation of *AtST4a, -4b* and *-4c* expression, we analyzed their expression in roots of wild type Arabidopsis at different time points following treatments with *t*-zeatin.

The best way to study the function of a gene is to study the phenotype of plants that are lacking it. Therefore, homozygous *AtST4a*, *AtST4b* and *AtST4c* T-DNA insertion mutants were isolated and subjected to a number of metabolic and phenotypic analyses. To identify the biochemical function of *AtST4a, -4b* and *-4c in vitro*, their coding sequence was expressed in *E. coli* and their enzyme activity was tested using radioactive PAPS and purified plant metabolites. Using High Performance Liquid Chromatography (HPLC), neutral loss mass spectrometry and liquid chromatography-tandem mass spectrometry (LC-MS/MS) analyses, we were able to characterize the substrate of *AtST4b*. Finally, the consequence of changing the sulfated metabolome of *AtST4*a, *AtST4b* and *AtST4c* single mutants was analyzed by monitoring a number of growth parameters known to be under the control of cytokinins. The results of these investigations are presented in the next chapters.

Chapter 2- Materials and Methods

2.1) Materials

Seeds of wild type *A. thaliana,* ecotype Columbia 0 (Col-0) were obtained from Lehle seeds (USA). The Arabidopsis lines carrying a T-DNA insertion allele for *AtST4a* (GABI_177E08) and *AtST4b* (GABI_231G06) were obtained from Gabi-Kat (http://www.gabi-kat.de/), and *AtST4c* (FLAG_334F06) from INRA (http://www.inra.fr/). All the mutant lines were generated in a Col-0 background.

2.2) Methods

2.2.1) Plant growth conditions

The Arabidopsis plants were grown either in soil or on vertical petri dishes containing full-strength Murashige and Skoog (MS) medium (1% sucrose, 0.4% Gelrite, 0.05% MES, PH 5.7) under long day conditions (16 hours light/8 hours dark) at a light intensity of ~130 $\mu mol\ m^{-2}s^{-1}$. The temperature was kept at 20 °C during night-time and gradually increased to 22 °C during day-time.

2.2.2) Seed sterilization

The Arabidopsis seeds were sterilized by a 30 seconds immersion in 70% ethanol, 5 minutes shaking in a mixture of 10% bleach and 0.02% SDS solution and several times rinsing with sterile distilled water. The seeds were then vernalized by keeping them 2-4 days at 4°C in dH_2O before planting.

2.3) Regulation studies of the *AtST4* subfamily

2.3.1) Transcript expression study of the *AtST4* subfamily in response to cytokinins

For transcript expression analysis, 16-day-old plants were sprayed with 20 μM *t*-zeatin dissolved in 50% dimethylsulfoxide (DMSO) for 30 minutes, 2 hours, 4 hours and 6 hours. RNA samples were extracted from root tissue using the RNeasy Plant Mini Kit (Qiagen). For reverse transcription polymerase chain reaction (RT-PCR) experiments, 2 μg of total RNA was treated with 2 μl Expand Reverse Transcriptase Buffer 5x (Roche) and 0.2 μl DNase I 40 U/μl (Roche). The volume was adjusted to 20 μl using DEPC-treated water. The reaction was incubated 15 minutes at room temperature, followed by the addition of 2 μl of 30 mM EDTA. DNase I was heat-inactivated at 65°C for 10 minutes and tubes were put on ice for 2 minutes and centrifuged for a short time. Following DNase I treatment, 8 μl of 50 μM Oligo dT (15 mers) was added to each reaction. Then, the tubes were incubated 10 minutes at 65°C, put on ice for 2 minutes and centrifuged for a short time. A mix of 10 μl Expand RT Buffer 5x (Roche), 5 μl dTT (100 mM), 2 μl dNTP (25 mM), 2 μl Expand Reverse Transcriptase 50 U/μl (Roche) was added to each reaction, followed by 60 minutes incubation at 43°C. The synthesized cDNAs were then used in PCR reactions.

The absence of genomic DNA contamination was verified by PCR using the *Actin* primers which span introns of 8 *Actin* genes. Furthermore, the *Actin* genes were used as internal control for RNA calibration. The volumes of cDNA, used as template for PCR, were adjusted after a preliminary calibration based on the levels of *Actin* PCR products. The following thermocycling program was used: initial denaturation at 94°C for 2 minutes, followed by the specified number

of cycles at 94°C for 30 seconds, 55°C for 45 seconds (except for Actin at 60°C), and 72°C for 1 minute, and a final extension at 72°C for 5 minutes.

The following primers were used:

Actin-F (5'-GCTGATGGTGAAGACATTCA-3')

Actin-R (5'-CATAGCAGGGGCATTGAAAG-3')

AtST4a-F (5'-CGGGATCCATGGATGAAAAAGATAGACCAA-3')

AtST4a-R (5'-GGGGTACCTTAGAATTTCAA-3')

AtST4b-F (5'-TGCCATGGGTGAGAAAGATATTCCA-3')

AtST4b-R (5'-CGGGATCCCTACAATTTCAAACCAGAGCC-3')

AtST4c-F (5'- CGCTTAAACTACCCTTGAAG-3')

AtST4c-R (5'-AGAACAAAAACCACACATCA-3')

The primers were used at a concentration of 0.4 μM.

2.4) Molecular characterization of T-DNA insertion mutants

2.4.1) Genomic DNA extraction

The genomic DNA was extracted from leaf tissue of at least 20 individual plants according to the Extract-N-Amp plant PCR kit (Sigma-Aldrich).

2.4.2) Screening for T-DNA insertion mutants

The wild type *AtST4a, AtST4b* and *AtST4c*, and their knockout alleles were identified by means of polymerase chain reaction (PCR) using the following primers.

- The wild type *AtST4a* allele was identified using the following primers in PCR:

  AtST4a-F (5'-GGACCCGCTTCAAGTACC-3')

  AtST4a-R (5'-TCAATTTTGTCTACCATTTCAGG-3')

The AtST4a-R in combination with Gabi-Kat LB (5'-ATATTGACCATCATACTCATTGC-3') was used for detection of *AtST4a*-KO allele.

- The wild type *AtST4b* allele was identified using the following primers in PCR:

  AtST4b-F (5'-CTCTTATGCCACCAAATACAAG-3')

  AtST4b-R (5'- CGGGATCCCTACAATTTCAAACCAGAGCC-3')

  The AtST4b-R in combination with Gabi-Kat LB (5'-ATATTGACCATCATACTCATTGC-3') was used for detection of the *AtST4b*-KO allele.

- The wild type *AtST4c* allele was identified using the following primers in PCR:

  AtST4c-F (5'-CGCTTAAACTACCCTTGAAG-3')

  AtST4c-R (5'- AGAACAAAAACCACACATCA-3')

  The AtST4c-F in combination with INRA LB (5'-CTACAAATTGCCTTTTCTTATCGAC-3') was used for detection of the *AtST4c*-KO allele.

10-15 ng of genomic DNA was used as a template in all PCR reactions. In all cases, the *actin* gene was used as a positive internal control. The thermocycling program was as follows: initial denaturation at 94°C for 2 minutes, followed by 37 cycles at 94°C for 45 seconds, 55°C for 1 minute (except for AtST4a at 58°C), and 72°C for 1 minute, and a final extension at 72°C for 7 minutes. The PCR was performed using Ex Taq DNA polymerase (Takara Biomedicals).

2.4.3) RT-PCR analysis of T-DNA insertion mutants

The two-week old wild type and mutant plants were either treated with 20 μM *t*-zeatin for 2 hours or mock treated. The RNA was extracted from root tissue using the RNeasy Plant Mini Kit (Qiagen) and cDNA was generated as explained in section 2.3.1. The resulting cDNAs were used as template for knockout confirmation analysis. The following gene specific primers were used in PCR:

AtST4a-F (5'-GGACCCGCTTCAAGTACC-3')

AtST4a-R (5'-TCAATTTTGTCTACCATTTCAGG-3')

AtST4b-F (5'-ATGGGTGAGAAAGATATTCCA-3')

AtST4b-R (5'- CTACAATTTCAAACCAGAGCC-3')

AtST4c-F (5'-CGCTTAAACTACCCTTGAAG-3')

AtST4c-R (5'-AGAACAAAAACCACACATCA-3')

Actin-F (5'- GCTGATGGTGAAGACATTCA-3')

Actin-R (5'-CATAGCAGGGGCATTGAAAG-3')

The PCR program was as follows: initial denaturation at 94°C for 2 minutes, followed by specific number of cycles at 94°C for 45 seconds, 55°C for 1 minute (except for AtST4a at 58°C and Actin at 60°C), and 72°C for 1 minute, and a final extension at 72°C for 7 minutes.

2.5) Phenotype analysis of mutant plants

2.5.1) Root growth analysis

Seedlings of wild type and Arabidopsis mutants were grown vertically on MS media. The length of the primary root was marked on the petri dishes at around the same time every

day within the 10 days after germination (DAG) and measured by a ruler. The emerging lateral roots were counted using a Nikon dissecting microscope (Nikon SMZ1500). The plants were photographed 7 DAG with a Nikon D70 camera.

2.5.2) Determination of rosette diameter, seed size, seed and silique number

Rosette diameter and number of leaves of soil-grown plants were determined 14, 21 and 26 days after germination (DAG). For each plant, two measurements of rosette diameter were taken with a ruler, and the average of the two values was used for data analysis.

Seed size of wild-type, *AtST4b* and *AtST4c* mutant lines were determined measuring the length and width of 40 seeds. The volume was estimated based on formula of volume = 4/3 X π X length X width X depth (Riefler *et al.* 2006). The number of seeds per silique was counted for 30 mature siliques of each genotype. The number of siliques was measured 36 and 46 DAG.

2.5.3) Statistical analysis

Data analysis was performed using the PASW Statistics 18 (formerly known as SPSS) software. Since the data were not generally suitable for parametric statistics, comparisons of means from multiple groups were analyzed by the Kruskal-Wallis test. If this test found a significant effect, the differences between each of independent mutant groups and wild type group were analyzed by the Mann-Whitney U. When the data were suitable for parametric analysis, we compared two groups using two-independent-sample test (t-test). A P value of 0.05 or less was considered significant in all cases.

2.6) Enzymology

2.6.1) Expression and purification of recombinant enzymes in *E. coli.*

The coding sequences of *AtST4a*, *AtST4b* and *AtST4c* were previously cloned in a bacterial expression system (pQE-30, Qiagen) and transformed in *E.coli* strain XL1-blue. A culture of *E. coli* harboring *AtST4a, -4b* and *-4c* ($O.D_{600} = 0.7$) was induced with 1mM isopropylthio-β-D-galactopyranoside (IPDG) for 10 hours at 22^0C. Bacterial cells were collected by centrifugation and resuspended in lysis buffer (50mM sodium phosphate, 0.3M NaCl, 10mM imidazole and 14 mM ß-mercaptoethanol, pH 8.0). The cells were lysed by sonication, and the recombinant proteins were recovered in the soluble fraction by centrifugation at 13,000 rpm for 20 minutes at 4^0C. The soluble recombinant proteins were purified by affinity chromatography onto a nickel-nitrolotriacetic acid agarose matrix (Qiagen) under native condition. Protein concentration was estimated using the Bradford Reagent (Bio Rad) and bovine serum albumin as a reference protein. To verify the solubility and evaluate the level of purity of the recombinant proteins after chromatography, aliquots were subjected to 12% polyacrylamide gel electrophoresis according to the method of Laemmli. The proteins were visualized by 15 minutes staining in 0.1% Coomassie Blue. The gel was later destained with several changes of 40% methanol and 10% of acetic acid for removal of the background coloration.

2.6.2) Sulfotransferase assays

The reaction mixture (50 μl) contained 50 pmol [^{35}S] PAPS (NEN Life science products, Boston, MA), 5μl of hydrolyzed metabolite extract (dissolved in 50% methanol) and approximately 2 μg of the recombinant enzyme preparation (extracted in 50 mM Tris-Cl,

pH 7.5). The reactions were allowed to proceed for 10 minutes at 22°C and then stopped by the addition of 10 μl 2.5% acetic acid. The sulfated enzymatic product was extracted in ice-cold n-butanol and an aliquot was counted for radioactivity using a liquid scintillation counter. The remaining fraction was lyophilized for product identification by high performance liquid chromatography (HPLC), thin layer chromatography (TLC) and mass spectrometry.

2.6.3) Preparation of *Arabidopsis thaliana* extracts for the detection of the endogenous substrate

Roots of 16 day-old *A. thaliana* plants grown vertically on MS media were ground to a fine powder in liquid nitrogen, and the powder was homogenized in 50% methanol (approximately 3 ml/g of plant tissue) for 1 hour. Methanol was evaporated and the aqueous phase extracted with 1:1 volume of n-butanol. The butanol extract was lyophilized and resuspended in 50% aqueous methanol. To release the endogenous substrate, the extract was hydrolyzed in 0.1N HCl by boiling at 98°C for 10 minutes and subsequently neutralized in 0.1N NaOH. This fraction was tested directly as substrate for enzymatic assays or purified on a Novapak C_{18} reverse phase column equilibrated with solvent A (0.05% acetic acid in water) using a Waters 625 LC HPLC system. The column was washed for 5 minutes in 100% solvent A. Metabolites were eluted with a linear gradient of solvent A into solvent B (100% methanol, 0.05% acetic acid) in 50 minutes, followed by 10 minutes in 100% solvent B at a flow rate of 0.5 ml/min. Fractions of 0.5 ml were collected and assayed for activity with the recombinant enzymes. The fractions exhibiting the highest activity were selected and assayed to get enough purified products for HPLC, TLC and mass spectrometry.

2.6.4) Preparation of *Arabidopsis thaliana* extracts for the detection of the endogenous enzymatic products

Approximately 100,000 dpm of ^{35}S-labeled sulfate product (dissolved in 100 µl of 50% methanol) produced according to the protocol described in section 2.6.3, was fractionated on a Novapack C_{18} reverse phase column equilibrated with solvent A (0.05% acetic acid and 5 mM ammonium acetate in water) using a Waters 625 LC HPLC system. The column was washed for 5 minutes in 100% solvent A. Plant metabolites were eluted with a linear gradient of solvent A into solvent B (100% methanol, 0.05% acetic acid and 5 mM ammonium acetate) in 50 minutes, followed by 10 minutes in 100% solvent B at a flow rate of 0.5 ml/min. Fractions of 0.5 ml were collected and counted for radioactivity using a liquid scintillation counter. Using the same conditions, 1 gram of non-hydrolyzed, non-radiolabeled root extract from wild type and mutant plants were purified on the HPLC system. The fractions corresponding to the elution time of the radioactive product were lyophilized and redissolved in 100 µl 50% methanol for mass spectrometry analysis.

2.6.5) Mass spectrometry

Electrospray ionization tandem mass spectrometry (ESI-MS/MS) was used for analysis of the HPLC-purified product of wild type and T-DNA insertion mutant lines. Data acquisition and evaluation was performed using the Masslynx software. The catalyzed reaction products were analyzed using neutral loss scan in the negative and positive mode in search of a parent ion which gives a neutral loss of 80 mass unit (mass of sulfuryl group). The analyses were preformed on a Quattro triple quadrupole from Micromass using a cone voltage of 20 eV and collision induced dissociation (CID) energy of 35 eV (2.5 mTorr argon). To get structural information and accurate mass of the AtST4b-

sulfated product, the corresponding peak was further analyzed on a Q-TOF2 mass spectrometer (Micromass, UK).

2.6.6) Thin Layer Chromatography

Approximately 15,000 dpm of purified assay products were spotted on cellulose TLC plates (Analtech, 100 microns) and migrated in a mobile phase consisting of butanol, water, and acetic acid (6:2:2, V/V/V). The dried plates were later exposed to Kodak BioMax film for 7 days and then the autoradiograms were developed and scanned.

Chapter 3- Results

3.1) Regulation study of the *AtST4* subfamily

3.1.1) Introduction

Genome-wide microarray analysis revealed that members of the *AtST4* subfamily are regulated by cytokinins (Hoth *et al.* 2003; Brenner *et al.* 2005; Kiba *et al.* 2005; Lee *et al.* 2007; Yokoyama *et al.* 2007). An examination of the available microarray data showed that *AtST4b* is strongly induced by cytokinins in seedlings of *A. thaliana* (Genevestigator: ~4.92 fold induction after 1 hour and 3 hours treatment with 1μM zeatin). In contrast, *AtST4a* and/or *AtST4c* are slightly repressed by cytokinins on the same data set (Genevestigator: ~0.8 fold repression after 1 hour and 3 hours treatment with 1μM zeatin in seedlings). Furthermore, results from Gene Atlas and the electronic Fluorescent Pictograph (eFP) browser engine showed that the members of the *AtST4* subfamily are expressed mainly in the elongation zone of seedling roots (Zimmermann *et al.* 2004; Winter *et al.* 2007). Based on these results, a reverse transcription polymerase chain reaction (RT-PCR) experiment was performed to evaluate the effect of cytokinins on transcript expression of the members of the *AtST4* subfamily in root tissue.

In addition, since the members of the *AtST4* subfamily are regulated by cytokinins, we searched for putative cytokinin response cis-elements upstream of the coding region of *AtST4a*, *AtST4b* and *AtST4c*. The results of these analyses are discussed in the following sections.

3.1.2) Transcript expression study of the *AtST4* subfamily in response to cytokinins

Transcript expression analysis using gene specific primers on 16-days-old Arabidopsis confirmed the regulation of the *AtST4* subfamily members by the cytokinin *trans*-zeatin (*t*-zeatin) in roots. As shown in Fig. 8, 30 minutes after treatment with *t*-zeatin, *AtST4b* transcript level was low, but gradually increased with time. In contrast to *AtST4b*, the expression of *AtST4c* was repressed by *t*-zeatin in roots. While *AtST4c* expression was high in the absence of cytokinins, it decreased gradually following *t*-zeatin treatment, until there was no detectable level of transcript 6 hours after treatment. The *AtST4a* expression level was too low to be detected under the conditions of our experiment.

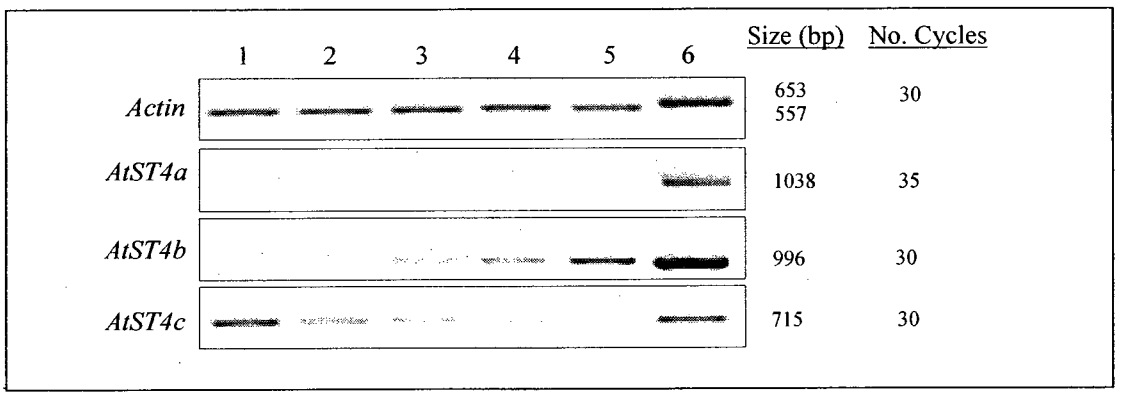

Figure 8. Transcript expression profile of the members of the *AtST4* subfamily in response to cytokinins. Total RNA was extracted from roots of 16-day-old Arabidopsis (Col-0) vertically grown on MS media treated or non-treated with 20μM *t*-zeatin for various time. The *Actin* was used to quantify the amounts of cDNAs and to test for genomic DNA contamination. Lane 1: 0 hour, lane 2: 30 minutes, lane 3: 2 hours, lane 4: 4 hours, lane 5: 6 hours and lane 6: genomic DNA.

3.1.3) Study of the presence of cytokinin-responsive elements in the upstream region of the *AtST4* genes

As mentioned earlier in Chapter 1, type-B ARRs are classified as transcriptional factors in the multi-step phosphorelay signal transduction of the cytokinin pathway in Arabidopsis. Analysis of the structure of type-B ARRs has revealed that, in addition to the acidic domain, nuclear localization domain and glutamine-rich domain, they contain a DNA binding domain in the C-terminal extension. This domain is called the B motif or GARP motif and is composed of 60 amino acids. The GARP motif is representative of the plant Myb-related transcription factors. The plant Myb proteins are distinctly related to the well-known mammalian Myb-repeat transcription factors, which bind DNA in a sequence-specific manner (Sakai *et al.* 1998; Imamura *et al.* 1999; Riechmann *et al.* 2000). In an attempt to characterize the DNA target of the plant Myb factors, Hosoda *et al.* found that the B motif derived from ARR 10, a representative of type-B ARR binds specifically to the optimal DNA sequence 5'-AGATT-3' in *in vitro* assays (Hosoda *et al.* 2002). In a different research study, the B motif of ARR1 and ARR2 was shown to have the highest binding affinity to the same core sequence (5'-AGATT-3') through gel retardation assays (Sakai *et al.* 2000). The core sequences 5'-GGATC-3' and 5'-GGATT-3' were found to be bound by the B motif of ARR1 and ARR2 with less affinity. Moreover, Sakai *et al.* showed that transgenic plants expressing a reporter gene under the control of multiple copies of the sequence 5'-GGATT-3' are significantly activated by ARR1 and ARR2. Following the same procedure, Imamura *et al.* found that a truncated version of ARR11, encompassing the receiver domain and GARP motif, binds more preferably to the sequence motif 5'-GGATT-3', rather than 5'-AGATT-3' in *in vitro*

assays (Imamura *et al.* 2003). In addition, Rashotte *et al.* performed a genome-wide microarray analysis to study the genes that are regulated by cytokinins. They found that genes that are consistently induced by cytokinins (for example, type-A ARRs), contain a significantly high proportion of the core sequence motif 5'-AAGATC-3' within the 1 kbp upstream of their translation start site. Interestingly, they found that the frequency of this motif in the upstream region of type-A ARRs is positively correlated with the induction level (Rashotte *et al.* 2003). For example, while the sequence motif 5'-AAGATC-3' should randomly occur approximately 0.38 times per kilobase pair, cytokinin up-regulated and down-regulated genes contained on average 14 and 6 times this motif within their upstream region, respectively. Overall, the optimal binding core sequence for the type-B ARRs seems to be 5'-(A/G)GAT(T/C)-3' with a specific requirement for the central GAT. However, since this short motif occurs frequently in the Arabidopsis genome, the existence of additional factors has been proposed in order to increase the specificity of the response (Sakai *et al.* 2000).

Since the members of the *AtST4* subfamily are regulated by cytokinins, we searched for the putative cis-acting motifs, mentioned above, in the 1,000 bp upstream of the predicted translation start site of *AtST4a*, *AtST4b* and *AtST4c*. The upstream coding region of *ARR 5* (At3g48100) and *ARR15* (At1g19050) (representatives of type-A ARRs) were used as references for genes that are up-regulated by cytokinins (Genevestigator: ~5.63 and 4.05 fold induction for *ARR5* and *ARR15*, respectively, after 1 hour and 3 hours treatment of seedlings with 1μM zeatin). The upstream coding region of a peroxidase (At5g19890) and auxin-responsive gene (At5g50760) were used as references for genes that are down-regulated by cytokinins (Rashotte *et al.* 2003; Lee *et al.* 2007) (Genevestigator: ~0.67 and

0.53 fold repression, respectively, after 1 hour and 3 hours treatment of seedlings with 1μM zeatin). The promoter regions of *Actin8* (At1g49240) and α-*tubulin* (At1g04820) were used as references for genes that are not regulated by cytokinins (Genevestigator: ~0.92 and 1.06 fold changes for *Actin8* and *α-tubulin*, respectively, after 1 hour and 3 hours treatment of seedlings with 1μM zeatin).

As shown in Table 1, the core sequence motif 5'-(A/G)GAT(T/C)-3'occurs more frequently in the upstream promoter region of the putative cytokinin up-regulated genes (*ARR5*, *ARR15*) than the cytokinin down-regulated and the cytokinin non-regulated reference genes. The occurrence of this motif in the upstream region of the members of the *AtST4* subfamily is less than *ARR5* and *ARR15*, but is more than that of the cytokinin non-regulated genes and close to that of the cytokinin down-regulated genes.

Altogether, the results show that the members of the *AtST4* subfamily, especially *AtST4b* and *AtST4c*, contain a higher number of the potential cytokinin-response elements compared to their random occurrence in the Arabidopsis genome. Their occurrence in the *AtST4* promoters is similar to what is observed for the putative cytokinin-regulated genes. Therefore, they have the potential to be regulated by cytokinin transcriptional activators such as type-B ARRs and subsequently be part of the cytokinin response.

Sequence motif / Gene (AGI)	5'-AAGATC-3' (Rashotte *et al.*, 2003)	5'-AGATT-3' (Hosoda *et al.*, 2003; Sakai *et al.*, 2000)	5'-GGATC-3' (Sakai *et al.*, 2000)	5'-GGATT-3' (Imamura *et al.*, 2003; Sakai *et al.*, 2000)	5'-AGATC-3' (Rashotte *et al.*, 2003)	5'-(A/G)GAT(C/T)-3' (Sakai *et al.*, 2000)
AtST4a (At2g14920)	**0**	**4**	**0**	**1**	**1**	**6**
AtST4b (At1g13420)	**2**	**5**	**1**	**2**	**3**	**11**
AtST4c (At1g13430)	**3**	**5**	**1**	**0**	**4**	**10**
ARR15 (At1g19050)	**6**	**7**	**4**	**2**	**7**	**20**
ARR5 (At3g48100)	**5**	**6**	**2**	**2**	**9**	**19**
Peroxidase (At5g19890)	**0**	**5**	**0**	**3**	**1**	**9**
Auxin-responsive gene (At5g50760)	**1**	**5**	**0**	**3**	**2**	**10**
Act8 (At1g49240)	**0**	**0**	**0**	**3**	**0**	**3**
α-tubuline (At1g04820)	**1**	**1**	**0**	**2**	**1**	**4**

Table 1. Putative cytokinin cis-acting motifs in promoters of the *AtST4* genes. The 1,000 bp upstream of the predicted translation start site of the genes were retrieved from ATTEDII (http://atted.jp/) and analyzed for the presence of cis-acting sequence motifs. The *ARR5* and *ARR15*, peroxidase and auxin-responsive gene and, *Actin8* and *α-tubulin* were used as references for the putative cytokinin up-regulated genes (pink), down-regulated genes (blue) and non-regulated genes (yellow), respectively. The numbers show the frequency of the respective motifs in forward and complementary strands.

3.2) Molecular characterization of T-DNA insertion mutants

3.2.1) Introduction

The primary aim of this study was to determine the role of the *AtST4* genes in plant growth and development. Using a reverse genetic approach, we identified loss of function mutants for *AtST4a, AtST4b* and *AtST4c*. Subsequently, we conducted a number of metabolic and phenotypic analyses to determine the biochemical and biological function of the *AtST4* genes in Arabidopsis.

3.2.2) Isolation of T-DNA insertion homozygous mutants

Arabidopsis lines carrying a T-DNA insertion in the *AtST4a* (GABI_177E08), *AtST4b* (GABI_231G06) and *AtST4c* (FLAG_334F06) loci were identified from the publicly available T-DNA insertion libraries. In all these Columbia 0 mutant lines, the T-DNA insertion is located within the intronless coding region. The site of T-DNA insertion was estimated by nucleotide blast using the sequencing information of the T-DNA borders retrieved from the TAIR web site (Fig. 9A). The *AtST4a* and *AtST4c* mutants carry an insertion near the end of their coding sequence (737 bp and 870 bp downstream of their translation start sites, respectively), which separates the regions encoding for the sulfotransferase catalytic domain (region I) and PAPS binding domain (region I and region IV). In the *AtST4b* mutant, the T-DNA insertion is located 74 bp downstream of the translational start site, which is adjacent to the region I involved in catalytic and PAPS binding activity. PCR analysis using gene-specific primers flanking the insertion site and the T-DNA left border (LB) primer showed that the *AtST4a, AtST4b* and *AtST4c* mutants are homozygous for the T-DNA insertion. As shown in Fig. 9B, while the intact

gene amplification product was not detected, the PCR-amplified T-DNA insertion product was identified in the mutant lines. In contrast, wild type Arabidopsis showed the presence of only the intact gene amplification product.

3.2.3) Transcript expression analysis of the T-DNA insertion homozygous mutants

To determine if the T-DNA insertion has affected the transcript level of the genes, RT-PCR analysis was performed on RNA samples of the homozygous *AtST4a, AtST4b* and *AtST4c* mutant plants. The presence of the respective gene-specific transcripts in wild type plants and their absence in the mutant plants confirmed that *AtST4a, AtST4b* and *AtST4c* homozygous mutant lines are null alleles (Fig. 9C). Therefore, the resultant T-DNA insertion mutants were designated as *AtST4a*-knockout (*AtST4a*-KO), *AtST4b*-knockout (*AtST4b*-KO) and *AtST4c*-knockout (*AtST4c*-KO) lines. It is important to note that in contrast with Fig. 8, we could detect amplification of the *AtST4a* transcript. This was obtained using a different primer pair generating a shorter PCR product. In the future, studies of *AtST4a* expression will have to be conducted using this primer set.

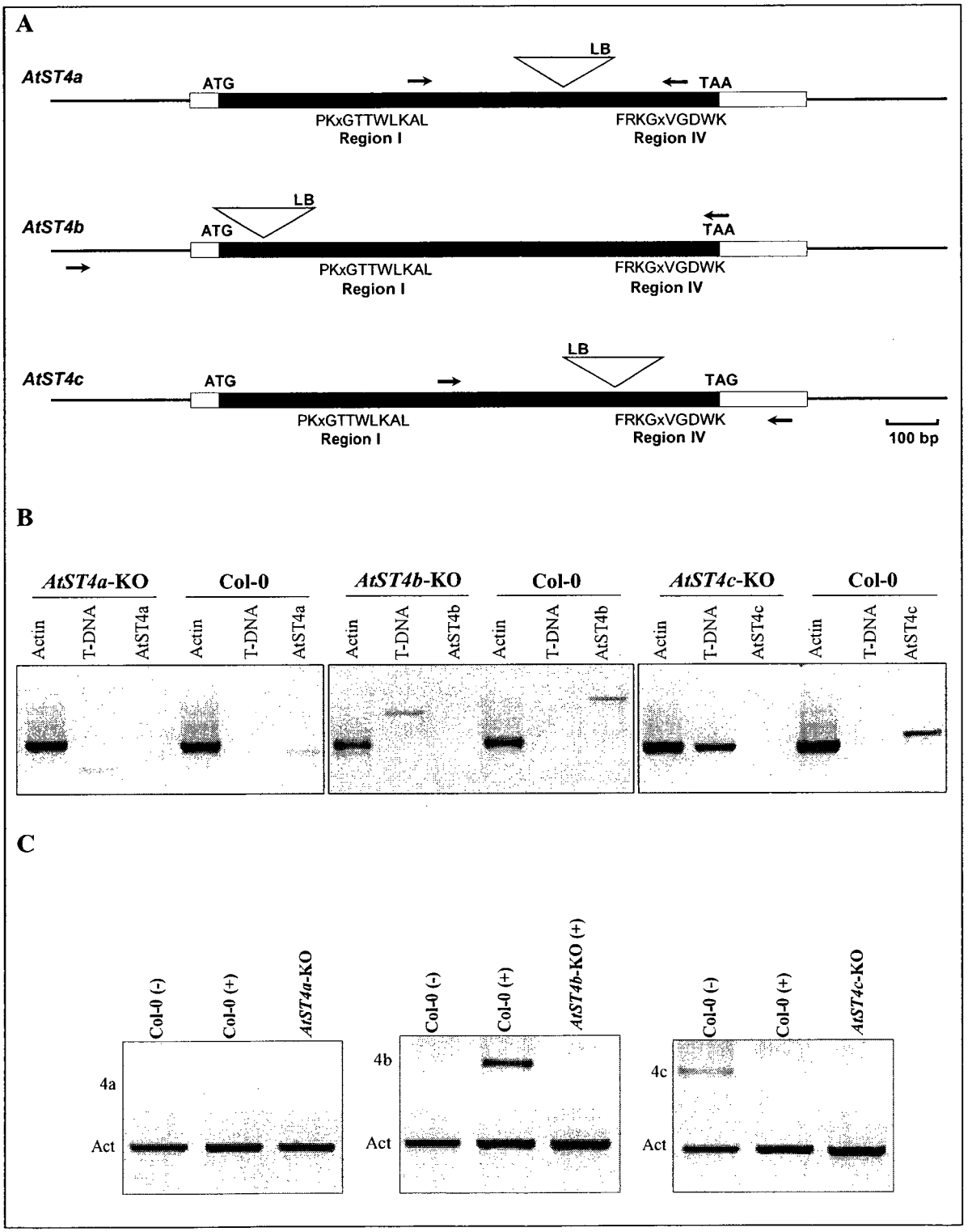

Figure 9. Identification of T-DNA insertion homozygous lines of the *AtST4* genes. (A) Schematic representation of the chromosomal region encompassing the *AtST4* genes and their T-DNA insertion site. The black boxes represent: exons, white boxes: 5' and 3'UTRs, triangles: T-DNA insertion sites, arrows:

gene-specific primers, LB: T-DNA left border. The consensus sequence from region I (PKxGTTWLKAL) and region IV (FRKGxVGDWK) were used to identify the regions involving in catalytic and PAPS binding activity. **(B)** PCR screening of the T-DNA insertion lines. Genomic DNA was extracted from leaves of three-week old *AtST4a* (GABI_177E08), *AtST4b* (GABI_231G06) and *AtST4c* (FLAG_334F06) T-DNA insertion lines and used as a template for PCR screening. The *Actin* gene was used as a positive control. **(C)** RT-PCR analysis of the *AtST4* T-DNA insertion homozygous lines and wild type plants. The two-week old mutant and wild type plants were treated (+) or non-treated (-) two hours with 20μM *t*-zeatin. Total RNA was extracted from roots and subjected to RT-PCR analysis using gene specific primers. 4a, 4b, 4c and Act are abbreviations for *AtST4a*, *AtST4b*, *AtST4c* and *Actin* genes, respectively.

3.3) Biochemical characterization of AtST4b

3.3.1) Introduction

To identify the substrate of the AtST4b sulfotransferase, plant metabolites were extracted and purified from roots of 14-day-old Arabidopsis. Subsequently, we used radiolabeled PAPS as sulfonate donor to assay the activity of the recombinant enzyme with the plant extract. To confirm the identity of the product of the reaction and to demonstrate its accumulation *in vivo*, the metabolite profile of the *AtST4b* T-DNA insertion homozygous line was compared with that of wild type plants using neutral loss mass spectrometry and liquid chromatography-tandem mass spectrometry (LC-MS/MS) analyses.

3.3.2) Expression of AtST4b recombinant sulfotransferase

To determine the biochemical function of AtST4b, the coding sequence was cloned in an *E.coli* expression plasmid as a fusion protein with 6 histidine residues at the N-terminus. The His-tag was used for affinity purification of the enzyme on Ni-agarose column. The partially purified recombinant enzyme corresponded to the expected size of the protein (~37.71 KDa) on SDS-PAGE (Fig. 10).

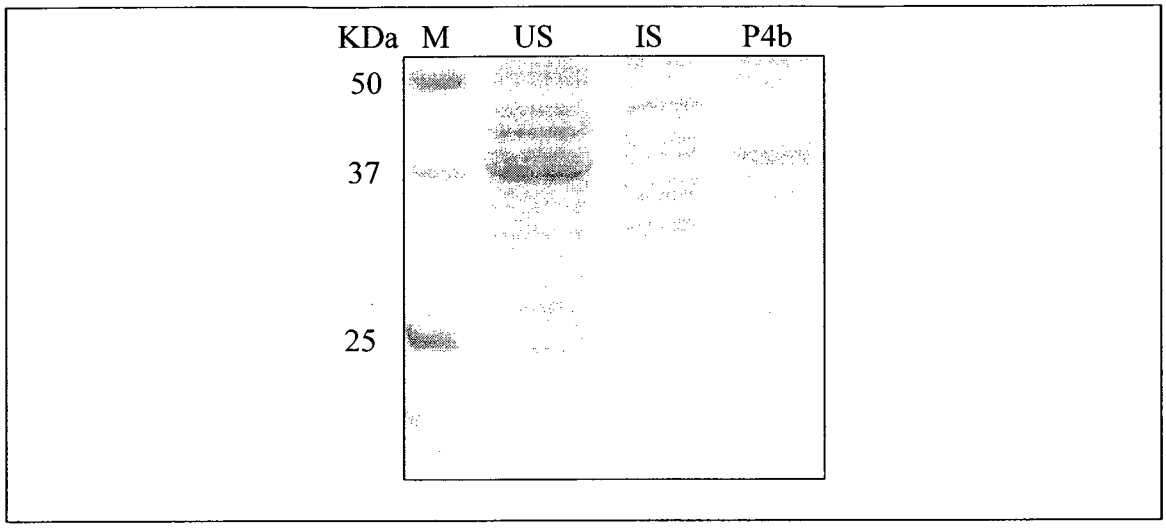

Figure 10. SDS-PAGE of partially purified AtST4b recombinant sulfotransferase. Cultures of bacteria expressing the recombinant enzyme were grown 14 hours at room temperature, induced or non-induced by IPTG and subjected to SDS-PAGE analysis. An aliquot of the induced culture was used for purification by affinity chromatography on Ni-NTA agarose. M: protein molecular marker, US: non-induced soluble proteins, IS: induced soluble proteins and P4b: purified AtST4b.

3.3.3) HPLC purification of AtST4b substrate and product

HPLC purification of AtST4b substrate

To determine the substrate of AtST4b, enzyme assays were performed on a library of chemicals including the previously reported sulfotransferase substrates, but none of them were accepted by the recombinant enzyme.

Based on the available microarray data on Genevestigator, the enzyme is expressed almost exclusively in roots of *A. thaliana*, therefore, root extracts were used to purify the potential substrate of AtST4b (Zimmermann *et al.* 2004). In order to remove the sulfonate group of the extracted metabolites, mild acid hydrolysis was performed prior to the assay and purification. The total root extracts were later fractionated using reverse

phase High Performance Liquid Chromatography (HPLC) and the individual fractions were assayed with the AtST4b recombinant enzyme. The results show that fraction 34, 37 and 42 have the highest enzymatic activity (Fig. 11). The presence of multiple peaks can be explained in part by the nature of the substrate of the enzyme which might contain chiral carbons giving rise to stereoisomers that could be resolved on the HPLC column.

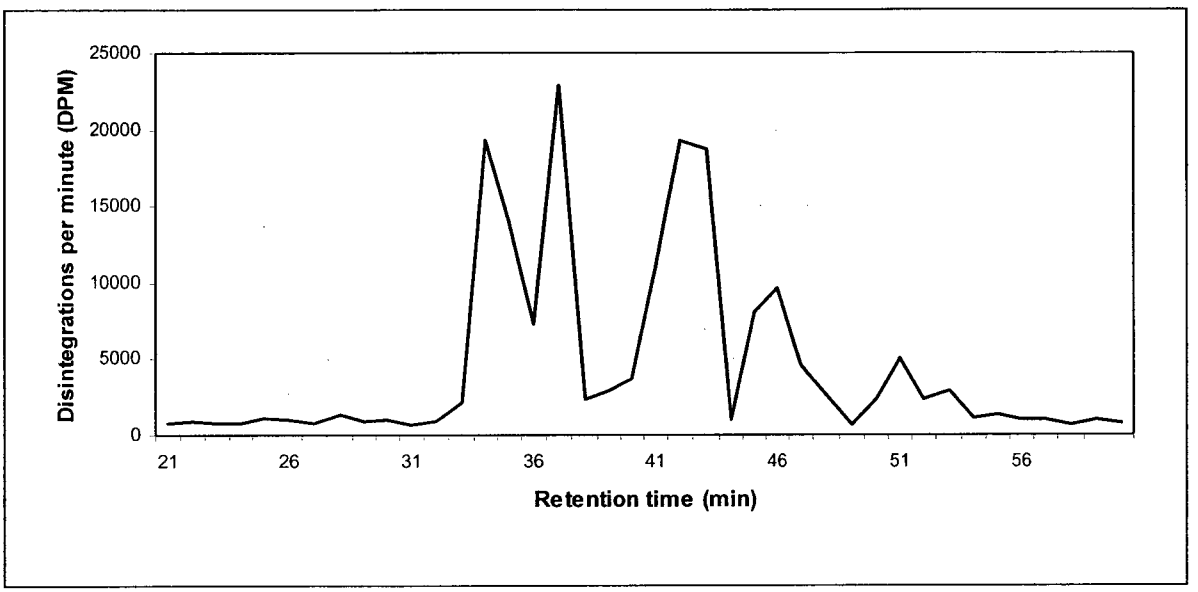

Figure 11. HPLC profile of an acid hydrolyzed root extract. Fraction 34, 37 and 42 showed the highest enzyme activity.

HPLC purification of AtST4b enzymatic reaction product

To identify the product of the reaction, enzyme assays were performed on fraction 37 that exhibited the highest enzyme activity. Following the enzyme assay, the AtST4b radiolabeled-sulfated product was purified by reverse phase HPLC. The results show that the product elutes at 27 min (Fig. 12).

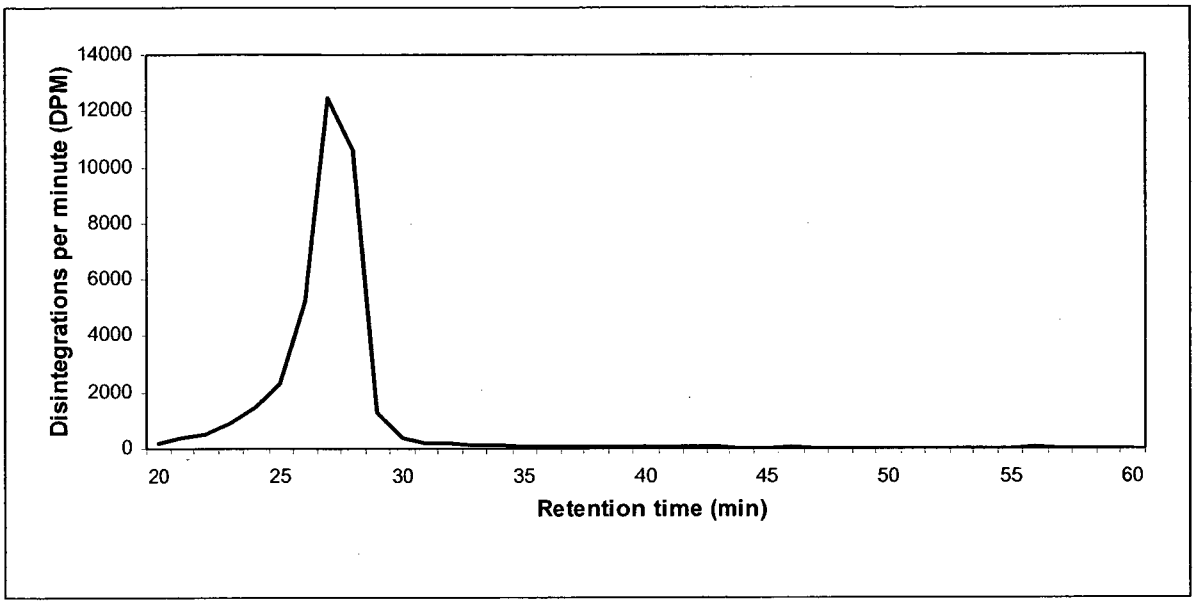

Figure 12. HPLC purification of the AtST4b radiolabeled enzymatic product. The highest radioactivity was recovered in fraction 27.

3.3.4) Neutral loss mass spectrometry of AtST4b purified product

Because of their fragility, sulfonated compounds can easily be detected using neutral loss mass spectrometry. By increasing the collision energy, the sulfuryl group (SO_3^-) is easily removed from the parent molecule. This chemical feature can be used to identify sulfonated compounds in a complex mixture by looking for parent ions losing a mass of 80 daltons (SO_3^-) following the increase in collision energy. We used this diagnostic tool to identify the sulfonated compound(s) present in fraction 27 of a purified root extract from wild type plants. Figure 13 (upper graph) shows that several putative sulfonated metabolites are present in this fraction with a major one (more than 98% of ion count) having a mass-to-charge ratio (m/z) of 514 daltons in negative mode ($[M-H]^-$). To identify the AtST4b enzymatic product in the fraction, we compared the wild type neutral loss metabolite profile with the one obtained with an *AtST4b*-KO root extract under the same condition. The root extract of the *AtST4b* T-DNA insertion homozygous line

showed almost the same profile as the wild type extract, except for the absence of the 514 $[M-H]^-$ peak (Fig. 13 lower graph). These results indicate that the reaction product synthesized *in vitro* by the recombinant *AtST4b* enzyme accumulate *in vivo* and has a mass of m/z 514 daltons $[M-H]^-$.

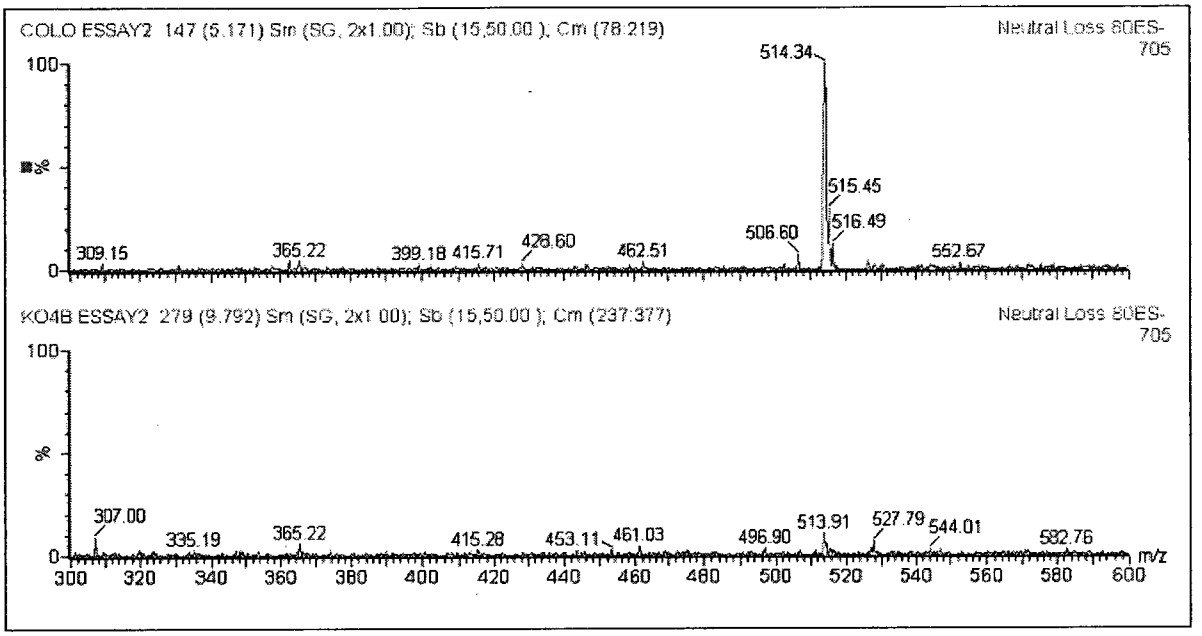

Figure 13. Mass spectrometry analysis of AtST4b-reaction product. Neutral loss profiles of a root extract from wild type (upper graph) and AtST4b-KO mutant (lower graph) plants in negative mode. The major peak at m/z 514 is missing in the AtST4b-KO scan.

3.3.5) LC-MS/MS analysis of AtST4b purified product

To elucidate the chemical structure of the compound having a mass of 514 $[M-H]^-$ daltons, a cytokinin-treated root extract was subjected to reverse phase liquid chromatography-tandem mass spectrometry (LC-MS/MS) analysis. Initially, the fragmentation pattern was obtained using a nano liquid chromatograph coupled with a tandem quadrupole time-of-flight (Q-TOF) mass spectrometer at the Centre for

Biological Applications of Mass Spectrometry (CBAMS, Concordia University). Fig. 14A shows the fragmentation pattern of the AtST4b enzymatic product. In the positive ion electrospray mass spectrum, the AtST4b sulfonated product produced a protonated molecular ion at m/z 516 ($[M+H]^+$). The MS/MS fragmentation of this compound gave major fragment ions at m/z 348 and 291, which correspond to the loss of spermidine or a fragment of it (Fig. 14A and B). The molecular ion at m/z 436 is due to the cleavage of the sulfonate moiety from the parent ion (m/z 516). Further fragmentation of the 436 $[M+H]^+$ ion, produced the ions at m/z 419 (due to loss of NH_3), 362, 348, 320, 291, 265, 263 and 203 which have been previously reported in the MS/MS fragmentation of cadabicine from *Capparis spinosa* (Khanfar *et al.* 2003). The structure and accurate mass of cadabicine and cadabicine-sulfate was further determined by Dr. Jurgen Schmidt from the Institute of Plant Biochemistry (Halle, Germany) using Fourier Transform Ion Mobility Spectrometry (FT-IMS) (Fig. 14B). Even though cadabicine has been reported to occur in nature in the root bark of Capparaceae (*Capparis spinosa* and *Capparis decidua*) and in seeds of Brassicaceae (*Brassica napus*), it is the first time that it is identified from *A. thaliana* (Khanfar *et al.* 2003; Baumert *et al.* 2005). Furthermore, it is the first report of the natural occurrence of its sulfonated derivative.

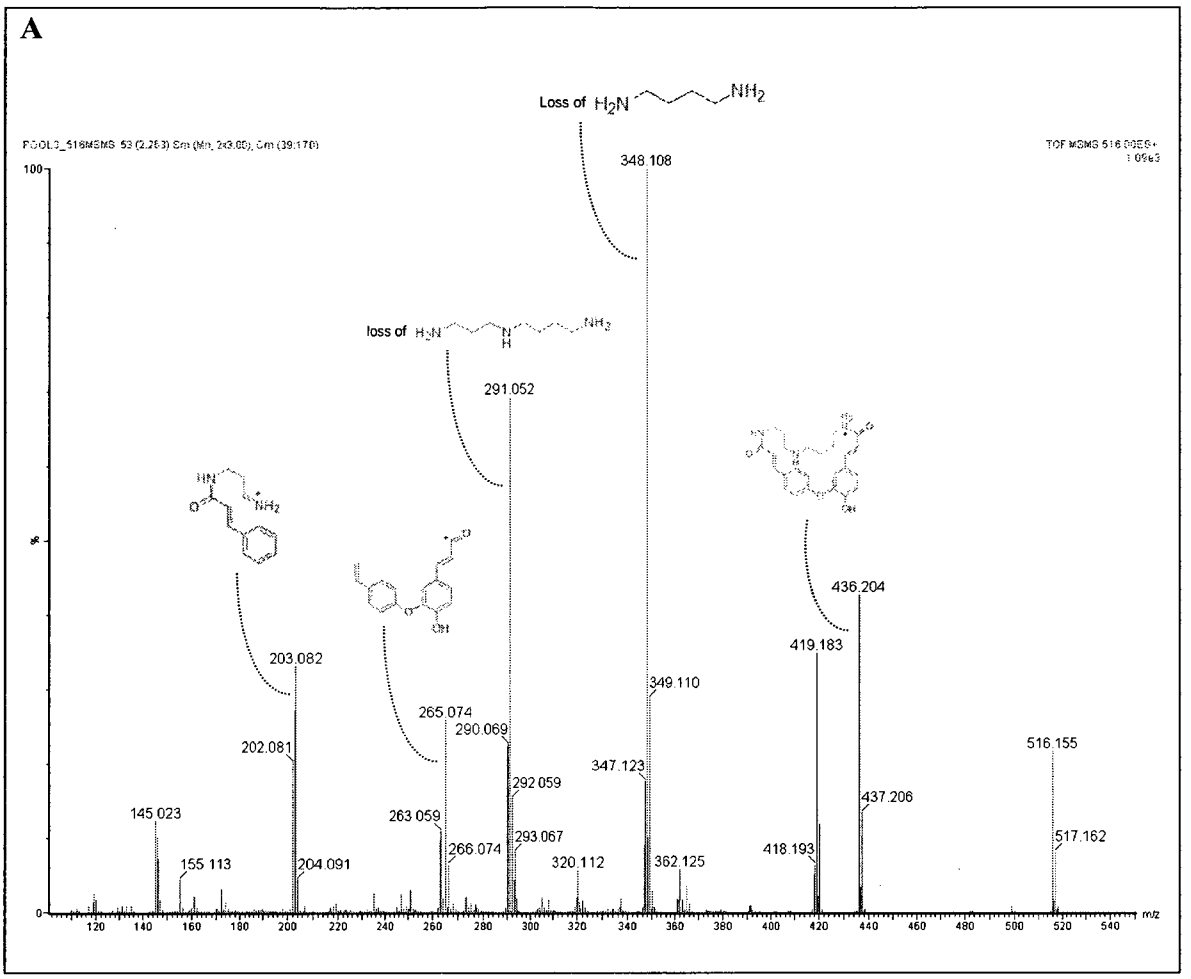
A
Loss of
loss of
348.108
291.052
436.204
419.183
203.082
349.110
265.074
290.069
202.081
347.123
516.155
292.059
437.206
145.023
263.059
293.067
517.162
155.113
266.074
204.091
320.112
362.125
418.193
100
%
0
120
140
160
180
200
220
240
260
280
300
320
340
360
380
400
420
440
460
480
500
520
540
m/z

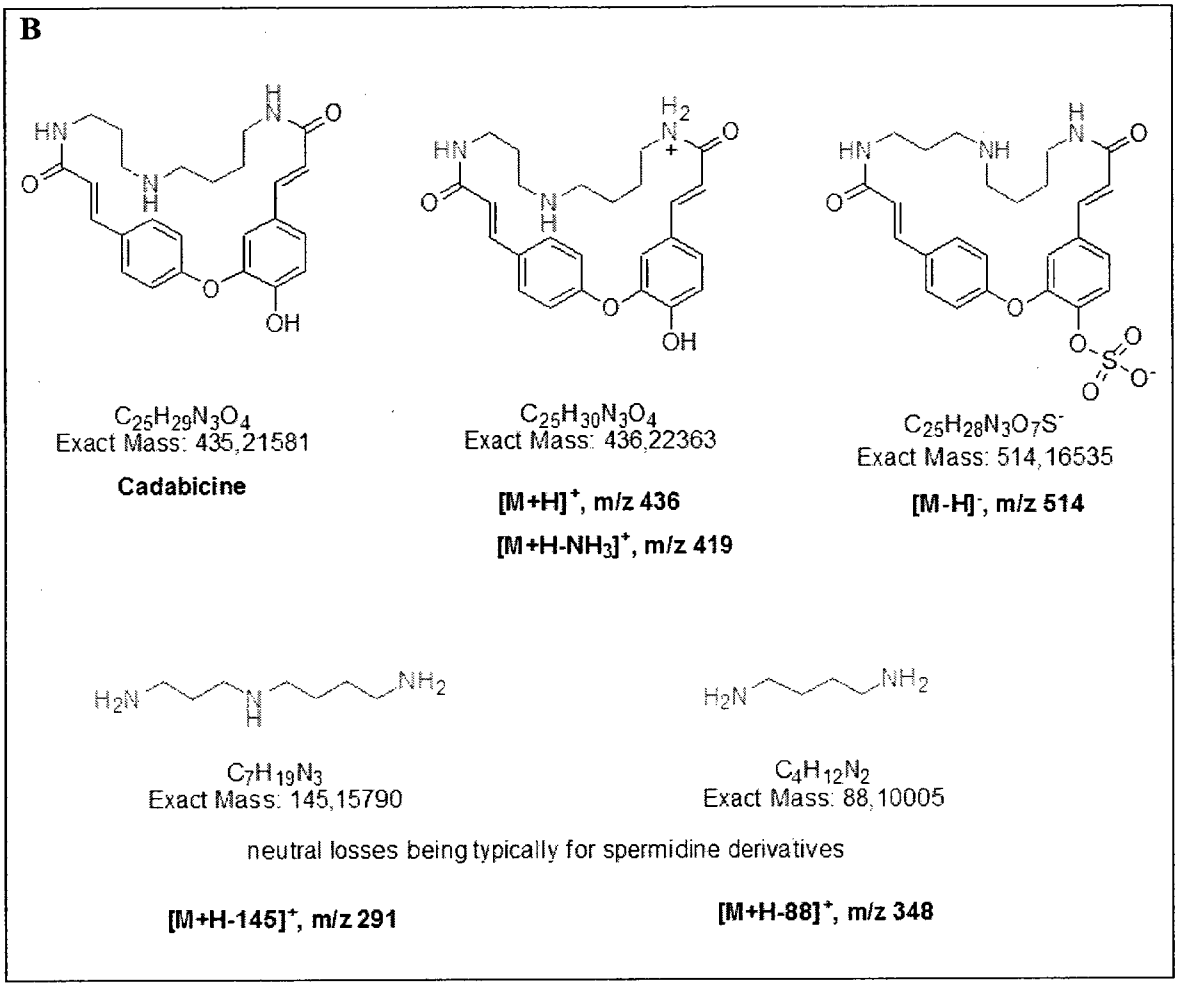

Figure 14. Identification of AtST4b-sulfated product. (A) LC-MS/MS spectrum of the AtST4b sulfated product in positive mode. The possible structure of some major fragments is shown. **(B)** Structure of cadabicine and cadabicine sulfate with exact mass determination using FT-IMS. Cadabicine contains an amide conjugate (spermidine, shown in red) and two acyl conjugates (hydroxycinnamic acid, shown in black and blue).

3.4) Characterization of *AtST4b* biological function

3.4.1) Introduction

Having identified the structure of the AtST4b enzymatic product, we attempted to determine its function *in planta* by comparing the growth behavior of the *AtST4b* T-DNA insertion homozygous mutant (*AtST4b*-KO) with wild type plants.

3.4.2) Primary root length analysis

Cytokinins inhibit root elongation. Furthermore, cytokinin receptor double mutants exhibit longer roots and increased number of lateral roots (Higuchi *et al.* 2004; Riefler *et al.* 2006). Moreover, as it was shown earlier, *AtST4b* expression is regulated by cytokinins and its expression is restricted to root tissue (Marsolais *et al.* 2007). Consequently, we analyzed the root growth behavior in the *AtST4b*-KO mutant in presence and absence of cytokinins.

Observation of primary root growth 10 days after germination (DAG) under *in vitro* conditions demonstrated that the root length of *AtST4b*-KO had increased 6.5 to 16.5% more than that of wild type seedlings (Fig. 15A and B). Interestingly, the *AtST4b*-KO plants had a greater growth rate in the beginning and mid (between 2 to 7 DAG with the highest increase at 4 DAG) than at the end of our analysis. To determine the role of *AtST4b* in the cytokinin response pathway, we examined root elongation in response to the exogenous application of the cytokinin *t*-zeatin. We compared primary root elongation of wild type and the *AtST4b*-KO line in presence of 1 and 5μM *t*-zeatin at different stages of development. Fig. 15C shows that 5 DAG, roots of *AtST4b* mutant plants are less sensitive to different concentrations of cytokinins. Similar differences were

also obtained 7, 12, and 14 DAG (data not shown). Such an effect has been reported for cytokinin receptor mutants and cytokinin deficient plants (Werner *et al.* 2001; Higuchi *et al.* 2004; Nishimura *et al.* 2004). Altogether, our results suggested that *AtST4b* participate in the root growth inhibition mediated by cytokinins.

3.4.3) Number of lateral roots

Formation of lateral roots is also inhibited by cytokinins (Werner *et al.* 2001; Werner *et al.* 2003). To assess the effect of *AtST4b* on lateral root formation, we counted the number of lateral roots in 12- and 14-day-old wild type and *AtST4b*-KO plants. As shown in Fig. 15D, even though the number of lateral roots had been increased 24% to 25% in the *AtST4b*-KO plants, there is no statistically significant difference between the wild type and *AtST4b*-KO lines 12 and 14 DAG with a *P*-value of 0.06 at 14 DAG. Even though the trend for increased lateral root is evident, the small sample size used for the analyses probably did not allow assessing the differences between the mutant line and control plants. A larger sample size will be required to evaluate the role of *AtST4b* in the growth of secondary roots.

A

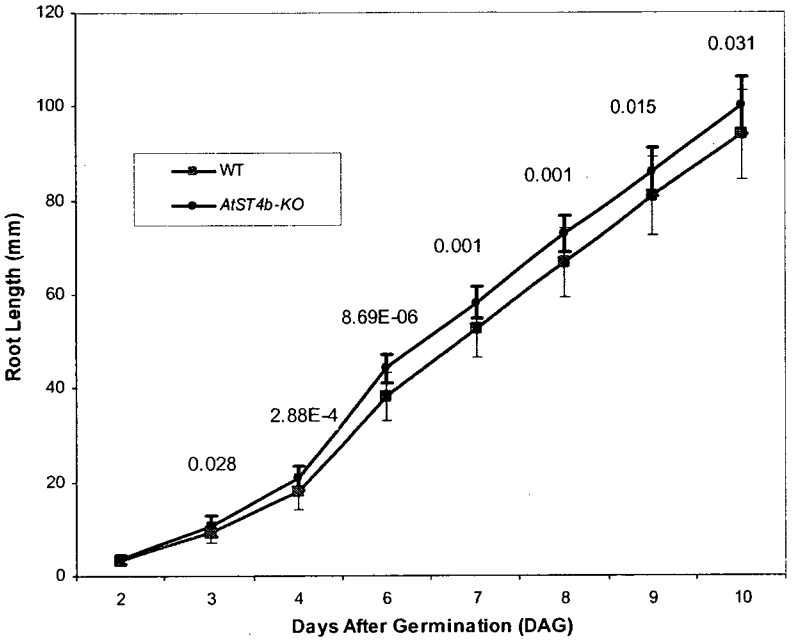
120
100
80
60
40
20
0
Root Length (mm)
WT
AtST4b-KO
0.028
2.88E-4
8.69E-06
0.001
0.001
0.015
0.031
2
3
4
6
7
8
9
10
Days After Germination (DAG)

B

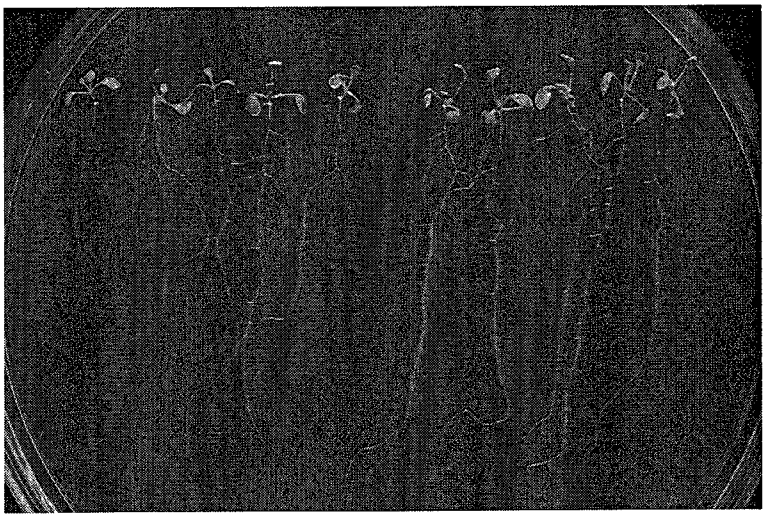

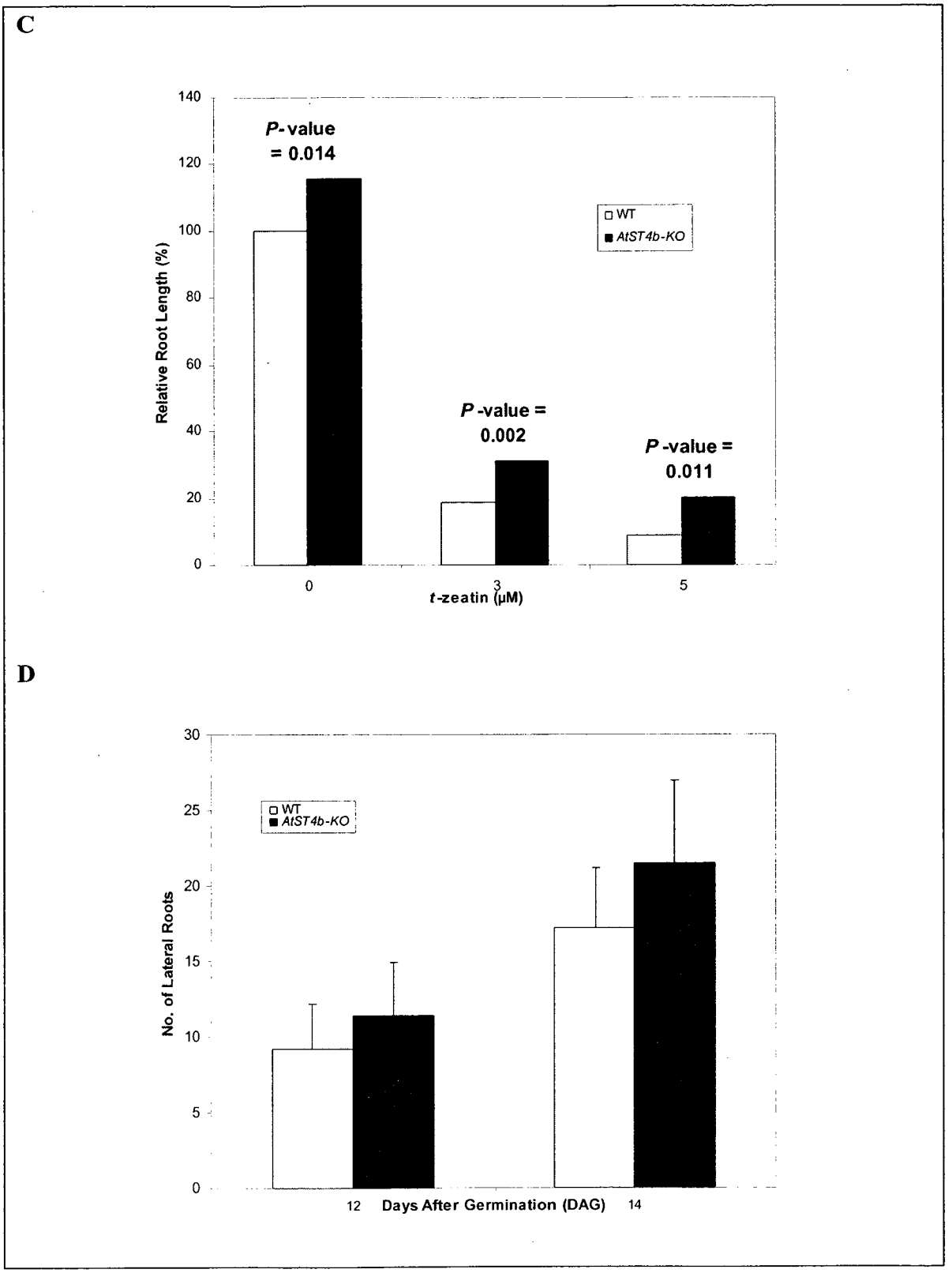

Figure 15. Root phenotype of the *AtST4b*-KO mutants. (A) Kinetic of root elongation in wild type (Col-0) and *AtST4b*-KO plants. Plants were grown vertically on MS agar plates under long day conditions and

root length was measured every day. Label for each day shows the corresponding significant *P*-value. Error bars represent standard deviation (SD) ($27 \leq n \leq 44$). **(B)** Root system of *in vitro* grown wild type (left) and *AtST4b*-KO (right) plants 7 DAG. **(C)** Relative changes of primary roots length in wild type (Col-0) and *AtST4b*-KO plants 5 DAG in presence of increasing concentration of *t*-zeatin. Root length of wild type plants in the absence of cytokinins was set at 100%. Length of roots in the absence of *t*-zeatin was: WT: 0.81 ± 0.11 (mean ± SD), *AtST4b*-KO: 0.93 ± 0.18. (n=19). **(D)** Number of lateral roots 12 and 14 DAG in plants grown vertically on MS agar plates. Error bars represent SD ($9 \leq n \leq 12$). Analysis of the significance level between wild type and the *AtST4b*-KO plants was performed by either Kruskal-Wallis test followed by Mann-Whitney U test or by two-independent-sample test (t-test). Only *P*-values with a significant level less than 0.05 are shown. See Annex 1 for details of statistical values.

3.4.4) Rosette diameter

Study of cytokinin-deficient plants and cytokinin receptor mutants indicate that shoot growth is impaired in these plants (Werner *et al.* 2001; Higuchi *et al.* 2004; Nishimura *et al.* 2004; Riefler *et al.* 2006). Analysis of the rosette structure of the *AtST4b*-KO showed that even though there is a statistical increase in size at 21 DAG (*P*-value=0.028), the significance level is relatively high and there is no general pattern of significant increase at 14 and 26 DAG (Fig. 16A). It is important to mention that this experiment was repeated earlier, in which there was a statistically significant increase in rosette size of the *AtST4b*-KO plants (17% to 30% increase) compare to wild type plants (*P*-value was equal to $2.53E^{-5}$, $4.96E^{-4}$ and $2.82E^{-5}$ at 14, 21 and 26 DAG, respectively) (see the rosette structure in Fig. 16C). The changes in the significance level could arise from a number of parameters such as sample size, variance or changes of experimental conditions such as light, soil, seeds, etc. On the other hand, based on the general trend of increase in the *AtST4b*-KO plants in both analyses, it can be said that *AtST4b* might negatively control rosette size.

3.4.5) Number of leaves

Further analysis of shoot development showed that the rate of leaf formation is affected during the vegetative growth in the *AtST4b*-KO mutants. As shown in Fig. 16B the *AtST4b*-KO plants developed approximately 6% to 9 % more leaves than wild type plants of the same age (14, 21 DAG) (*P*-value is equal to 0.013 and $4.21E^{-4}$ at 14 and 21 DAG, respectively). The increase in number of leaves of *AtST4b*-KO plants was reproducible and observed in a separate experiment.

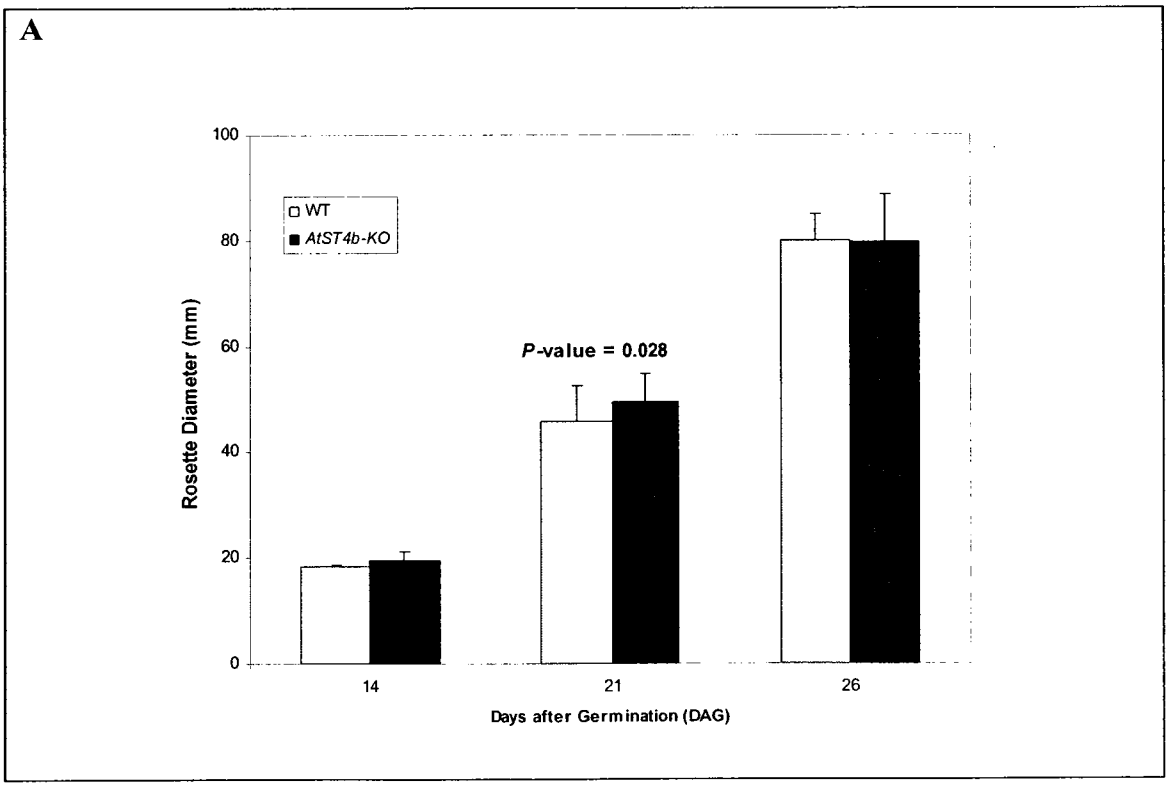

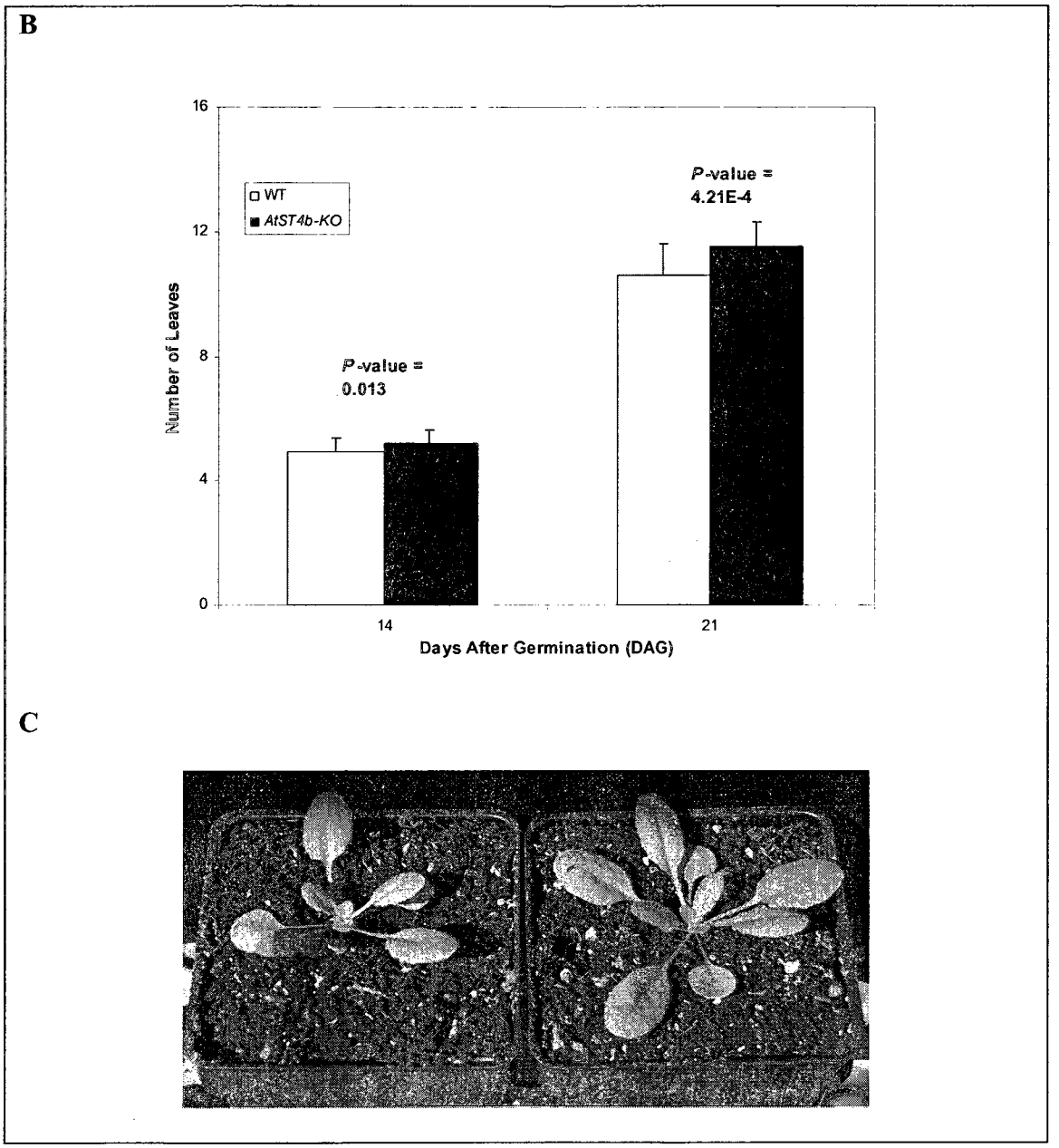

Figure 16. Shoot phenotype of the *AtST4b*-KO plants. (A) Rosette diameter of in-soil grown plants 14, 21 and 26 DAG. Error bars represent SD ($21 \leq n \leq 32$). **(B)** Number of leaves of in-soil grown plants 14, 21 DAG. Error bars represent SD ($21 \leq n \leq 39$). **(C)** Rosette of wild type (left) and *AtST4b*-KO (right) plants 21 DAG. Analysis of the significance level between wild type and the *AtST4b*-KO plants was performed by a Kruskal-Wallis test followed by a Mann-Whitney U test. Only *P*-values with a significant level less than 0.05 are shown. See Annex 2 for details of statistical values.

3.4.6) Flowering time

To assess the role of *AtST4b* during reproductive development, a number of phenotype analyses were conducted. Based on these analyses, there are no apparent changes in flowering time and flower structure between wild type Arabidopsis and the *AtST4b*-KO mutants.

3.4.7) Seed production

Increased grain production has been linked to the reduced level of cytokinin oxidase activity and the subsequent accumulation of cytokinins in the inflorescence of rice (Ashikari *et al.* 2005). In Arabidopsis, the reduced cytokinin content of cytokinin oxidase overexpression lines reduced the number of flowers and seeds in siliques, but increased the size of the seeds (Werner *et al.* 2003). Under long day conditions, the *AtST4b*-KO plants produced on average ~33% more siliques than wild type plants during reproductive development (36 and 46 DAG) (Fig. 17A and C). These results were reproducible and seen in a separate experiment (data not shown). Moreover, no significant changes were found in the number of seeds in mature siliques (*P*-value=0.06) (Fig. 17B).

A

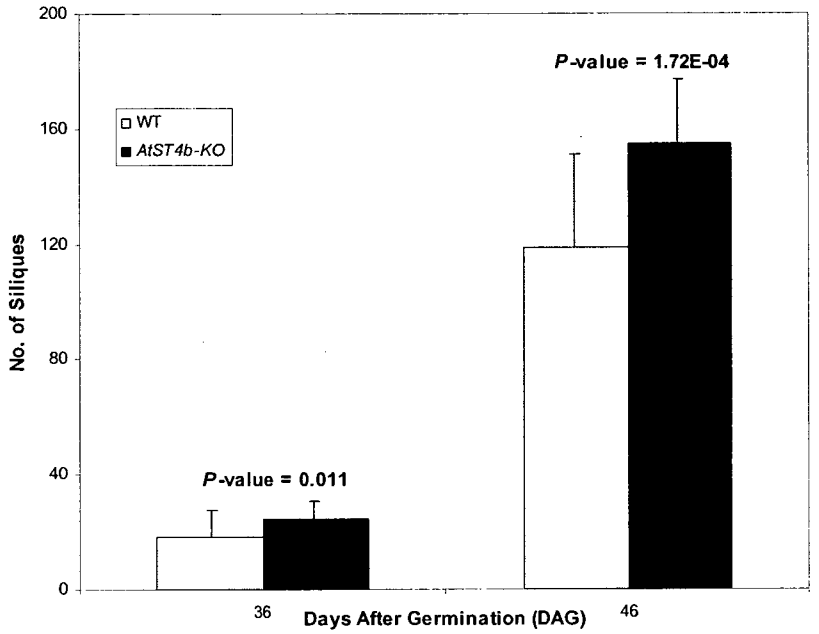
200
160
120
80
40
0
No. of Siliques
WT
AtST4b-KO
P-value = 1.72E-04
P-value = 0.011
36
46
Days After Germination (DAG)

B

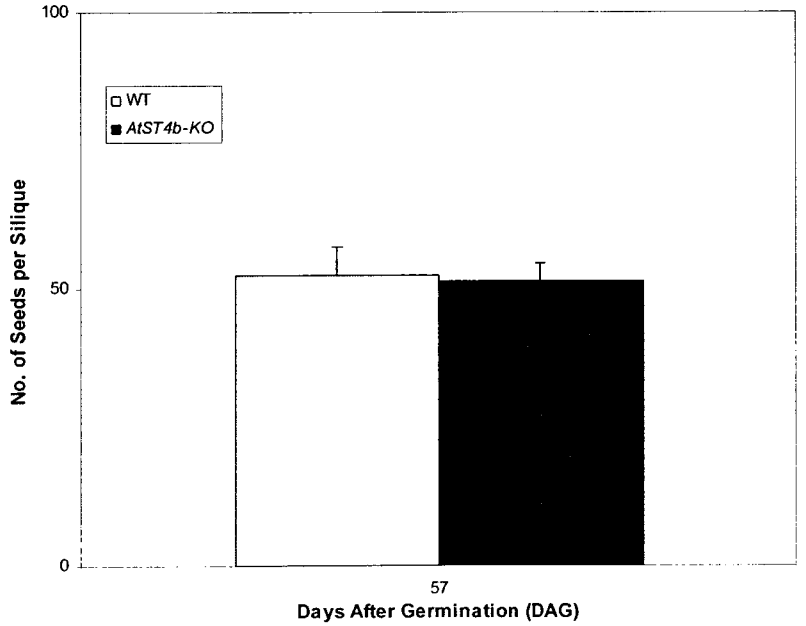
100
50
0
No. of Seeds per Silique
WT
AtST4b-KO
57
Days After Germination (DAG)

C

Figure 17. Reproductive development is improved in the *AtST4b*-KO line. (A) Number of siliques per plant 36 and 46 DAG. Error bars represent SD ($21 \leq n \leq 24$). **(B)** Number of seeds per mature siliques 57 DAG. Error bars represent SD (n=30). **(C)** Photograph of wild type (left) and *AtST4b*-KO (right) plants 5 weeks after germination. Analysis of the significance level between wild type and the *AtST4b*-KO plants was performed by a Kruskal-Wallis test followed by a Mann-Whitney U test. Only *P*-values with a significant level less than 0.05 are shown. See Annex 3 for details of statistical values.

3.4.8) Seed size and volume

As mentioned earlier, plants with impaired cytokinin signaling (cytokinin receptor mutants) and plants with reduced cytokinin content (cytokinin oxidase overexpressor lines) produce bigger seeds (Werner *et al.* 2003; Riefler *et al.* 2006). To investigate the role of *AtST4b* in seed development, the size of wild type and mutant seeds were measured under a dissecting microscope. As shown in Fig. 18A and B, the average length and width of the mutant seeds are about 7.4% and 4.5% greater than that of wild type

seeds, respectively. These changes increased the seed volume up to ~17% in the *AtST4b*-KO plants (Fig. 18C).

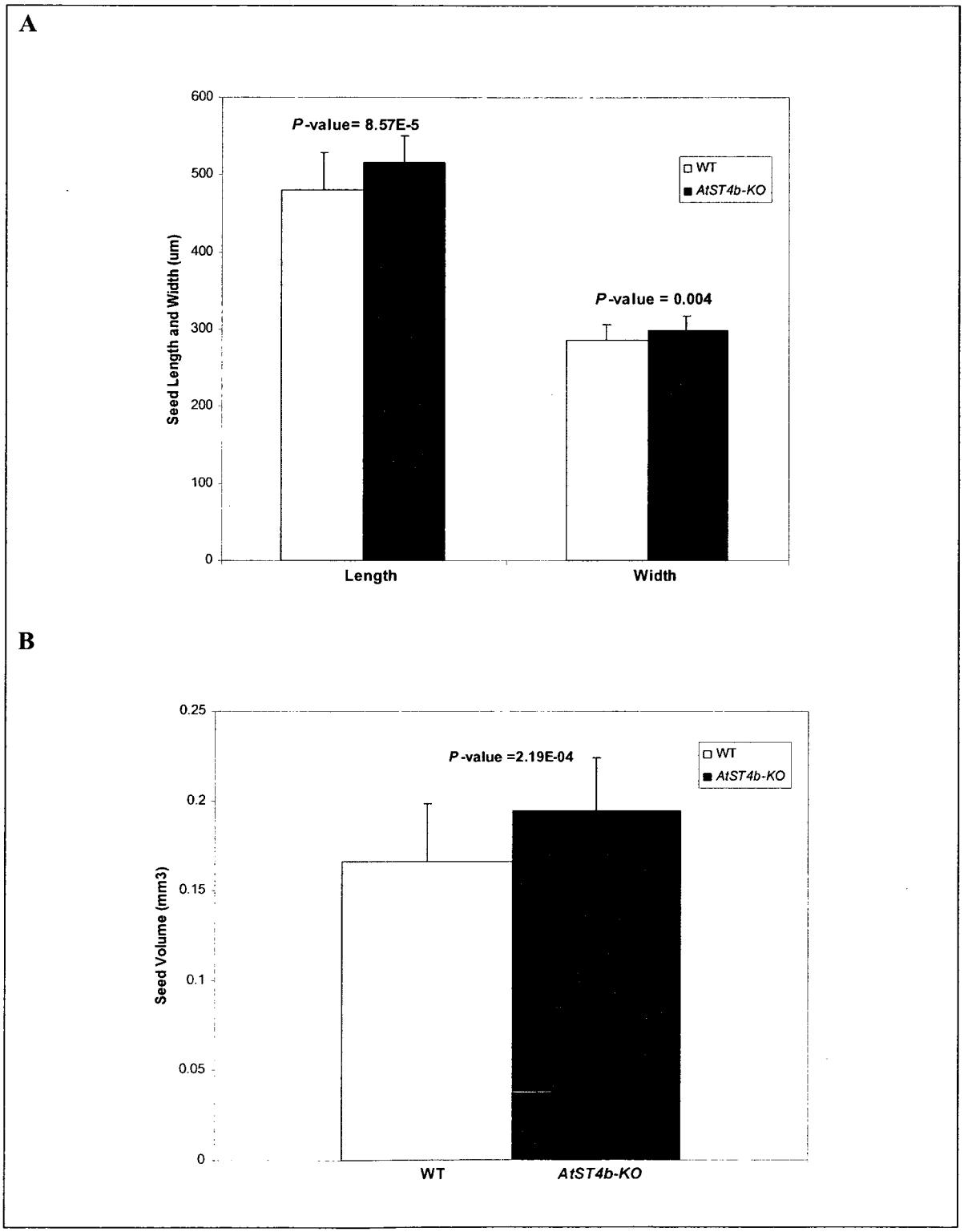

C

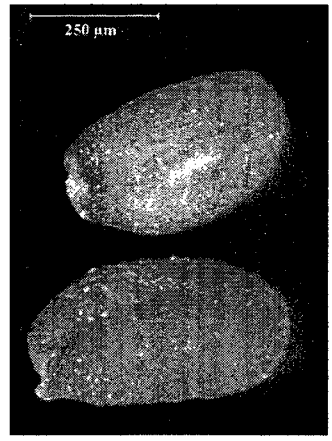

Figure 18. Seed size of the *AtST4b*-KO plants. (A) The length and width of seeds from wild type and the *AtST4b*-KO plants. Error bars represent SD (n=40). **(B)** Calculated volume of wild type and the *AtST4b*-KO seeds based on the formula: volume = 4/3 x π x length x width x depth (Riefler et al. 2006). Error bars represent SD (n=40). **(C)** Wild type (top) compared to the *AtST4b*-KO seeds (bottom). Analysis of the significance level between wild type and the *AtST4b*-KO seeds was performed by a Kruskal-Wallis test followed by a Mann-Whitney U test. Only *P*-values with a significant level less than 0.05 are shown. See Annex 3 for details of statistical values.

3.5) Biochemical characterization of AtST4a and AtST4c

3.5.1) Introduction

In a previous study, Marsolais *et al.* showed that AtST4a has brassinosteroid sulfotransferase activity *in vitro* while AtST4b and AtST4c were inactive with the same substrate (Marsolais *et al.* 2007). This study was limited since it was conducted with a small number of pure compounds from our laboratory library collection. In order to elucidate the biochemical function of AtST4a and AtST4c *in vivo*, sulfated metabolite profiles of wild type and knockout plants were analyzed using a combination of HPLC

and mass spectrometry. Metabolites were also purified form *A. thaliana* and assayed *in vitro* with recombinant AtST4b and AtST4c.

3.5.2) Expression of AtST4a and AtST4c recombinant sulfotransferases

The coding sequences of *AtST4a* and *AtST4c* were previously cloned in the bacterial expression plasmid pQE 30 (Qiagen) containing a 6x His-tag at the N-terminus. Expression of the enzymes produced proteins with the expected size of 38.8 and 37.7 kDa for AtST4a and AtST4c, respectively (Fig. 19).

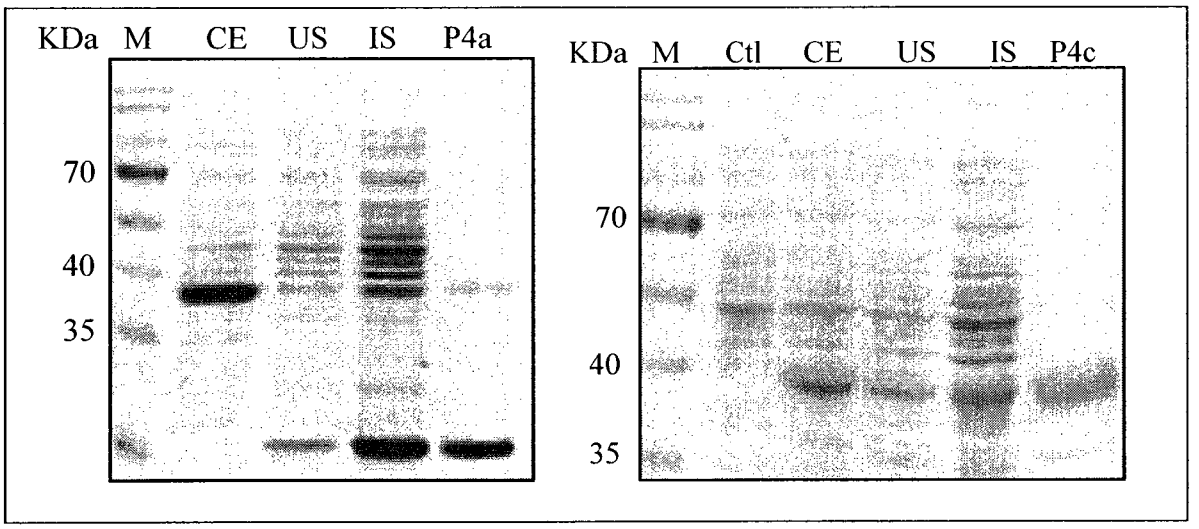

Figure 19. SDS-PAGE of AtST4a and AtST4c recombinant sulfotransferases. IPTG-induced or control cultures of bacteria expressing the recombinant enzymes were grown 14 hours at room temperature and their protein extracts were subjected to SDS-PAGE analysis. Aliquots of the induced culture were used for purification by affinity chromatography on Ni-NTA agarose. M: protein molecular marker, Ctl: PQE30 empty vector, CE: bacterial crude extract (25μg), US: non-induced soluble proteins (25μg), IS: induced soluble proteins (25μg) and P4a and P4c: purified AtST4a and AtST4c (10μg).

3.5.3) HPLC purification of the substrate and product

HPLC purification of AtST4a and AtST4c substrate

Gene regulation studies showed that *AtST4a* and *AtST4c* are expressed only in the root system of Arabidopsis (Marsolais *et al.* 2007). Accordingly, root extracts were used to purify the endogenous substrate and product of AtST4a and AtST4c. Following mild acid hydrolysis (to release the potential substrate from its conjugated form), the extract was fractionated by reverse phase HPLC. Each fraction was assayed with recombinant AtST4a and AtST4c to detect the presence of the substrate. The results show that the substrate of both enzymes elute in fraction 32 (Fig. 20).

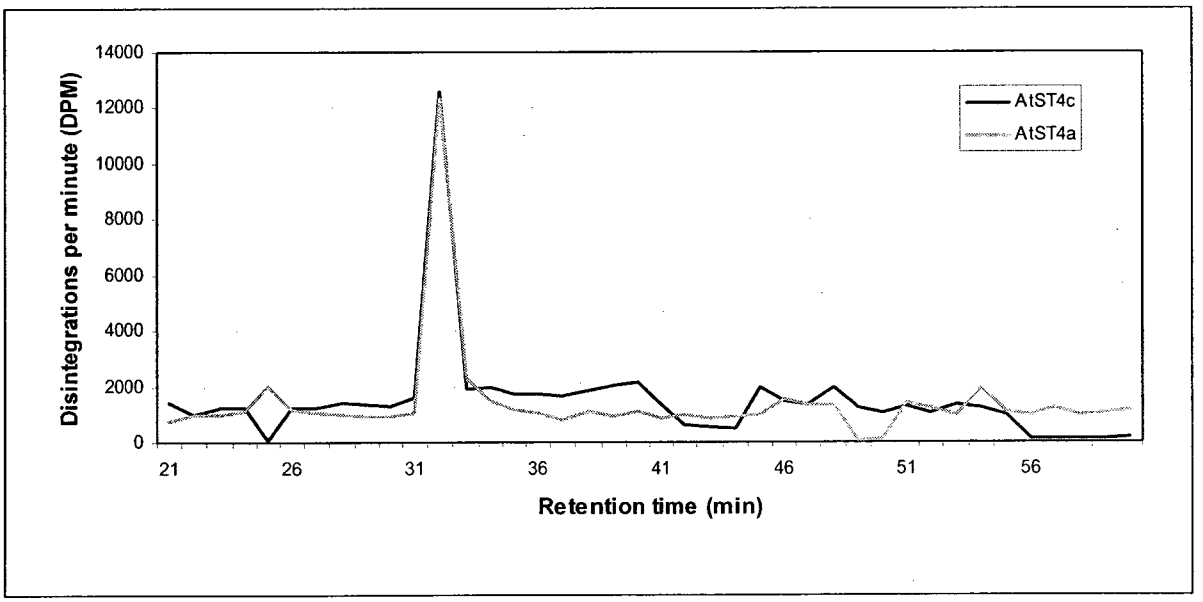

Figure 20. HPLC purification of AtST4a and AtST4c endogenous substrate. Individual fractions were assayed for activity with recombinant AtST4a and AtST4c.

HPLC purification of AtST4a and AtST4c reaction products

To identify the elution time of the reaction products of AtST4a and AtST4c, enzymatic assays were performed on the purified fraction containing the potential substrate (fraction 32) in order to produce the radiolabeled-sulfated products. Subsequently, the reaction products were purified on a reverse phase HPLC column and the individual fractions counted for radioactivity. The results show that the reaction product of both enzymes elute in fraction 24 (Fig. 21).

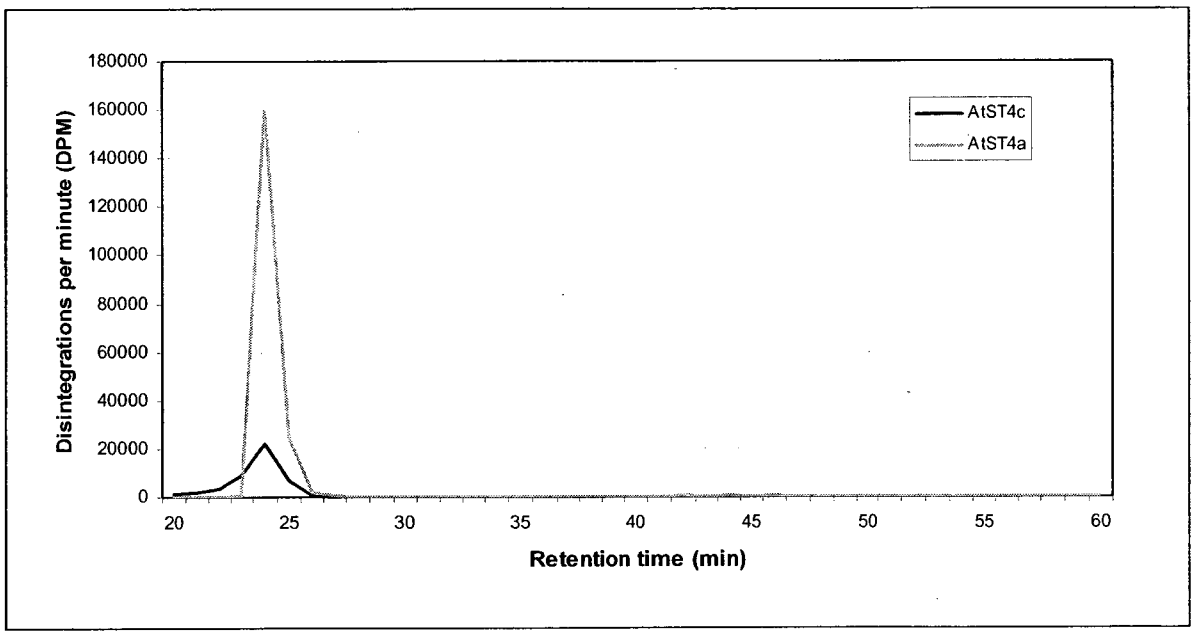

Figure 21. HPLC purification of AtST4a and AtST4c radiolabeled product. The highest activity was recovered in fraction 24.

3.5.4) Neutral loss mass spectrometry of AtST4a and AtST4c reaction products

Having determined the elution time of AtST4a and AtST4c enzymatic reaction products, root metabolites of wild type and *AtST4a*- or *AtST4c*-KO plants were purified under the

same conditions and their respective HPLC fractions (fraction 24) were analyzed by neutral loss mass spectrometry. We did not find any difference in the sulfated metabolite profile of the two knockout plants when compared with the wild type purified fraction 24. This result is not totally unexpected when we consider that the substrate and the product of both enzymes co-elute on HPLC suggesting a redundant function for AtST4a and AtST4c. It is also possible that the abundance of the *in vivo* products is too low for detection under our experimental conditions. Transgenic lines overexpressing AtST4a or AtST4c will have to be produced and analyzed to help in the detection of the endogenous sulfated product.

3.5.5) Thin layer chromatography of AtST4a and AtST4c reaction products

We further examined the purified AtST4a and AtST4c radiolabeled enzymatic products on TLC plates. As shown in Fig. 22, the reaction products are exhibiting the same chromatographic behavior, suggesting that the two enzymes sulfonate the same substrate from the purified fraction 32.

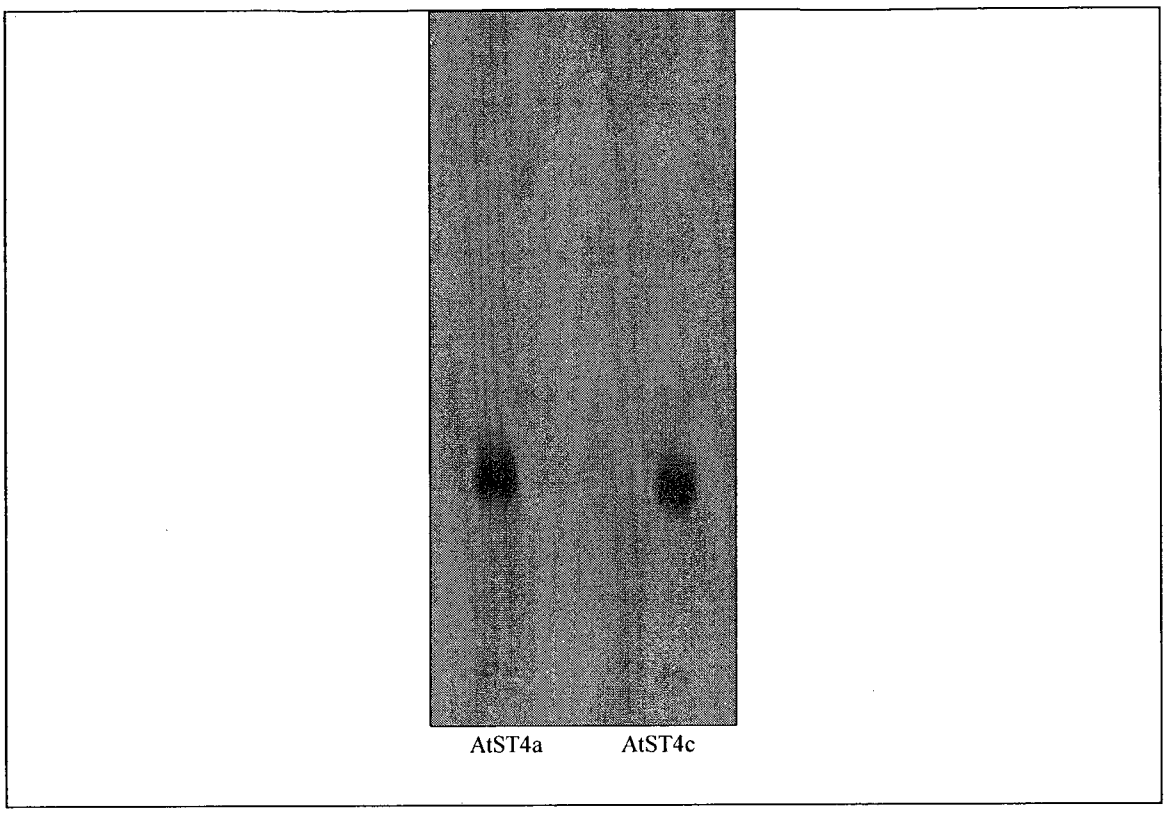

Figure 22. Thin layer chromatography of AtST4a and AtST4c sulfated products. 15,000 DPM of purified AtST4a and AtST4c products were spotted on a cellulose TLC plate.

3.6) Characterization of *AtST4a* and *AtST4c* biological function

3.6.1) Introduction

In order to determine their biological function, the consequence of changing the sulfated metabolome of *AtST4*a and *AtST4c* single mutant was analyzed by monitoring a number of growth parameters known to be under the control of cytokinins.

3.6.2) Primary root length analysis

As mentioned earlier, the three members of the *AtST4* subfamily are expressed in the root system which is also the site of synthesis of cytokinins (Marsolais *et al.* 2007). To

determine the role of these genes in root growth and development, *AtST4a*-KO and *AtST4c*-KO plants were grown vertically on MS agar plates, and their primary root length was measured for 10 days under long day growth conditions. The results show that the roots of *AtST4c*-KO plants were statistically shorter than those of the wild type plants (9 to 37% shorter) for the first eight days after germination (Fig. 23A). The decrease in the root growth rate of *AtST4c*-KO was greater at the beginning of their lifespan (28% between 2 to 6 DAG as opposed to 9% between 6 to 8 DAG). In contrast, *AtST4a*-KO plants showed a significant decrease in root lenght only after 8 days of growth. Moreover, the decrease in primary root growth rate was not as great as the one observed for the *AtST4c*-KO plants (6.5 to 14% decrease between 8 DAG and 10 DAG).

3.6.3) Number of lateral roots

A loss of function mutation in *AtST4a* did not cause a strong effect on the number of lateral roots at 10 and 13 DAG. In contrast, *AtST4c*-KO plants produced 17% to 28% less lateral roots than wild type plants (*P*-value is $4.49E^{-4}$ and 0.069 at 10 DAG and 13 DAG, respectively) (Fig. 23B).

A

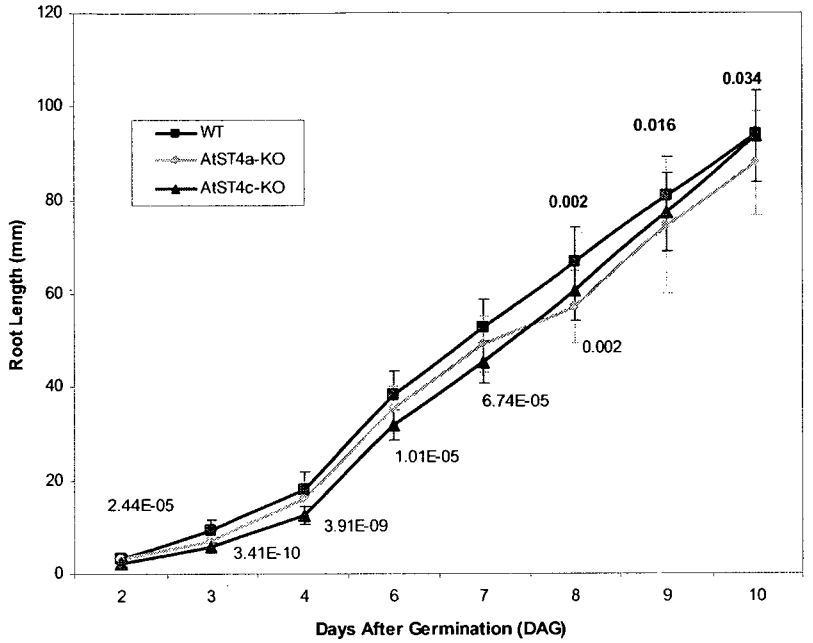
120
100
80
60
40
20
0
Root Length (mm)
WT
AtST4a-KO
AtST4c-KO
0.034
0.016
0.002
0.002
6.74E-05
1.01E-05
3.91E-09
3.41E-10
2.44E-05
2
3
4
6
7
8
9
10
Days After Germination (DAG)

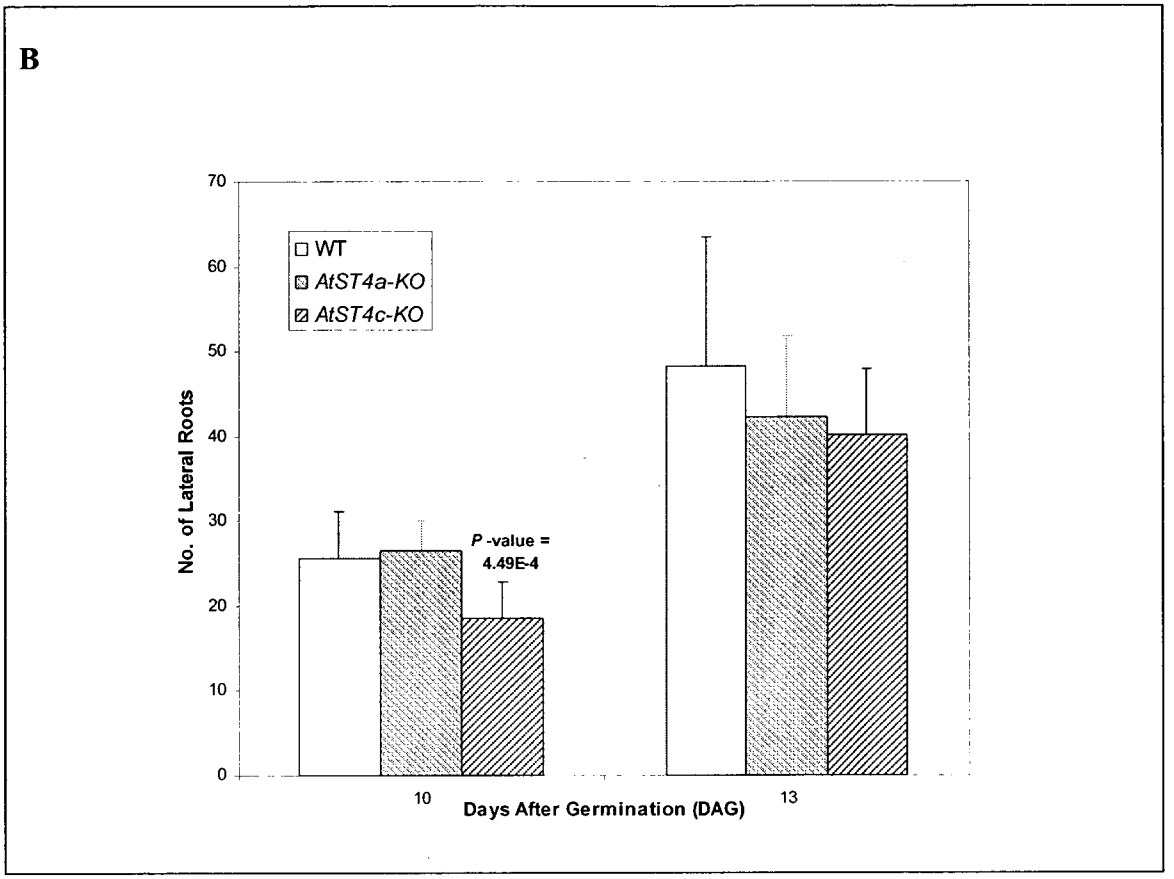

Figure 23. Root development of *AtST4a*-KO and *AtST4c*-KO. (A) Kinetic of root growth in wild type, *AtST4a*-KO and *AtST4c*-KO plants. Plants were grown vertically on MS agar plates and the root length was measured daily. Labels for each day show the corresponding *P*-value for *AtST4a* (green) and *AtST4c* (blue). Error bars represent standard deviation (SD) ($17 \leq n \leq 44$). **(B)** Number of lateral roots of plants grown on MS agar plates 10 and 13 DAG. Error bars represent SD ($12 \leq n \leq 21$). Statistical analysis was performed by a Kruskal-Wallis test followed by a Mann-Whitney U test. Only *P*-values less than 0.05 are shown. See Annex 1 for detailed statistical values.

3.6.4) Rosette diameter

It is well known that cytokinins promote cell division and shoot development in plants (Mok and Mok 2001; Werner *et al.* 2003). Analysis of the Genevestigator (web-browser data mining interface for Affymetrix Gene Chip data) showed that cytokinins slightly repress *AtST4a* and/or *AtST4c* expression in seedlings (~0.8 fold repression after 1h and

3h treatment with 1μM *t*-zeatin). Analysis of long day grown *AtST4a*-KO plants showed a slight increase in rosette diameter 21 DAG compared to wild type plants (*P*-value=0.035). However, the change is very small and the significance of the result is weak. By contrast, *AtST4c*-KO showed a slight decrease in rosette diameter 26 DAG compared to wild type plants (*P*-value=0.014) (Fig. 24A). This experiment was repeated for *AtST4c*-KO plants and we observed a significant decrease of 13% (*P*-value=0.017) to 30% (*P*-value $=1.03E^{-7}$) in rosette size compared to wild type plants 21 and 26 DAG, respectively (data not shown). The consistent reduction in rosette size observed in both experiments suggests that *AtST4c* might play a positive role in the growth of the aerial tissue in Arabidopsis.

We also observed that the rosette of *AtST4c*-KO plants is bending towards the ground. A careful observation of the seedlings showed an increase in hypocotyl length in the *AtST4c*-KO plants (Fig. 24C).

3.6.5) Number of leaves

We also examined leaf formation in *AtST4a*-KO and *AtST4c*-KO plants. The number of leaves of *AtST4a*-KO plants was slightly increased when compared to wild type plants (~6.8% more at 21 DAG, *P*-value=0.010) (Fig. 24B). However, the contribution of *AtST4a* on growth is marginal when we consider the very small increase in leaf number and the relatively high *P*-value observed in this experiment. In contrast, leaf number was significantly reduced in *AtST4c*-KO plants with ~43% less leaves 21 DAG (*P*-value=$9.03E^{-12}$).

3.6.6) Flowering time

Under long day conditions, *AtST4c*-KO plants flowered earlier than wild type plants, while *AtST4a*-KO showed no apparent changes in the time of flowering. Approximately 25 DAG, wild type plants have 12 to 14 leaves and start to flower. In contrast, *AtST4c*-KO plants initiated flowering 21 DAG and have 6 to 7 leaves (Fig. 24D). The morphology of the flowers in *AtST4a*-KO and *AtST4c*-KO was found to be similar to wild type plants.

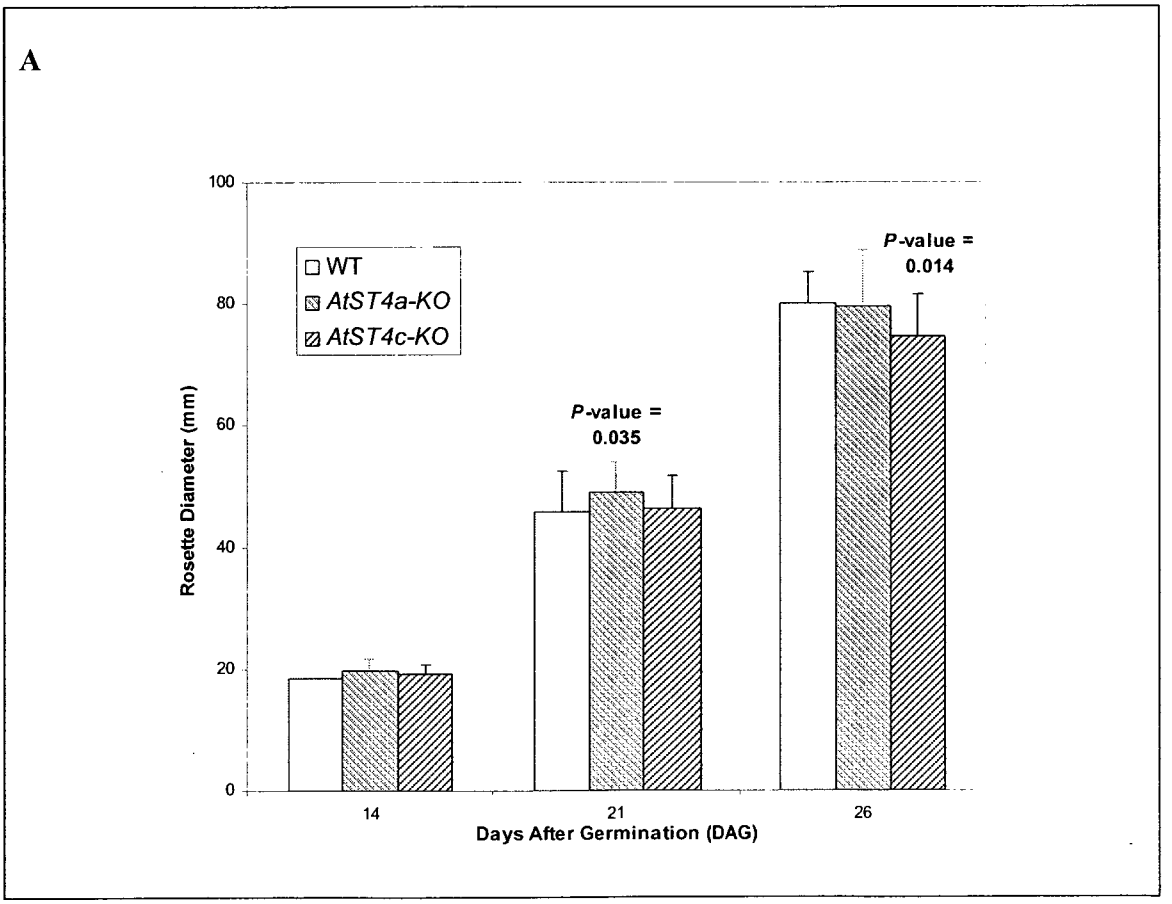

B

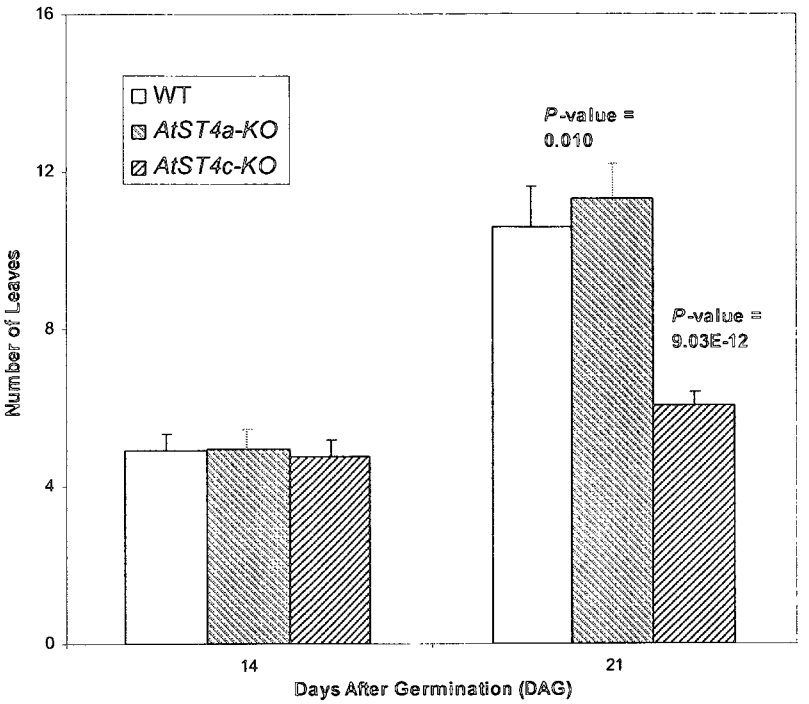
16
12
8
4
0
Number of Leaves
WT
AtST4a-KO
AtST4c-KO
P-value =
0.010
P-value =
9.03E-12
14
21
Days After Germination (DAG)

C

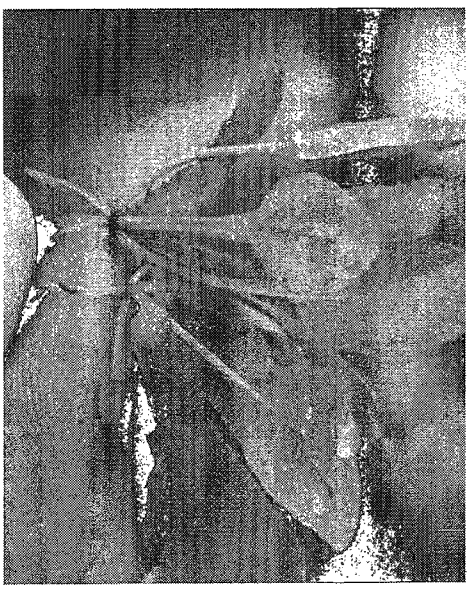

D

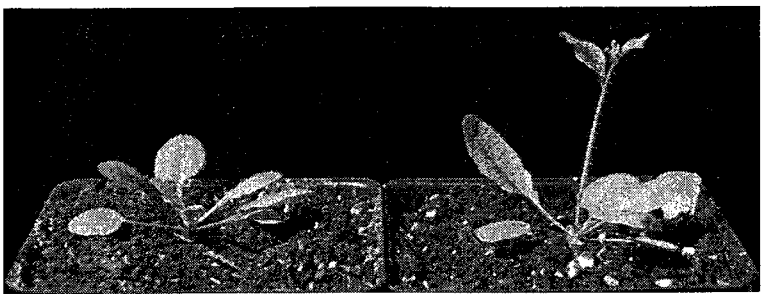

Figure 24. Shoot phenotype of *AtST4a*-Ko and *AtST4c*-KO. (A) Rosette diameter of in-soil grown plants 14, 21 and 26 DAG. Error bars represent SD ($21 \leq n \leq 27$). **(B)** Number of leaves of in-soil grown plants 14, 21 DAG. Error bars represent SD ($21 \leq n \leq 39$). **(C)** Comparison of hypocotyl region in wild type (top) and *AtST4c*-KO (bottom). **(D)** Early flowering phenotype of *AtST4c*-KO (right) was compared to wild type (left) plants at 22 DAG. Analysis of significance between wild type and mutant lines was performed using a Kruskal-Wallis test followed by a Mann-Whitney U test. Only *P*-values with a significance level less than 0.05 are shown. See Annex 2 for detailed statistical values.

3.6.7) Seed production

The number of siliques was higher in *AtST4a*- and *AtST4c*-KO plants than wild type plants. *AtST4a*-KO plants produced on average 62% more siliques 36 and 46 DAG as compared to wild type plants. Silique number was even higher in the *AtST4c*-KO line (~360% and 76% more siliques 36 and 46 DAG, respectively) than that of *AtST4a* (Fig. 25A and C). Analysis of mature siliques showed that the number of seeds per silique was not changed significantly in *AtST4a*-KO. However, there was a ~17% reduction in seed number in the siliques of *AtST4c*-KO plants compared to the wild type counterparts (*P*-value=$4.94E^{-7}$) (Fig. 25B).

A

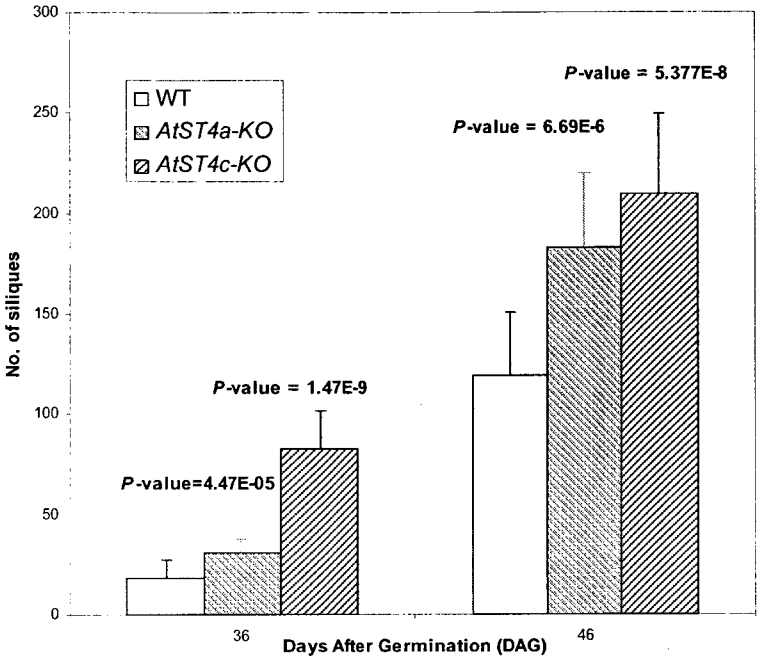
300
250
200
150
100
50
0
No. of siliques
WT
AtST4a-KO
AtST4c-KO
P-value = 5.377E-8
P-value = 6.69E-6
P-value = 1.47E-9
P-value=4.47E-05
36
46
Days After Germination (DAG)

B

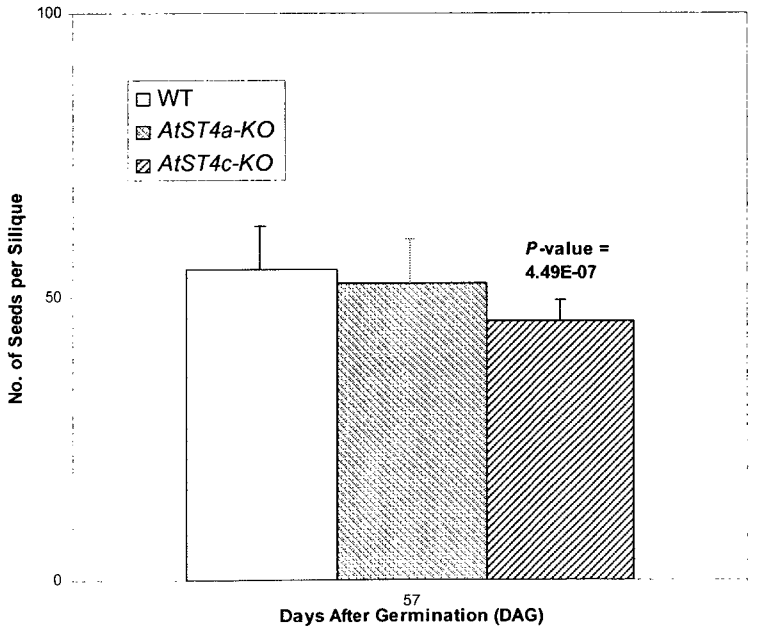
100
50
0
No. of Seeds per Silique
WT
AtST4a-KO
AtST4c-KO
P-value =
4.49E-07
57
Days After Germination (DAG)

C

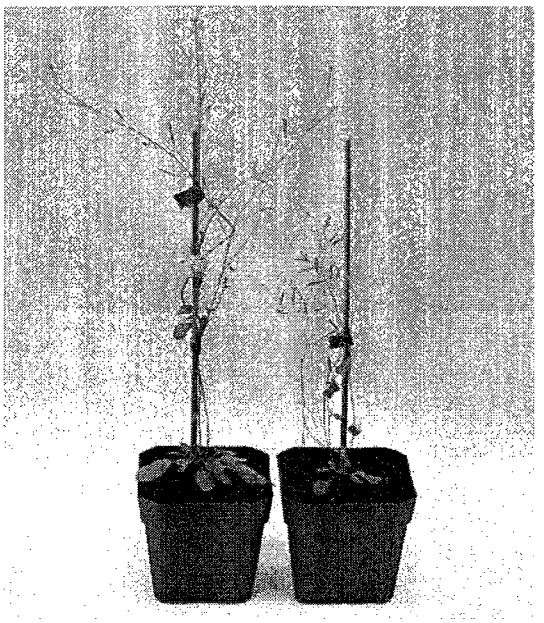

Figure 25. Reproductive developments of *AtST4a*- and *AtST4c*-KO. (A) Number of siliques per plant 36 and 46 DAG. Error bars represent SD ($n \geq 23$). **(B)** Number of seeds per mature siliques 57 DAG. Error bars represent SD (n=30). **(C)** Photograph of wild type (left) and *AtST4c*-KO (right) plants 5 weeks after germination. Analysis of significance between wild type and mutant lines was performed using a Kruskal-Wallis test followed by a Mann-Whitney U test. Only *P*-values with a significant level less than 0.05 are shown. See Annex 3 for detailed statistical values.

3.6.8) Seed size and volume of the *AtST4c*-KO plants

Analysis of seed size was only performed on the *AtST4c*-KO plants. The results presented in Fig. 26A and 26C show that mutant seeds are smaller than wild type seeds. *AtST4c*-KO seeds are approximately 6.2% (length) and 8.6% (width) smaller when compared to wild type seeds. As a consequence of the reduction in seed length and width, the *AtST4c*-KO seed volume is decreased by 21.5% compared to wild type seed volume (Fig. 26B).

A

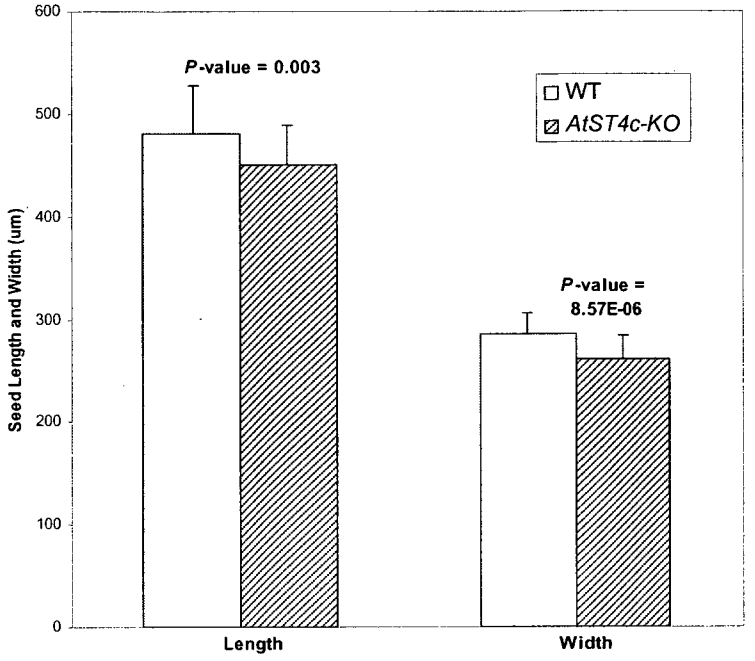
600
500
400
300
200
100
0
Seed Length and Width (um)
P-value = 0.003
P-value =
8.57E-06
WT
AtST4c-KO
Length
Width

B

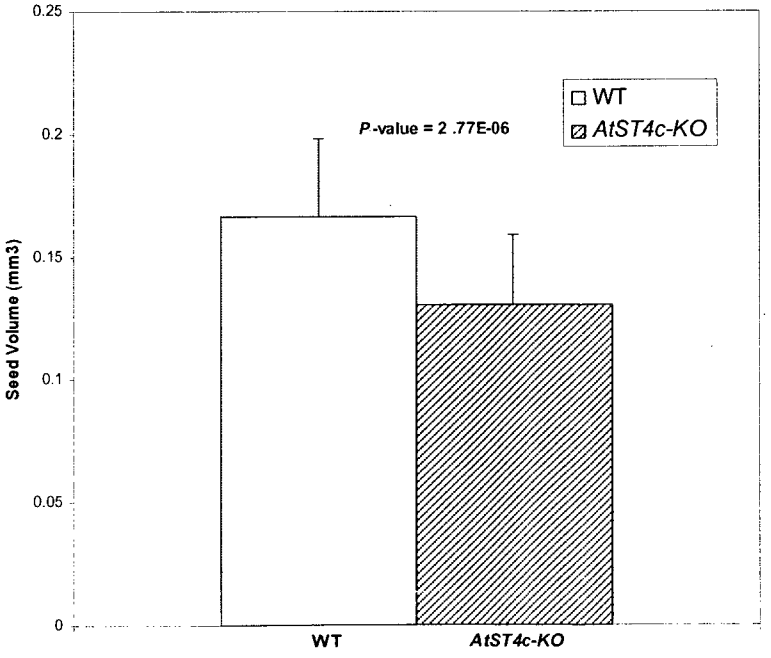
0.25
0.2
0.15
0.1
0.05
0
Seed Volume (mm3)
P-value = 2 .77E-06
WT
AtST4c-KO
WT
AtST4c-KO

C

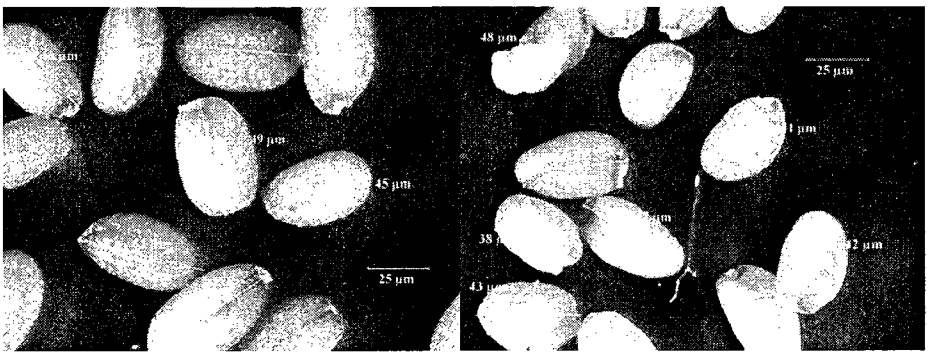

Figure 26. Seed size of *AtST4c*-KO plants. (A) Width and length of seeds in wild type and *AtST4c*-KO plants. Error bars represent SD (n=40). **(B)** Calculated volume of wild type and *AtST4c*-KO seeds based on the formula 4/3 π x length x width x depth (Riefler et al. 2006). Error bars represent SD (n=40). **(C)** Wild type seeds (right) compared to *AtST4c*-KO seeds (left). Analysis of significance between wild type and mutant lines was performed using a Kruskal-Wallis test followed by a Mann-Whitney U test. Only *P*-values less than 0.05 are shown. See Annex 3 for detailed statistical values.

Chapter 4- Discussion and Future work

Soluble sulfotransferases are a superfamily of enzymes that are widely distributed in plants, bacteria and mammals. Our knowledge about their function in plants is suffering from the lack of systematic investigations of plant sulfated metabolomes. Out of the 18 sulfotransferase-coding genes in *A. thaliana*, seven have been fully characterized. Herein, we describe the results of our studies on the biochemical and biological characterization of the three members of the *AtST4* subfamily (*AtST4a*, *AtST4b*, and *AtST4c*) in *A. thaliana*.

4.1) Biochemical and biological characterization of AtST4b

AtST4b shares 72% amino acid sequence identity with AtST4a and 77% amino acid sequence identity with AtST4c (for the phylogenic tree, refer to Fig. 2). Analysis of the publicly available microarray data showed that *AtST4b* is specifically expressed in roots of young seedlings and up-regulated by cytokinins (Zimmermann *et al.* 2004). Such an up-regulation of *AtST4b* by cytokinins has been reported in several genome-wide microarray studies of *A. thaliana* (Hoth *et al.* 2003; Kiba *et al.* 2005; Lee *et al.* 2007; Yokoyama *et al.* 2007) (for a summary refer to Chapter 1). These results were confirmed by transcript expression analysis of the roots of Arabidopsis where *AtST4b* showed gradual up-regulation by the exogenous application of the cytokinin *t*-zeatin (Fig. 8). The detailed analyses of the microarray data showed that in transgenic plants that over-express ARR22 (a type-B ARR), *AtST4b* is up-regulated 11.3 fold compared to wild-type plants (Kiba *et al.* 2005). A change in expression of *AtST4b* is also reported in the microarray analysis of the ARR10 and ARR12 double mutant (two type-B ARRs)

(Yokoyama *et al.* 2007). These results are consistent with the presence of a relatively high number of cytokinin response elements recognized by type-B ARRs in the promoter region of the *AtST4b* gene (Table 1). Taken together, these results support the hypothesis that the function of the *AtST4b* gene might be related to the cytokinin plant response.

Metabolite analysis of *AtST4b*-KO plants revealed that cadabicine (a dicoumaroyl spermidine conjugate) is the substrate of AtST4b in *A. thaliana* and that the formation of cadabicine sulfate is dependent on AtST4b sulfotransferase activity (Fig. 13). Metabolite profiling of the wild type and mutant plants showed that although cadabicine sulfate is missing in the *AtST4b*-KO plants, the substrate (cadabicine, m/z 436) is present in the root extract of both *AtST4b*-KO and wild type plants (data not shown).

Cadabicine has only been reported to occur in members of the Capparaceae and Brassicaceae family which belong to the Brassicales order (Khanfar *et al.* 2003; Baumert *et al.* 2005). In this study, we demonstrate for the first time that cadabicine sulfate occurs naturally in roots and leaves (data not shown) of *A. thaliana*. To date, there is no information available on the function of spermidine conjugates such as cadabicine on growth and development. Our results suggest that the sulfonation of cadabicine might be related to the effects mediated by cytokinins on root and shoot development.

The results of several experiments revealed the important role of the polyamine spermidine during growth and development in various organisms. For example, the study of the spermidine synthesis coding gene mutant (Δspe2), showed that spermidine and/or spermine are absolutely required for the growth and cell division of *Saccharomyces cerevisiae* cells (Chattopadhyay *et al.* 2002). Other studies have shown that it is the presence of spermidine and not spermine, which is absolutely necessary for the growth of

yeast cells (Hamasaki-Katagiri *et al.* 1997; Hamasaki-Katagiri *et al.* 1998). Similar results were obtained in higher plants. Imai *et al.* showed that even though spermine is not essential for survival, suppression of the two genes involved in spermidine biosynthesis (*SPDS1* and *SPDS2*) is lethal in Arabidopsis, and results in embryonic arrest in the double mutant seeds (Imai *et al.* 2004; Imai *et al.* 2004).

Acylated polyamines are synthesized by members of the BAHD acyltransferase family. These enzymes are widely distributed in plants and play regulatory roles during plant growth and development (for a review refer to (Facchini *et al.* 2002; Bienz *et al.* 2005). The accumulation of hydroxycinnamic acid spermidine conjugates has only recently been reported in *A. thaliana* (Grienenberger *et al.* 2009; Luo *et al.* 2009). Using functional genomics and metabolic profiling, Luo *et al.* determined that sinapoyl and disinapoyl spermidine are the major polyamine conjugates that accumulate in Arabidopsis seeds. Furthermore, they characterized At2g25150 encoding for a spermidine dicoumaroyl transferase (SCT) that transfers two coumaric acids to its spermidine acyl acceptor molecule. Interestingly, SCT is predominantly expressed in root tips and up-regulated by *t*-zeatin. Its co-regulation and co-expression with *AtST4b* suggests that the N1, N8-di(couamaroyl)-spermidine produced by SCT is a precursor for the synthesis of cadabicine, the substrate of *AtST4b*. In support of this hypothesis, metabolite analysis of SCT-knockout Arabidopsis plants conducted in our laboratory showed the absence of cadabicine and cadabicine sulfate in root tissue (data not shown).

It has been shown previously that the exogenous application of cytokinins increase the accumulation of free polyamines and of their conjugates in plants (Altman 1988; Sergive *et al.* 1995). More recently, the up-regulation of spermidine synthesis coding genes was

reported in response to the application of cytokinins on Arabidopsis seedlings (Hanzawa *et al.* 2002). In addition, several recent studies show that there is an interaction between the cytokinins and polyamines signaling pathways. Different polyamines, especially spermine, prevent cytokinin-induced expression of ARR5, a type-A response regulator gene, in Arabidopsis and Amaranthus (Rakova and Romanov 2005). The antagonistic function of cytokinins and of the polyamines spermine and spermidine has been reported in other older studies as well (Naika *et al.* 1980; Feray *et al.* 1992). Considering the similarity of their physiological activity, and based on the above information, it has been proposed that cytokinins mediate their function partially through the regulation of polyamines homeostasis.

The negative role of cytokinins on root growth and development has been known for a long time (Cary *et al.* 1995). Analysis of the *AtST4b* loss-of-function mutant revealed a negative regulatory role of this gene on root growth in Arabidopsis (Fig. 15). Furthermore, *AtST4b* homozygous mutants showed reduced sensitivity to different concentrations of cytokinins (Fig. 15A and 15C). The reduced sensitivity to cytokinin inhibition of root growth is also reported in plants with impaired-cytokinin signaling such as the Arabidopsis cytokinin receptor mutants (Higuchi *et al.* 2004; Nishimura *et al.* 2004), the Arabidopsis histidine phosphotransfer (AHPs) mutants (Hutchison *et al.* 2006), the Arabidopsis type-B ARR mutants (Mason *et al.* 2005) and the cytokinin-deficient tobacco plants that overexpress different cytokinin oxidases (CKXs) (Werner *et al.* 2001). However, the role of *AtST4b* in shoot and reproductive development is not consistent with the known cytokinin function. The *AtST4b*-KO plants produce more leaves, slightly bigger rosette, more siliques and bigger seeds than wild type plants. In

contrast, cytokinin *ahk2/3/4* triple receptor mutants and cytokinin-deficient plants produce stunted shoots (with decreased leaf size and number), less seeds per siliques or infertile but bigger seeds (Werner *et al.* 2001; Werner *et al.* 2003; Higuchi *et al.* 2004; Nishimura *et al.* 2004; Riefler *et al.* 2006).

Several hypotheses can be proposed to explain the overall improved root and shoot growth of *AtST4b*-KO plants. In the first hypothesis, we can consider that cadabicine is a positive growth regulator and is inactivated by sulfonation. A similar inactivation function has been previously proposed for *AtST2a* in controlling the biological activity of 12-hydroxyjasmonic acid in *A. thaliana* (Gidda *et al.* 2003). Accumulation of polyamine conjugates has been shown to promote cell division, flower formation, organogenesis and tuber induction in plants (Facchini *et al.* 2002). In this scenario, it is the accumulation of cadabicine in *AtST4b* mutant plants that induces plant growth. The results of mass spectrometry analyses support this hypothesis, and show that endogenous levels of free cadabicine is much higher in roots of *AtST4b*-KO plants compared to wild type plants (data not shown). Alternatively, cadabicine sulfate might be a general growth inhibitor and its absence would explain the improved growth observed for the *AtST4b*-KO plants. In order to find out which of the two possibilities is right, a careful examination of the growth parameters of the *sct* mutant which can not synthesize cadabicine and cadabicine sulfate will be required. AtST4b can also be part of a pathway that copes with excess polyamines or polyamine conjugates in plants. Interestingly, the increase in the intracellular polyamines induces the spermidine/spermine N1-acetyltransferase (SSAT) gene which in turn inactivates the excess spermine and spermidine in humans (Moinard *et al.* 2005). To our knowledge, there is no SSAT in the genome of Arabidopsis.

However, a similar inactivation mechanism can be proposed in Arabidopsis in which spermidine dicoumaroyl transferase (SCT) and AtST4b control excessive spermidine accumulation in cells. Other conjugating enzymes might partly complement the missing SCT or AtST4b to prevent the toxic accumulation of spermidine but allowing an increase in spermidine accumulation sufficient to explain the improved growth phenotype.

In order to better understand the function of cadabicine and cadabicine sulfate in plants, several experiments will have to be conducted in the future.

- Comparison of the levels of spermidine and of its derivatives in *AtST4b-KO, sct-KO* and wild type plants. The results of these studies would allow to characterize other molecules that could affect growth in Arabidopsis and to have a better understanding of the dynamic of the accumulation of these important molecules.
- Study the tissue distribution of spermidine and its derivatives in Arabidopsis. *SCT* and *AtST4b* are only expressed in the root system. However, we could detect accumulation of cadabicine in the aerial parts suggesting a transport mechanism. The cytokinin-dependent sulfonation reaction taking place in the roots might block the transport of active cadabicine in the aerial parts. This would explain the increased growth of the shoot and root system of the *AtST4b* mutant plants.
- Careful examination of the growth behavior of the *sct* mutant. This mutant cannot synthesize cadabicine and cadabicine sulfate. A reduced growth phenotype would support a positive role for cadabicine. In contrast, an improved growth phenotype would support an inhibitory role of the final product, cadabicine sulfate.
- Construction and analysis of growth parameters of a transgenic line overexpressing *AtST4b*. The availability of this overexpressor line would allow a

cytokinin independent reduction of the pool of cadabicine in the aerial part of the plant and to study its effect on shoot growth and seed set.

4.2) Biochemical and biological characterization of AtST4a and AtST4c

Based on their amino acid sequence similarity, AtST4a and AtST4c are more closely related to each other (80% amino acid sequence identity) than to AtST4b. Analysis of the Genevestigator microarray database and our RT-PCR experimental results show that both genes are expressed mainly in roots and are down-regulated by cytokinins (Fig. 8 and Fig. 9C) (Zimmermann *et al.* 2004; Marsolais *et al.* 2007). Investigation of their promoter region also confirmed the presence of cytokinin regulatory motifs (Table 1). However, in contrast with *AtST4b*, *AtST4a* and *AtST4c* are repressed by cytokinins suggesting that they might have opposite functionalities.

Unfortunately, we were not able to identify the reaction products of AtST4a and AtST4c *in vivo*. The sulfated metabolome of *AtST4a*- and *AtST4c*-KO root extracts is almost identical to the wild type one, suggesting a redundant function for the two enzymes (Fig. 20, Fig. 21, and Fig. 22). However, the loss of function mutation of the two genes gave different phenotypes suggesting that the two enzymes might have different substrates with very similar chemical properties. Alternatively, the two genes might sulfonate the same substrate in different tissues explaining the different phenotypes.

Recently, AtST4a has been characterized *in vitro* and was shown to exhibit a relatively broad specificity toward brassinosteroids (Marsolais *et al.* 2007). However, the natural occurrence of sulfated brassinosteroids (BRs) has not been reported yet. BRs are widely distributed in plants, and play several regulatory roles during growth and development. Analysis of BR-deficient and -insensitive mutants confirmed their essential role for cell

elongation, male fertility, senescence and vascular differentiation (Clouse *et al.* 1996; Altmann 1998).

The crosstalk between cytokinins and BRs regulatory pathways is reported in several studies. For example, BRs interact with cytokinins and other phytohormones like auxin to regulate ethylene biosynthesis in plants (Arteca and Arteca 2008; Hansen *et al.* 2009). The physiological roles of cytokinins and BRs are similar in some aspects. BRs, like cytokinins, stimulate cell division through up-regulation of cyclin D3, a member of a family of proteins that allow progression through the cell cycle, and BRs can even substitute cytokinins in cell cultures of Arabidopsis. However, it is postulated that the pathway by which BRs regulate cyclin D3 is different from the one induced by cytokinins (Hu *et al.* 2000). The shoot growth promoting activity of BRs is also similar to the one induced by cytokinins (for a review see (Clouse and Sasse 1998). On the other hand, the effect of BRs on root growth is intriguing and contradictory results have been explained by the use of different experimental conditions. For example, even though low concentrations (<pM) of exogenous BRs stimulate root growth in wild type plants, higher concentrations were found to be inhibitory (Clouse *et al.* 1996; Mussig *et al.* 2003).

Based on the fact that CKs and BRs have inhibitory and stimulatory effects on growth, cytokinin-mediated repression of a brassinosteroid sulfotransferase can be part of a pathway in which both CKs and BRs are working together in order to regulate root and shoot growth in *A.thaliana*. This hypothesis will be confirmed only when we will be able to demonstrate that the AtST4a and/or AtST4c enzymes are sulfonating brassinosteroids *in vivo*.

Phenotypic analyses of the loss of function mutants revealed that, unlike *AtST4b*, *AtST4c* seems to play a positive function in root and shoot growth in Arabidopsis. *AtST4c*-KO plants produced shorter primary roots, reduced number of lateral roots, slightly smaller rosettes, reduced number of leaves, less seeds per siliques and finally smaller seeds. Based on the repression of *AtST4c* expression by cytokinins and the phenotype of the loss of function mutant, one can conclude that *AtST4c*, as opposed to *AtST4b*, positively regulates plant growth and that this positive effect is repressed by the cytokinin signaling pathway. In general, loss of *AtST4a* did not cause a strong phenotype in root and shoot growth. This mild effect is consistent with the weak expression of this gene seen in RT-PCR reactions (Fig. 8 and Fig. 9C).

AtST4c-KO plants flower earlier than wild type Arabidopsis. This phenotype was highly reproducible and observed in soil and *in vitro* grown plants. The late-flowering phenotype has also been reported in some cytokinin-deficient (Werner *et al.* 2003) and cytokinin-insensitive Arabidopsis mutants (Nishimura *et al.* 2004; Riefler *et al.* 2006) suggesting a positive role of cytokinins in flower induction. Furthermore, the relationship between *AtST4c* expression and flowering is strengthened by the fact that *AtST4c* (or *AtST4a*) is repressed by the *LEAFY* (*LFY*) gene (~9.84 and 13.14 fold induction in lfy-12 and 35S::amiR-lfy-1, respectively) (Zimmermann *et al.* 2004). *LEAFY* is a floral-meristem identity gene that regulates transition to flowering and the subsequent patterning of young floral meristems (Schultz and Haughn 1991; Huala and Sussex 1992). The link between the floral meristem-identity genes and flowering-time genes has been difficult to assess, but it is presumed that the former regulate onset of flowering in response to environmental stimuli and action of the genes that induce flowering time.

Taken together, these results suggest that the general growth reduction of the *AtST4c-KO* mutant growth might be the result of a premature switch from vegetative to reproductive growth, which is accompanied by a general growth arrest. In order to clarify the role of *AtST4c* in cytokinin-mediated growth control and its role in flowering, the following experiments should be performed in the future.

- Identify the endogenous substrate of AtST4c. Two approaches should be used: Overexpression of *AtST4c* to allow the identification of the sulfated product and analysis of the sulfated metabolome of the *AtST4a/4c* double mutant.
- Localize the site of expression of *AtST4a* and *AtST4c* in whole plants by the construction of promoter-GFP fusions.
- Study *AtST4c* expression in other meristem identity mutants of Arabidopsis.
- Study the regulation of meristem identity genes in the *AtST4c*-KO mutant.

References:

Altman, A. (1988). Polyamines and plant hormones. The Physiology of Polyamines. I. U. Bachrach and Y. M. Heimer, CRC Press Inc, Boca Raton, FL. **11**.

Altmann, T. (1998). "Recent advances in brassinosteroid molecular genetics." Curr Opin Plant Biol **1**(5): 378-383.

Arteca, R. N. and J. M. Arteca (2008). "Effects of brassinosteroid, auxin, and cytokinin on ethylene production in Arabidopsis thaliana plants." J Exp Bot **59**(11): 3019-3026.

Ashikari, M., H. Sakakibara, S. Lin, T. Yamamoto, T. Takashi, A. Nishimura, E. R. Angeles, Q. Qian, H. Kitano and M. Matsuoka (2005). "Cytokinin oxidase regulates rice grain production." Science **309**(5735): 741-745.

Baumert, A., C. Milkowski, J. Schmidt, M. Nimtz, V. Wray and D. Strack (2005). "Formation of a complex pattern of sinapate esters in Brassica napus seeds, catalyzed by enzymes of a serine carboxypeptidase-like acyltransferase family?" Phytochemistry **66**(11): 1334-1345.

Bienz, S., P. Bisegger, A. Guggisberg and M. Hesse (2005). "Polyamine alkaloids." Nat Prod Rep **22**(5): 647-658.

Blanchard, R. L., R. R. Freimuth, J. Buck, R. M. Weinshilboum and M. W. Coughtrie (2004). "A proposed nomenclature system for the cytosolic sulfotransferase (SULT) superfamily." Pharmacogenetics **14**(3): 199-211.

Bonneau, L., M. Carre and Martin-Tanguy J. (1994). "Polyamines and related enzymes in rice seeds differing in germination potential." Plant Growth Regulation **15**: 75 -82.

Brenner, W. G., G. A. Romanov, I. Kollmer, L. Burkle and T. Schmulling (2005). "Immediate-early and delayed cytokinin response genes of Arabidopsis thaliana identified by genome-wide expression profiling reveal novel cytokinin-sensitive processes and suggest cytokinin action through transcriptional cascades." Plant J **44**(2): 314-333.

Cary, A. J., W. Liu and S. H. Howell (1995). "Cytokinin action is coupled to ethylene in its effects on the inhibition of root and hypocotyl elongation in Arabidopsis thaliana seedlings." Plant Physiol **107**(4): 1075-1082.

Chang, C. and R. C. Stewart (1998). "The two-component system. Regulation of diverse signaling pathways in prokaryotes and eukaryotes." Plant Physiol **117**(3): 723-731.

Chapman, E., M. D. Best, S. R. Hanson and C. H. Wong (2004). "Sulfotransferases: structure, mechanism, biological activity, inhibition, and synthetic utility." Angew Chem Int Ed Engl **43**(27): 3526-3548.

Chattopadhyay, M. K., C. W. Tabor and H. Tabor (2002). "Absolute requirement of spermidine for growth and cell cycle progression of fission yeast (Schizosaccharomyces pombe)." Proc Natl Acad Sci U S A **99**(16): 10330-10334.

Clouse, S. D., M. Langford and T. C. McMorris (1996). "A brassinosteroid-insensitive mutant in Arabidopsis thaliana exhibits multiple defects in growth and development." Plant Physiol **111**(3): 671-678.

Clouse, S. D. and J. M. Sasse (1998). "BRASSINOSTEROIDS: Essential Regulators of Plant Growth and Development." Annu Rev Plant Physiol Plant Mol Biol **49**: 427-451.

D'Agostino, I. B., J. Deruere and J. J. Kieber (2000). "Characterization of the response of the Arabidopsis response regulator gene family to cytokinin." Plant Physiol **124**(4): 1706-1717.

D'Agostino, I. B. and J. J. Kieber (1999). "Phosphorelay signal transduction: the emerging family of plant response regulators." Trends Biochem Sci **24**(11): 452-456.

D'Auria, J. C. (2006). "Acyltransferases in plants: a good time to be BAHD." Curr Opin Plant Biol **9**(3): 331-340.

Dello Ioio, R., F. S. Linhares, E. Scacchi, E. Casamitjana-Martinez, R. Heidstra, P. Costantino and S. Sabatini (2007). "Cytokinins determine Arabidopsis root-meristem size by controlling cell differentiation." Curr Biol **17**(8): 678-682.

Facchini, P. J., Hagel Jillian and Z. K. G. (2002). "Hydroxycinnamic acid amide metabolism:
physiology and biochemistry." Can. J. Bot. **80**: 577-589.

Farzan, M., T. Mirzabekov, P. Kolchinsky, R. Wyatt, M. Cayabyab, N. P. Gerard, C. Gerard, J. Sodroski and H. Choe (1999). "Tyrosine sulfation of the amino terminus of CCR5 facilitates HIV-1 entry." Cell **96**(5): 667-676.

Feray, A., A. Hourmant, M. Penot, C. Moisan-Cann and J. Caroff (1992). "Effects of interaction between polyamines and benzyladenine on betacyanin." Journal of plant physiology **139**(6): 680-684.

Ferreira, F. J. and J. J. Kieber (2005). "Cytokinin signaling." Curr Opin Plant Biol **8**(5): 518-525.

Gan, S. and R. M. Amasino (1995). "Inhibition of leaf senescence by autoregulated production of cytokinin." Science **270**(5244): 1986-1988.

Gidda, S. K., O. Miersch, A. Levitin, J. Schmidt, C. Wasternack and L. Varin (2003). "Biochemical and molecular characterization of a hydroxyjasmonate sulfotransferase from Arabidopsis thaliana." J Biol Chem **278**(20): 17895-17900.

Gidda, S. K. and L. Varin (2006). "Biochemical and molecular characterization of flavonoid 7-sulfotransferase from Arabidopsis thaliana." Plant Physiol Biochem **44**(11-12): 628-636.

Grienenberger, E., S. Besseau, P. Geoffroy, D. Debayle, D. Heintz, C. Lapierre, B. Pollet, T. Heitz and M. Legrand (2009). "A BAHD acyltransferase is expressed in the tapetum of Arabidopsis anthers and is involved in the synthesis of hydroxycinnamoyl spermidines." Plant J **58**(2): 246-259.

Hamasaki-Katagiri, N., Y. Katagiri, C. W. Tabor and H. Tabor (1998). "Spermine is not essential for growth of Saccharomyces cerevisiae: identification of the SPE4 gene (spermine synthase) and characterization of a spe4 deletion mutant." Gene **210**(2): 195-201.

Hamasaki-Katagiri, N., C. W. Tabor and H. Tabor (1997). "Spermidine biosynthesis in Saccharomyces cerevisae: polyamine requirement of a null mutant of the SPE3 gene (spermidine synthase)." Gene **187**(1): 35-43.

Hansen, M., H. S. Chae and J. J. Kieber (2009). "Regulation of ACS protein stability by cytokinin and brassinosteroid." Plant J **57**(4): 606-614.

Hanzawa, Y., A. Imai, A. J. Michael, Y. Komeda and T. Takahashi (2002). "Characterization of the spermidine synthase-related gene family in Arabidopsis thaliana." FEBS Lett **527**(1-3): 176-180.

Hernàndez-Sebastiá, C., L. Varin and F. Marsolais (2008). Sulfotransferases from Plants, Algae and Phototrophic Bacteria, Advances in Photosynthesis and Respiration, Springer Netherlands.

Heyl, A. and T. Schmulling (2003). "Cytokinin signal perception and transduction." Curr Opin Plant Biol **6**(5): 480-488.

Higuchi, M., M. S. Pischke, A. P. Mahonen, K. Miyawaki, Y. Hashimoto, M. Seki, M. Kobayashi, K. Shinozaki, T. Kato, S. Tabata, Y. Helariutta, M. R. Sussman and T. Kakimoto (2004). "In planta functions of the Arabidopsis cytokinin receptor family." Proc Natl Acad Sci U S A **101**(23): 8821-8826.

Honke, K. and N. Taniguchi (2002). "Sulfotransferases and sulfated oligosaccharides." Med Res Rev **22**(6): 637-654.

Hosoda, K., A. Imamura, E. Katoh, T. Hatta, M. Tachiki, H. Yamada, T. Mizuno and T. Yamazaki (2002). "Molecular structure of the GARP family of plant Myb-related DNA binding motifs of the Arabidopsis response regulators." Plant Cell **14**(9): 2015-2029.

Hoth, S., Y. Ikeda, M. Morgante, X. Wang, J. Zuo, M. K. Hanafey, T. Gaasterland, S. V. Tingey and N. H. Chua (2003). "Monitoring genome-wide changes in gene expression in response to endogenous cytokinin reveals targets in Arabidopsis thaliana." FEBS Lett **554**(3): 373-380.

Hu, Y., F. Bao and J. Li (2000). "Promotive effect of brassinosteroids on cell division involves a distinct CycD3-induction pathway in Arabidopsis." Plant J **24**(5): 693-701.

Huala, E. and I. M. Sussex (1992). "LEAFY Interacts with Floral Homeotic Genes to Regulate Arabidopsis Floral Development." Plant Cell **4**(8): 901-913.

Hutchison, C. E., J. Li, C. Argueso, M. Gonzalez, E. Lee, M. W. Lewis, B. B. Maxwell, T. D. Perdue, G. E. Schaller, J. M. Alonso, J. R. Ecker and J. J. Kieber (2006). "The Arabidopsis histidine phosphotransfer proteins are redundant positive regulators of cytokinin signaling." Plant Cell **18**(11): 3073-3087.

Hwang, I. and J. Sheen (2001). "Two-component circuitry in Arabidopsis cytokinin signal transduction." Nature **413**(6854): 383-389.

Igarashi, K. and K. Kashiwagi (2000). "Polyamines: mysterious modulators of cellular functions." Biochem Biophys Res Commun **271**(3): 559-564.

Imai, A., T. Akiyama, T. Kato, S. Sato, S. Tabata, K. T. Yamamoto and T. Takahashi (2004). "Spermine is not essential for survival of Arabidopsis." FEBS Lett **556**(1-3): 148-152.

Imai, A., T. Matsuyama, Y. Hanzawa, T. Akiyama, M. Tamaoki, H. Saji, Y. Shirano, T. Kato, H. Hayashi, D. Shibata, S. Tabata, Y. Komeda and T. Takahashi (2004). "Spermidine synthase genes are essential for survival of Arabidopsis." Plant Physiol **135**(3): 1565-1573.

Imamura, A., N. Hanaki, A. Nakamura, T. Suzuki, M. Taniguchi, T. Kiba, C. Ueguchi, T. Sugiyama and T. Mizuno (1999). "Compilation and characterization of Arabidopsis thaliana response regulators implicated in His-Asp phosphorelay signal transduction." Plant Cell Physiol **40**(7): 733-742.

Imamura, A., T. Kiba, Y. Tajima, T. Yamashino and T. Mizuno (2003). "In vivo and in vitro characterization of the ARR11 response regulator implicated in the His-to-Asp phosphorelay signal transduction in Arabidopsis thaliana." Plant Cell Physiol **44**(2): 122-131.

Inoue, T., M. Higuchi, Y. Hashimoto, M. Seki, M. Kobayashi, T. Kato, S. Tabata, K. Shinozaki and T. Kakimoto (2001). "Identification of CRE1 as a cytokinin receptor from Arabidopsis." Nature **409**(6823): 1060-1063.

Kakimoto, T. (1996). "CKI1, a histidine kinase homolog implicated in cytokinin signal transduction." Science **274**(5289): 982-985.

Khanfar, M. A., S. S. Sabri, M. H. Zarga and K. P. Zeller (2003). "The chemical constituents of Capparis spinosa of Jordanian origin." Nat Prod Res **17**(1): 9-14.

Kiba, T., T. Naitou, N. Koizumi, T. Yamashino, H. Sakakibara and T. Mizuno (2005). "Combinatorial microarray analysis revealing arabidopsis genes implicated in cytokinin responses through the His->Asp Phosphorelay circuitry." Plant Cell Physiol **46**(2): 339-355.

Kiba, T., M. Taniguchi, A. Imamura, C. Ueguchi, T. Mizuno and T. Sugiyama (1999). "Differential expression of genes for response regulators in response to cytokinins and nitrate in Arabidopsis thaliana." Plant Cell Physiol **40**(7): 767-771.

Klein, M. and J. Papenbrock (2004). "The multi-protein family of Arabidopsis sulphotransferases and their relatives in other plant species." J Exp Bot **55**(404): 1809-1820.

Klein, M., M. Reichelt, J. Gershenzon and J. Papenbrock (2006). "The three desulfoglucosinolate sulfotransferase proteins in Arabidopsis have different substrate specificities and are differentially expressed." FEBS J **273**(1): 122-136.

Klose, M. K., J. K. Atkinson and A. J. Mercier (2002). "Effects of a hydroxy-cinnamoyl conjugate of spermidine on arthropod neuromuscular junctions." J Comp Physiol A Neuroethol Sens Neural Behav Physiol **187**(12): 945-952.

Kurakawa, T., N. Ueda, M. Maekawa, K. Kobayashi, M. Kojima, Y. Nagato, H. Sakakibara and J. Kyozuka (2007). "Direct control of shoot meristem activity by a cytokinin-activating enzyme." Nature **445**(7128): 652-655.

Kusano, T., T. Berberich, C. Tateda and Y. Takahashi (2008). "Polyamines: essential factors for growth and survival." Planta **228**(3): 367-381.

Kusano, T., K. Yamaguchi, T. Berberich and Y. Takahashi (2007). "Advances in polyamine research in 2007." J Plant Res **120**(3): 345-350.

Lee, D. J., J. Y. Park, S. J. Ku, Y. M. Ha, S. Kim, M. D. Kim, M. H. Oh and J. Kim (2007). "Genome-wide expression profiling of ARABIDOPSIS RESPONSE REGULATOR 7(ARR7) overexpression in cytokinin response." Mol Genet Genomics **277**(2): 115-137.

Luo, J., C. Fuell, A. Parr, L. Hill, P. Bailey, K. Elliott, S. A. Fairhurst, C. Martin and A. J. Michael (2009). "A novel polyamine acyltransferase responsible for the accumulation of spermidine conjugates in Arabidopsis seed." Plant Cell **21**(1): 318-333.

Mahonen, A. P., A. Bishopp, M. Higuchi, K. M. Nieminen, K. Kinoshita, K. Tormakangas, Y. Ikeda, A. Oka, T. Kakimoto and Y. Helariutta (2006). "Cytokinin signaling and its inhibitor AHP6 regulate cell fate during vascular development." Science **311**(5757): 94-98.

Mahonen, A. P., M. Bonke, L. Kauppinen, M. Riikonen, P. N. Benfey and Y. Helariutta (2000). "A novel two-component hybrid molecule regulates vascular morphogenesis of the Arabidopsis root." Genes Dev **14**(23): 2938-2943.

Marsolais, F., J. Boyd, Y. Paredes, A. M. Schinas, M. Garcia, S. Elzein and L. Varin (2007). "Molecular and biochemical characterization of two brassinosteroid sulfotransferases from Arabidopsis, AtST4a (At2g14920) and AtST1 (At2g03760)." Planta **225**(5): 1233-1244.

Marsolais, F., C. H. Sebastia, A. Rousseau and L. Varin (2004). "Molecular and biochemical characterization of BNST4, an ethanol-inducible steroid sulfotransferase from Brassica napus, and regulation of BNST genes by chemical stress and during development." Plant science **166**(5): 12.

Mason, M. G., D. E. Mathews, D. A. Argyros, B. B. Maxwell, J. J. Kieber, J. M. Alonso, J. R. Ecker and G. E. Schaller (2005). "Multiple type-B response regulators mediate cytokinin signal transduction in Arabidopsis." Plant Cell **17**(11): 3007-3018.

Miller, C. O., F. Skoog, M. H. V. Saltza and F. M. Strong (1995). "KINETIN, A CELL DIVISION FACTOR FROM DEOXYRIBONUCLEIC ACID1." Journal of the American Chemical Society **77**(5).

Miyata, S., T. Urao, K. Yamaguchi-Shinozaki and K. Shinozaki (1998). "Characterization of genes for two-component phosphorelay mediators with a single HPt domain in Arabidopsis thaliana." FEBS Lett **437**(1-2): 11-14.

Moinard, C., L. Cynober and J. P. de Bandt (2005). "Polyamines: metabolism and implications in human diseases." Clin Nutr **24**(2): 184-197.

Mok, D. W. and M. C. Mok (2001). "Cytokinin Metabolism and Action." Annu Rev Plant Physiol Plant Mol Biol **52**: 89-118.

Mussig, C., G. H. Shin and T. Altmann (2003). "Brassinosteroids promote root growth in Arabidopsis." Plant Physiol **133**(3): 1261-1271.

Naika, B. I., V. Sharmaa and S. K. Srivastavaa (1980). "Interaction between growth regulator and polyamine effects on membrane permeability " Phytochemistry **19**(7): 1321-1322.

Negishi, M., L. G. Pedersen, E. Petrotchenko, S. Shevtsov, A. Gorokhov, Y. Kakuta and L. C. Pedersen (2001). "Structure and function of sulfotransferases." Arch Biochem Biophys **390**(2): 149-157.

Nishimura, C., Y. Ohashi, S. Sato, T. Kato, S. Tabata and C. Ueguchi (2004). "Histidine kinase homologs that act as cytokinin receptors possess overlapping functions in the regulation of shoot and root growth in Arabidopsis." Plant Cell **16**(6): 1365-1377.

Panicot, M., C. Masgrau, A. Borrell, A. Cordeiro, A. F. Tiburcio and T. Altabella (2002). "Effects of putrescine accumulation in tobacco transgenic plants with different expression levels of oat arginine decarboxylase." Physiol Plant **114**(2): 281-287.

Park, J. B. and N. Schoene (2006). "Clovamide-type phenylpropenoic acid amides, N-coumaroyldopamine and N-caffeoyldopamine, inhibit platelet-leukocyte interactions via suppressing P-selectin expression." J Pharmacol Exp Ther **317**(2): 813-819.

Pegg, A. E. (2008). "Spermidine/spermine-N(1)-acetyltransferase: a key metabolic regulator." Am J Physiol Endocrinol Metab **294**(6): E995-1010.

Piotrowski, M., A. Schemenewitz, A. Lopukhina, A. Muller, T. Janowitz, E. W. Weiler and C. Oecking (2004). "Desulfoglucosinolate sulfotransferases from Arabidopsis thaliana catalyze the final step in the biosynthesis of the glucosinolate core structure." J Biol Chem **279**(49): 50717-50725.

Rakova, N. Y. and G. A. Romanov (2005). "Polyamines Suppress Manifestation of Cytokinin Primary Effects." Russian Journal of Plant Physiology **25**(1): 50-57.

Rashotte, A. M., S. D. Carson, J. P. To and J. J. Kieber (2003). "Expression profiling of cytokinin action in Arabidopsis." Plant Physiol **132**(4): 1998-2011.

Riechmann, J. L., J. Heard, G. Martin, L. Reuber, C. Jiang, J. Keddie, L. Adam, O. Pineda, O. J. Ratcliffe, R. R. Samaha, R. Creelman, M. Pilgrim, P. Broun, J. Z. Zhang, D. Ghandehari, B. K. Sherman and G. Yu (2000). "Arabidopsis transcription factors: genome-wide comparative analysis among eukaryotes." Science **290**(5499): 2105-2110.

Riefler, M., O. Novak, M. Strnad and T. Schmulling (2006). "Arabidopsis cytokinin receptor mutants reveal functions in shoot growth, leaf senescence, seed size, germination, root development, and cytokinin metabolism." Plant Cell **18**(1): 40-54.

Riou-Khamlichi, C., R. Huntley, A. Jacqmard and J. A. Murray (1999). "Cytokinin activation of Arabidopsis cell division through a D-type cyclin." Science **283**(5407): 1541-1544.

Rivoal, J. and A. D. Hanson (1994). "Choline-O-Sulfate Biosynthesis in Plants (Identification and Partial Characterization of a Salinity-Inducible Choline Sulfotransferase from Species of Limonium (Plumbaginaceae)." Plant Physiol **106**(3): 1187-1193.

Rossi, A. and A. Superti-Furga (2001). "Mutations in the diastrophic dysplasia sulfate transporter (DTDST) gene (SLC26A2): 22 novel mutations, mutation review, associated skeletal phenotypes, and diagnostic relevance." Hum Mutat **17**(3): 159-171.

Rouleau, M., F. Marsolais, M. Richard, L. Nicolle, B. Voigt, G. Adam and L. Varin (1999). "Inactivation of brassinosteroid biological activity by a salicylate-inducible steroid sulfotransferase from Brassica napus." J Biol Chem **274**(30): 20925-20930.

Rupp, H. M., M. Frank, T. Werner, M. Strnad and T. Schmulling (1999). "Increased steady state mRNA levels of the STM and KNAT1 homeobox genes in cytokinin overproducing Arabidopsis thaliana indicate a role for cytokinins in the shoot apical meristem." Plant J **18**(5): 557-563.

Russo, A., M. Piovano, M. Clericuzio, L. Lombardo, S. Tabasso, M. C. Chamy, G. Vidari, V. Cardile, P. Vita-Finzi and J. A. Garbarino (2007). "Putrescine-1,4-dicinnamide from Pholiota spumosa (Basidiomycetes) inhibits cell growth of human prostate cancer cells." Phytomedicine **14**(2-3): 185-191.

Sakai, H., T. Aoyama, H. Bono and A. Oka (1998). "Two-component response regulators from Arabidopsis thaliana contain a putative DNA-binding motif." Plant Cell Physiol **39**(11): 1232-1239.

Sakai, H., T. Aoyama and A. Oka (2000). "Arabidopsis ARR1 and ARR2 response regulators operate as transcriptional activators." Plant J **24**(6): 703-711.

Sakakibara, H. (2006). "Cytokinins: activity, biosynthesis, and translocation." Annu Rev Plant Biol **57**: 431-449.

Schultz, E. A. and G. W. Haughn (1991). "LEAFY, a Homeotic Gene That Regulates Inflorescence Development in Arabidopsis." Plant Cell **3**(8): 771-781.

Sergive, I. G., V. S. Alexieva and E. N. Karanov (1995). "Cytokinin and anticytokinin effects on growth and free polyamine content in etiolated and green radish cotyledons." Journal of plant physiology **145**(3): 266-270.

Strott, C. A. (1996). "Steroid sulfotransferases." Endocr Rev **17**(6): 670-697.

Suzuki, T., K. Miwa, K. Ishikawa, H. Yamada, H. Aiba and T. Mizuno (2001). "The Arabidopsis sensor His-kinase, AHk4, can respond to cytokinins." Plant Cell Physiol **42**(2): 107-113.

Suzuki, T., K. Sakurai, A. Imamura, A. Nakamura, C. Ueguchi and T. Mizuno (2000). "Compilation and characterization of histidine-containing phosphotransmitters implicated in His-to-Asp phosphorelay in plants: AHP signal transducers of Arabidopsis thaliana." Biosci Biotechnol Biochem **64**(11): 2486-2489.

Suzuki, T., K. Sakurai, C. Ueguchi and T. Mizuno (2001). "Two types of putative nuclear factors that physically interact with histidine-containing phosphotransfer (Hpt) domains, signaling mediators in His-to-Asp phosphorelay, in Arabidopsis thaliana." Plant Cell Physiol **42**(1): 37-45.

Tajima, Y., A. Imamura, T. Kiba, Y. Amano, T. Yamashino and T. Mizuno (2004). "Comparative studies on the type-B response regulators revealing their distinctive properties in the His-to-Asp phosphorelay signal transduction of Arabidopsis thaliana." Plant Cell Physiol **45**(1): 28-39.

Thomas, T. and T. J. Thomas (2001). "Polyamines in cell growth and cell death: molecular mechanisms and therapeutic applications." Cell Mol Life Sci **58**(2): 244-258.

To, J. P., G. Haberer, F. J. Ferreira, J. Deruere, M. G. Mason, G. E. Schaller, J. M. Alonso, J. R. Ecker and J. J. Kieber (2004). "Type-A Arabidopsis response regulators are partially redundant negative regulators of cytokinin signaling." Plant Cell **16**(3): 658-671.

To, J. P. and J. J. Kieber (2008). "Cytokinin signaling: two-components and more." Trends Plant Sci **13**(2): 85-92.

Ueguchi, C., H. Koizumi, T. Suzuki and T. Mizuno (2001). "Novel family of sensor histidine kinase genes in Arabidopsis thaliana." Plant Cell Physiol **42**(2): 231-235.

Ueguchi, C., S. Sato, T. Kato and S. Tabata (2001). "The AHK4 gene involved in the cytokinin-signaling pathway as a direct receptor molecule in Arabidopsis thaliana." Plant Cell Physiol **42**(7): 751-755.

ul Haque, M. F., L. M. King, D. Krakow, R. M. Cantor, M. E. Rusiniak, R. T. Swank, A. Superti-Furga, S. Haque, H. Abbas, W. Ahmad, M. Ahmad and D. H. Cohn (1998). "Mutations in orthologous genes in human spondyloepimetaphyseal dysplasia and the brachymorphic mouse." Nat Genet **20**(2): 157-162.

Urano, K., T. Hobo and K. Shinozaki (2005). "Arabidopsis ADC genes involved in polyamine biosynthesis are essential for seed development." FEBS Lett **579**(6): 1557-1564.

Urao, T., B. Yakubov, R. Satoh, K. Yamaguchi-Shinozaki, M. Seki, T. Hirayama and K. Shinozaki (1999). "A transmembrane hybrid-type histidine kinase in Arabidopsis functions as an osmosensor." Plant Cell **11**(9): 1743-1754.

Varin, L., V. DeLuca, R. K. Ibrahim and N. Brisson (1992). "Molecular characterization of two plant flavonol sulfotransferases." Proc Natl Acad Sci U S A **89**(4): 1286-1290.

Varin, L., F. Marsolais, M. Richard and M. Rouleau (1997). "Sulfation and sulfotransferases 6: Biochemistry and molecular biology of plant sulfotransferases." FASEB J **11**(7): 517-525.

Weinshilboum, R. and D. Otterness (1994). "Sulfotransferase enzymes." Handbook of experimental pharmacology **ISSN** 0171-2004 **112**(6 p.1/4).

Weinshilboum, R. M., D. M. Otterness, I. A. Aksoy, T. C. Wood, C. Her and R. B. Raftogianis (1997). "Sulfation and sulfotransferases 1: Sulfotransferase molecular biology: cDNAs and genes." FASEB J **11**(1): 3-14.

Werner, T., V. Motyka, V. Laucou, R. Smets, H. Van Onckelen and T. Schmulling (2003). "Cytokinin-deficient transgenic Arabidopsis plants show multiple developmental alterations indicating opposite functions of cytokinins in the regulation of shoot and root meristem activity." Plant Cell **15**(11): 2532-2550.

Werner, T., V. Motyka, M. Strnad and T. Schmulling (2001). "Regulation of plant growth by cytokinin." Proc Natl Acad Sci U S A **98**(18): 10487-10492.

Wingler, A., A. v. Schaewen, R. C. Leegood, P. J. Lea and W. P. Quick (1998). "Regulation of leaf senescence by cytokinin, sugars, and light." Plant Physiology **116**: 329-335.

Winter, D., B. Vinegar, H. Nahal, R. Ammar, G. V. Wilson and N. J. Provart (2007). "An "electronic Fluorescent Pictograph" browser for exploring and analyzing large-scale biological data sets." PLoS ONE **2**(1): e718.

Yamada, H., T. Suzuki, K. Terada, K. Takei, K. Ishikawa, K. Miwa, T. Yamashino and T. Mizuno (2001). "The Arabidopsis AHK4 histidine kinase is a cytokinin-binding receptor that transduces cytokinin signals across the membrane." Plant Cell Physiol **42**(9): 1017-1023.

Yasuda, S., M. Suiko and M. C. Liu (2005). "Oral contraceptives as substrates and inhibitors for human cytosolic SULTs." J Biochem **137**(3): 401-406.

Yokoyama, A., T. Yamashino, Y. Amano, Y. Tajima, A. Imamura, H. Sakakibara and T. Mizuno (2007). "Type-B ARR transcription factors, ARR10 and ARR12, are

implicated in cytokinin-mediated regulation of protoxylem differentiation in roots of Arabidopsis thaliana." Plant Cell Physiol **48**(1): 84-96.

Zimmermann, P., M. Hirsch-Hoffmann, L. Hennig and W. Gruissem (2004). "GENEVESTIGATOR. Arabidopsis microarray database and analysis toolbox." Plant Physiol **136**(1): 2621-2632.

ANNEX 1

Table 1. Statistical data of root length phenotype analysis.

Root length analysis, DAG[1]=2, Kruskal-Wallis Asymp. Sig. [2]= 0.0

Genotype[3]	Mann-Whitney U	Asymp. Sig. (2-tailed)	Number[4]
Ctl & A	315	0.455	Ctl =42 A=17
Ctl & B	569.5	0.075	Ctl=42 B=35
Ctl & C	268	$2.44E^{-5}$	Ctl=42 C=29

Root length analysis, DAG=3, Kruskal-Wallis Asymp. Sig. = 0.0

Genotype	Mann-Whitney U	Asymp. Sig. (2-tailed)	Number
Ctl & A	268	0.001	Ctl =43 A=25
Ctl & B	535	0.028	Ctl=43 B=35
Ctl & C	99	$3.41E^{-10}$	Ctl=43 C=31

Root length analysis, DAG=4, Kruskal-Wallis Asymp. Sig. = 0.0

Genotype	Mann-Whitney U	Asymp. Sig. (2-tailed)	Number
Ctl & A	403	0.087	Ctl =43 A=25
Ctl & B	393	$2.88E^{-4}$	Ctl=43 B=35
Ctl & C	122	$3.91E^{-9}$	Ctl=43 C=30

[1] DAG= Days after Germination
[2] Asymp. Sig. stands for asymptotic significance
[3] Ctl, A, B and C stand for control, *AtST4a*-, *AtST4b*- and *AtST4c*-KO lines, respectively
[4] Number shows the numbers of replicates in each mutant line

Root length analysis, DAG=6, Kruskal-Wallis Asymp. Sig. = 0.0

Genotype	Mann-Whitney U	Asymp. Sig. (2-tailed)	Number
Ctl & A	426	0.076	Ctl =44 A=26
Ctl & B	295	$8.69E^{-6}$	Ctl=44 B=33
Ctl & C	259	$1.01E^{-5}$	Ctl=44 C=30

Root length analysis, DAG=7, Kruskal-Wallis Asymp. Sig. = 0.0

Genotype	Mann-Whitney U	Asymp. Sig. (2-tailed)	Number
Ctl & A	379	0.06	Ctl =42 A=25
Ctl & B	385	0.001	Ctl=42 B=33
Ctl & C	281	$6.74E^{-5}$	Ctl=42 C=30

Root length analysis, DAG=8, Kruskal-Wallis Asymp. Sig. = 0.0

Genotype	Mann-Whitney U	Asymp. Sig. (2-tailed)	Number
Ctl & A	176	0.002	Ctl =40 A=18
Ctl & B	343	0.001	Ctl=40 B=31
Ctl & C	336	0.002	Ctl=40 C=30

Root length analysis, DAG=9, Kruskal-Wallis Asymp. Sig. = 0.0

Genotype	Mann-Whitney U	Asymp. Sig. (2-tailed)	Number
Ctl & A	199	0.016	Ctl =37 A=18
Ctl & B	349	0.015	Ctl=37 B=29
Ctl & C	375	0.059	Ctl=37 C=28

Root length analysis, DAG=10, Kruskal-Wallis Asymp. Sig. = 0.002

Genotype	Mann-Whitney U	Asymp. Sig. (2-tailed)	Number
Ctl & A	215	0.034	Ctl =37 A=18
Ctl & B	341	0.031	Ctl=37 B=27
Ctl & C	411	0.62	Ctl=37 C=24

Table 2. Statistical data of hormone treatment analysis of root tissue.

Relative root length, Hormone dose=0μM, two-independent-samples test

Genotype	Levene's Test for Equality of Variances sig.	t-test for Equality of Means sig.	Number
Ctl & B	0.068	0.014	Ctl=19 B=19

Relative root length, Hormone dose=3μM, two-independent-samples test

Genotype	Levene's Test for Equality of Variances sig.	t-test for Equality of Means sig.	Number
Ctl & B	0.631	0.002	Ctl=20 B=18

Relative root length, Hormone dose=5μM

Genotype	Mann-Whitney U	Asymp. Sig. (2-tailed)	Number
Ctl & B	73.00	0.011	Ctl=18 B=16

Table 3. Statistical data of number of lateral root phenotype analysis.

Numbers of lateral roots, DAG=12, two-independent-samples test

Genotype	Levene's Test for Equality of Variances sig.	t-test for Equality of Means sig.	Number
Ctl & B	0.5	0.149	Ctl=10 B=10

Numbers of lateral roots, DAG=14, two-independent-samples test

Genotype	Levene's Test for Equality of Variances sig.	t-test for Equality of Means sig.	Number
Ctl & B	0.133	0.062	Ctl=9 B=12

Numbers of lateral roots, DAG=10, Kruskal-Wallis Asymp. Sig. = 0.001

Genotype	Mann-Whitney U	Asymp. Sig. (2-tailed)	Number
Ctl & A	120	0.836	Ctl =21 A=12
Ctl & C	48	$4.49E^{-4}$	Ctl=21 C=15

Numbers of lateral roots, DAG=13, Kruskal-Wallis Asymp. Sig. = 0.147

Genotype	Mann-Whitney U	Asymp. Sig. (2-tailed)	Number
Ctl & A	60.500	0.320	Ctl =20 A=8
Ctl & C	95.500	0.069	Ctl=20 C=15

ANNEX 2

Table 1. Statistical data of rosette diameter analysis.

Rosette diameter, DAG=14, Kruskal-Wallis Asymp. Sig. = 0.38
Rosette diameter, DAG=21, Kruskal-Wallis Asymp. Sig. = 0.015

Genotype	Mann-Whitney U	Asymp. Sig. (2-tailed)	Number
Ctl & A	334	0.035	Ctl =27 A=36
Ctl & B	288	0.028	Ctl=27 B=32
Ctl & C	451	0.76	Ctl=27 C=35

Rosette diameter, DAG=26, Kruskal-Wallis Asymp. Sig. = 0.008

Genotype	Mann-Whitney U	Asymp. Sig. (2-tailed)	Number
Ctl & A	297	0.48	Ctl =21 A=32
Ctl & B	296	0.867	Ctl=21 B=29
Ctl & C	165	0.014	Ctl=21 C=29

Table 2. Statistical data of numbers of leaves phenotype analysis.

Number of leaves, DAG=14, Kruskal-Wallis Asymp. Sig. = 0.001

Genotype	Mann-Whitney U	Asymp. Sig. (2-tailed)	Number
Ctl & A	391	0.7	Ctl =21 A=39
Ctl & B	298	0.013	Ctl=21 B=39
Ctl & C	326	0.331	Ctl=21 C=35

Number of leaves, DAG=21, Kruskal-Wallis Asymp. Sig. = 0.00

Genotype	Mann-Whitney U	Asymp. Sig. (2-tailed)	Number
Ctl & A	298	0.010	Ctl =29 A=32
Ctl & B	253	$4.21E^{-4}$	Ctl=29 B=34
Ctl & C	35	$9.03E^{-12}$	Ctl=29 C=35

ANNEX 3

Table 1. Statistical data of number of seeds per siliques analysis.

Number of seeds per silique, DAG=57, Kruskal-Wallis Asymp. Sig. = 0.00

Genotype	Mann-Whitney U	Asymp. Sig. (2-tailed)	Number
Ctl & A	387	0.355	Ctl =30 A=30
Ctl & B	321	0.056	Ctl=30 B=30
Ctl & C	109	$4.49E^{-7}$	Ctl=30 C=30

Table 2. Statistical data of number of siliques analysis.

Number of siliques per plants, DAG=36, Kruskal-Wallis Asymp. Sig. = 0.00

Genotype	Mann-Whitney U	Asymp. Sig. (2-tailed)	Number
Ctl & A	84.5	$4.47E^{-5}$	Ctl =23 A=24
Ctl & B	141	0.011	Ctl=23 B=22
Ctl & C	0.00	$1.47E^{-9}$	Ctl=23 C=27

Number of siliques per plants, DAG=46, Kruskal-Wallis Asymp. Sig. = 0.00

Genotype	Mann-Whitney U	Asymp. Sig. (2-tailed)	Number
Ctl & A	49	$6.69E^{-6}$	Ctl =24 A=20
Ctl & B	87	$1.72E^{-4}$	Ctl=24 B=21
Ctl & C	20	$5.377E^{-8}$	Ctl=24 C=23

Table 3. Statistical data of seed size phenotype analysis.

Seed length, Kruskal-Wallis Asymp. Sig. = 0.00

Genotype	Mann-Whitney U	Asymp. Sig. (2-tailed)	Number
Ctl & B	393	$8.57E^{-5}$	Ctl=40 B=40
Ctl & C	490	0.003	Ctl=40 C=40

Seed width, Kruskal-Wallis Asymp. Sig. = 0.00

Genotype	Mann-Whitney U	Asymp. Sig. (2-tailed)	Number
Ctl & B	504	0.004	Ctl=40 B=40
Ctl & C	341	$8.57E^{-5}$	Ctl=40 C=40

Seed volume, Kruskal-Wallis Asymp. Sig. = 0.00

Genotype	Mann-Whitney U	Asymp. Sig. (2-tailed)	Number
Ctl & B	416	$2.19E^{-4}$	Ctl=40 B=40
Ctl & C	313	$2.77E^{-6}$	Ctl=40 C=40